RESPONSES OF MICROORGANISMS TO ON-LINE CHEMICAL CLEANING WITH SODIUM HYPOCHLORITE IN MEMBRANE BIOREACTOR
CAI WEIWEI
2017

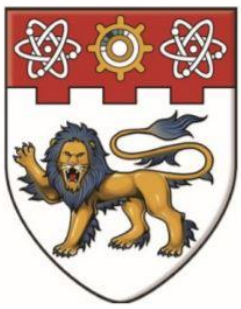

NANYANG TECHNOLOGICAL UNIVERSITY

RESPONSES OF MICROORGANISMS TO ON-LINE CHEMICAL CLEANING WITH SODIUM HYPOCHLORITE IN MEMBRANE BIOREACTOR

CAI WEIWEI

SCHOOL OF CIVIL AND ENVIRONMENTAL ENGINEERING

2017

RESPONSES OF MICROORGANISMS TO ON-LINE CHEMICAL CLEANING WITH SODIUM HYPOCHLORITE IN MEMBRANE BIOREACTOR

CAI WEIWEI

CAI WEIWEI

School of Civil and Environmental Engineering

A thesis submitted to the Nanyang Technological University

in partial fulfilment of the requirements for the degree of

Doctor of Philosophy

2017

ACKNOWLEDGMENTS

Firstly, I would like to express my deepest appreciation to my supervisor, Professor Liu Yu. Without his insightful guidance and constant encouragement, I would not conduct my research work smoothly. He always enlightens me and provides invaluable suggestions when I am confused about my study. His strong knowledge background and extraordinary insight also instruct me how to be a great researcher in the future. Meanwhile, he helps me know many truths of life through his rich life experience. Each time after meeting with him, I am highly motivated and full of passion not only in research, but also in every area of my life. I sincerely thank for his patient instruction, support and encouragement.

Secondly, I express my cordial gratitude to my co-supervisor Professor Ng Wun Jern for his support and guidance. Thanks to Associate Professor Zhang Xiangru and Dr. Liu Jiaqi in Hongkong University of Science and Technology for their kind assistance in my research work.

I greatly appreciate Dr. Xu Huijuan and Dr. Meng Shujuan for their heartfelt support during my PhD study. Thanks a lot to my friends, Mr. Wang Jingwei, Mr. Gu Jun, Ms. Yang Qin and Mr. Lim Weikang for their sincere help when I need their assistance.

I also express my thanks to those technicians in NEWRI AEBC laboratory, especially Mr. Lim Kee Chuan, Ms. Ong Qian Mei and Ms. Emily Mar'atusalihat for their technical support in lab.

I also highly appreciate School of Civil and Environmental Engineering, Nanyang Technological University for awarding me research scholarship, which provides me an economic support during my PhD period.

Last but not the least, sincere thanks go to my parents for their everlasting love and unlimited support throughout my pursuit of scientific research.

TABLE OF CONTENTS

SUMMARY

On-line chemical cleaning with sodium hypochlorite (NaClO) has been commonly employed for maintaining a constant permeability in membrane bioreactor (MBR) due to its simple and efficient operation. However, activated sludge is inevitably exposed to NaClO during this cleaning process. In spite of the broad applications of on-line chemical cleaning in MBR, such as chemical cleaning-in-place (CIP) and chemical enhanced backwash (CEB), little information is currently available about the microbial responses to NaClO in this prevalent practice, and their further impacts on MBR system.

During on-line chemical cleaning, the bulk suspension in MBR is exposed to NaClO, after which the treated sludge can partially revert back onto membrane when normal filtration restarts. Therefore, in the first phase of study, the potential effects of NaClO on biofouling re-development were investigated. Activated sludge was exposed to NaClO with different dosages, and treated sludge was used for study of subsequent fouling propensity in a crossflow microfiltration system. Results showed that NaClO could trigger bacterial lysis and release of EPS and AI-2. Compared to control, the membrane fouling rate of NaClO-treated sludge was significantly increased especially at high NaClO dosage, which could be attributed to the overproduction of EPS and AI-2. Despite a decline in cell viability observed after the exposure to NaClO, live cells in suspension showed a greater tendency to attach onto membrane surfaces, resulting in a faster fouling development. This may be due to the fact that under oxidizing stress imposed by NaClO, survived bacteria tended to move onto membrane surface in order to mitigate the damage potential. Consequently, this study raised a serious concern on on-line chemical cleaning-induced membrane biofouling.

Since the produced oxidative stress may trigger membrane biofouling formation, in the second phase of study, a subsequent investigation on the relationship between intracellular oxidative stress and biofouling formation was conducted. In this study, activated sludge microorganisms were exposed to NaClO with

various dosages for 30 min, leading to bacterial death and substantial generation of oxidative stress. Afterwards, the membrane fouling propensity of stressed biomass at different levels of reactive oxygen species (ROS) were systematically examined in a standard crossflow microfiltration system. Results showed that membrane fouling potential of stressed biomass was significantly increased due to the faster colonization of survived bacteria on the membrane surface. The confocal images provided the supportive evidence of such observation, i.e. live bacteria were found to the biofouling layer in the presence of oxidative stress, while significantly high number of dead bacteria cells was detected on the membrane surface in the absence of oxidative stress. It was also found that live bacteria more situated at the membrane surface, on the top of which a layer of dead bacteria was formed during the filtration of stressed bacteria. These suggested that the oxidative stress prompted survived bacteria to rapidly and predominantly adhere onto the membrane surface in order to protect themselves from harsh conditions. Consequently, survived bacteria after chemical cleaning by NaClO may accelerate the membrane biofouling formation and such developed adaptation phenotype in turn raises concern about the long-term effectiveness of chemical cleaning in MBR.

It appears from the above two phases that NaClO can trigger bacterial lysis, potentially leading to the release of dissolved organic matter (DOM) in liquid phase. In the third phase of study, a systematical characterization of these generated DOM and byproducts was carried out. The results showed the occurrence of significant DOM generation (up to 24.7 mg/L as DOC) after exposure of activated sludge to NaClO with various dosages. The dominant components of these emerging DOM were humic acid-like and protein-like substances. Furthermore, 19 kinds of chlorinated and brominated byproducts were identified by (UPLC)/ESI-tqMS, eight of which were confirmed with standard compounds. Many byproducts were found to be halogenated aromatic compounds, including halopyrroles and halo(hydro)benzoquinones, which had been reported to be significantly more toxic than the halogenated aliphatic ones. As a result, this study provides new insights into the practice of on-line chemical

cleaning, and opens up a window to re-examine the current operation of MBR by looking into the generation of micropollutants.

In the fourth phase, a continuous investigation on the fate of these generated DOM and byproducts in MBR were conducted. After exposure of activated sludge to 0 mg/L, 5 mg/L and 20 mg/L NaClO, it was found that around 39% of produced DOM was eventually removed in an aerobic MBR, among which protein-like substances were more readily eliminated than the humic-like substances. As for the halogenated byproducts, the MBR could only remove the byproducts partially, and 62.4%-84.5% of halogenated byproducts still ended up in the permeate at the NaClO dosages of 5 mg/L and 20 mg/L, respectively. This study shows the dark side of on-line chemical cleaning with NaClO, and raises serious concerns on the reuse and recycle of such MBR permeate.

In conclusion, this study clearly revealed the microbial responses to NaClO, and shed lights on the potentially unfavourable impacts of on-line chemical cleaning with NaClO on MBR system. Therefore, novel membrane cleaning strategies with environmental friendly features should be explored.

LIST OF PUBLICATIONS

1. Cai, W. and Liu, Y. (2016) Enhanced membrane biofouling potential by on-line chemical cleaning in membrane bioreactor. **Journal of Membrane Science** 511, 84-91.

2. Cai, W., Liu, J., Zhang, X., Ng, W.J. and Liu, Y. (2016) Generation of dissolved organic matter and byproducts from activated sludge during contact with sodium hypochlorite and its implications to on-line chemical cleaning in MBR. **Water Research** 104, 44-52.

3. Cai, W., Liu, J., Zhu, X., Zhang, X., and Liu, Y. (2017) Fate of dissolved organic matter and byproducts generated from on-line chemical cleaning with sodium hypochlorite in MBR. **Chemical Engineering Journal** 323, 233-242.

4. Cai, W. and Liu, Y. (2017) Oxidative stress induced membrane biofouling and its implications to on-line chemical cleaning in MBR. Submitted to **Journal of Membrane Science.**

LIST OF TABLES

LIST OF FIGURES

LIST OF SYMBOLS

AI-2	Autoinducer-2
CA	Cellulose acetate
CEB	Chemical enhanced backwash
CIP	Cleaning in place
CLSM	Confocal laser scanning microscopy
DBP	Disinfection byproduct
DOC	Dissolved organic carbon
DOM	Dissolved organic matter
DPD	4,5-dihydroxy-2,3-pentanedione
EDTA	Ethylene diamine tetraacetic acid
EEM	Excitation-emission matrix
EPS	Extracellular polymeric substances
F_{max}	Maximum fluorescence intensity
HRT	Hydraulic retention time
LMH	$L/(m^2h)$
MBR	Membrane bioreactor
MF	Microfiltration
MLSS	Mixed liquor suspended solid
NOM	Natural organic matter
NaClO	Sodium hypochlorite
PARAFAC	Parallel factor analysis
PBS	Phosphate buffered saline
PES	Polyethersulfone
PN	Proteins
PS	Polysaccharides
PVDF	Polyvinylidene fluoride
ROS	Reactive oxygen species
SDA	Specific dehydrogenases activity
SEM	Scanning electron microscopy
SMP	Soluble microbial products

SRT	Solid retention time
TMP	Trans-membrane pressure
TOBr	Total organic bromine
TOC	Total organic carbon
TOCl	Total organic chlorine
TOI	Total organic iodine
TOX	Total organic halogen
UF	Ultrafiltration
(UPLC)/ESI-tqMS	Ultra performance liquid chromatography / electrospray ionization-triple quadrupole mass spectrometry

CHAPTER 1 INTRODUCTION

1.1 BACKGROUND

Membrane bioreactor (MBR) is described as a combination of biological degradation process with a direct solid-liquid separation via membrane filtration. To date, it has gained increasing popularity in wastewater treatment worldwide, and more than 200 countries have adopted this promising technology for wastewater treatment and reclamation. Compared to conventional activated sludge treatment, MBR presents numerous advantages, such as smaller footprint, higher sludge concentration allowed, better effluent quality and less excess sludge production (Le-Clech et al. 2006). However, membrane fouling is a primary obstacle for cost-effective MBR operation, with reduced permeate flux or increased trans-membrane pressure (TMP) (Lee et al. 2012, Meng et al. 2009).

To cope with such a situation, membrane cleaning is often practiced, which substantially influences membrane performance. Although several cleaning strategies including relaxation, backwashing, enzyme cleaning, etc. have been developed to mitigate or prevent membrane fouling, chemical cleaning with sodium hypochlorite (NaClO) is considered as one of the most effective methods to eliminate both reversible and irreversible fouling in MBR (Lee et al. 2013, Porcelli and Judd 2010, Wei et al. 2011). During on-line chemical cleaning, NaClO is introduced into membrane from the permeate side with membrane modules submerging in bio-reactor (Wang et al. 2014b). Compared to off-line cleaning, on-line cleaning is generally preferable due to its simplicity, low cost and effectiveness. However, in this process, both membrane and activated sludge are unavoidably exposed to NaClO, potentially leading to various impacts on MBR system. Just recently, attention has been paid to possible effects of NaClO on the integrity of various types of membranes (Abdullah and Berube 2013, Puspitasari et al. 2010), however little information is currently available on the potential impacts of NaClO on microorganisms in MBR. Therefore, this study explored the diverse microbial responses to NaClO. It is expected that this study

should provide new insights into the prevalent practice of on-line chemical cleaning with NaClO, and shed lights on their further impacts on MBR performance.

1.2 OBJECTIVES AND SCOPE

The main objectives of this study are:

(1) To examine the effects of NaClO on microbial characteristics of activated sludge, while to study membrane fouling propensities of activated sludge microorganisms after exposure to NaClO with different dosages.

(2) To investigate the relationship between intracellular oxidative stress and biofouling formation. The biofilm structure as well as fouling behaviours of survived and dead bacteria were also studied in order to explore the underlying mechanisms behind them.

(3) To study the generation of DOM and byproduct upon exposure of activated sludge to NaClO. The specific components of these emerging DOM and halogenated DBPs were characterized by EEM and (UPLC)/ESI-tqMS, respectively.

(4) To further look into the fate of these generated DOM and byproducts in MBR. The biodegradability and final removability of specific components in MBR were also studied.

1.3 ORGANIZATION OF THE THESIS

This thesis contains the seven chapters:

(1) Chapter 1 presents an overview of current research background and specific objectives of this study.

(2) Chapter 2 offers a comprehensive literature review, including membrane fouling; various cleaning strategies with the focuses on on-line chemical cleaning and its potential impacts on MBR system.

(3) Chapter 3 demonstrates the NaClO-triggered biomass lysis and subsequent biofouling behaviours of the treated biomass. In this chapter, chemical cleaning-induced membrane biofouling was clearly shown, i.e. on-line chemical cleaning would negatively influence MBR performance by enhancing the attachment of survived bacteria onto membrane surface.

(4) Chapter 4 further establishes the relationship between intracellular oxidative stress and biofouling formation by studying the fouling behaviours of stressed and non-stressed biomass at the same cell viability.

(5) Chapter 5 focuses on the generation of DOM and byproducts from activated sludge after exposure to NaClO. It was found that the substantial amount of DOM was released, among which the dominant components were humic acid-like and protein-like substances. Meanwhile, 19 halogenated byproducts were identified containing halopyrroles and halo(hydro)benzoquinones, which may be more toxic than the halogenated aliphatic byproducts.

(6) Chapter 6 further shows the fate of the emerging DOM and byproducts in MBR. It was found that only a small part of produced DOM and byproducts could be biodegraded and removed by MBR.

(7) Chapter 7 summarizes the major findings of this study and outlines future work.

CHAPTER 2 LITERATURE REVIEW

2.1 MEMBRANE FOULING FORMATION IN MBR

Up to date, MBR encompassed various configurations based on different membrane geometries, membrane materials, hydraulic operations, biological process etc. Whilst numerous membrane geometries exist in the membrane market place, three dominant membrane configurations in MBR are flat-sheet, hollow fiber and multitube. In terms of membrane materials, polymeric (e.g. PVDF and PES) and ceramic membranes are the two most widely employed membrane materials. In addition, MBR are also classified into aerobic and anaerobic systems depending on the different biotreatment conditions. And two primary hydraulic operations (i.e. pumped and airlift) are generally employed.

2.1.1 Characteristics of membrane fouling in MBR

Membrane fouling in MBR is mainly attributed to the interactions between biomass and membrane surface or within membrane structure via series of physicochemical and biological mechanisms. In general, deposition and adherence of bio-solids take place as soon as the activated sludge contact with membrane, resulting in flux decline. Predominant fouling mechanisms in MBR involve a mixed of pore clogging and cake deposition. Even though the fouling behaviours in MBR are complicated due to the complex nature of activated sludge, a three-stage process that elaborates fouling mechanism in MBR has been proposed in the literature (Cho and Fane 2002, Zhang et al. 2006).

As illustrated in **Figure 2.1**, the first stage (conditioning fouling) presents an initial short-term rapid rise in TMP, which is caused by initial adsorption and pore clogging. With the biofilm formation and further pore blocking, the less steep stage (steady fouling) appears. The permeate flux at this stage is below critical flux required for particle deposition. In the third stage, a sharp increase known as TMP jump takes place due to the consequence of serious membrane

fouling. There are several existing hypotheses explaining the occurrence of TMP jump: (a) successive pore blocking causes local flux eventually exceeding critical value, and potential foulant deposit at a higher increasing rate (Van Der Gast et al. 2006, Ye et al. 2005); (b) Biofilm structure experiences sudden changes. With the increase in biofilm thickness during long-term operation, limited oxygen supply for bacteria in the inner layer accelerates cell death. Thereby, more extracellular polymeric substances (EPS) are released at the bottom layer, which are closely related to the biofilm structure as well as TMP changes (Hwang et al. 2008, Zhang et al. 2006); (c) Operation conditions may affect the stability of MBR system, and further change TMP (Pollice et al. 2005, Zhang et al. 2006).

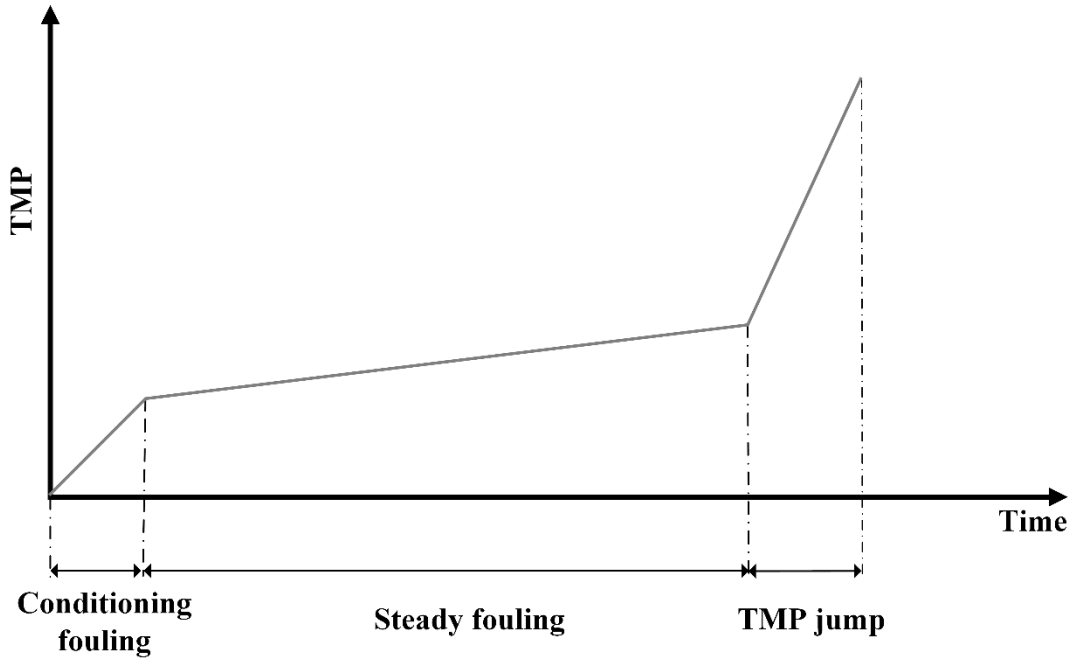

Figure 2.1 Schematic illustration of three-stage membrane fouling mechanism in MBR.

2.1.2 Classification of membrane fouling in MBR

Inorganic fouling, organic fouling and biofouling

From a viewpoint of foulant components, membrane fouling can be divided into three basic categories: inorganic fouling, organic fouling and biofouling (Liao et al. 2006). In general, inorganic fouling accounts for a small part and is caused by

chemical precipitation and biological precipitation as shown in **Figure 2.2**. Chemical precipitation refers to the deposition of large amount of cations and anions, such as Ca^{2+}, Mg^{2+}, PO_4^{3-}, and CO_3^{2-} on the membrane surface. When the concentration of accumulated chemical species increases until intrinsic saturation concentration is exceeded, chemical precipitation occurs (Bremere et al. 1999, Bremere et al. 1998). Additionally, the fouling layer formed on membrane could also resist shear force acting on the layer surface, resulting in higher concentration polarization and chemical precipitation tendency (Sheikholeslami 1999). Besides chemical precipitation, another contributor to inorganic fouling is biological precipitation. It can be attributed to some existing biopolymers containing various ionisable groups, which can easily trap metal ions and further form several types of complexes to accelerate flux decline (Costa et al. 2006). For example, COO^-, CO_3^{2-}, PO_4^{3-}, and OH^- are some common ionisable groups present in biofilm and biopolymers. In addition, metal ions could play a significant role in bridging cells and biopolymers to facilitate dense layer development, and this process also exacerbates membrane fouling formation. Even though inorganic fouling could be caused by two types of precipitations, it has not been considered as a main cause governing membrane fouling in MBR. Numerous investigations suggest that the severest fouling in MBR is due to microbial activities and natural organic matters (NOM). Thereby, only a few studies examined inorganic fouling in MBR, which also indicates inorganic fouling may not occur easily in MBR system (Kang et al. 2002, Ognier et al. 2002)**.**

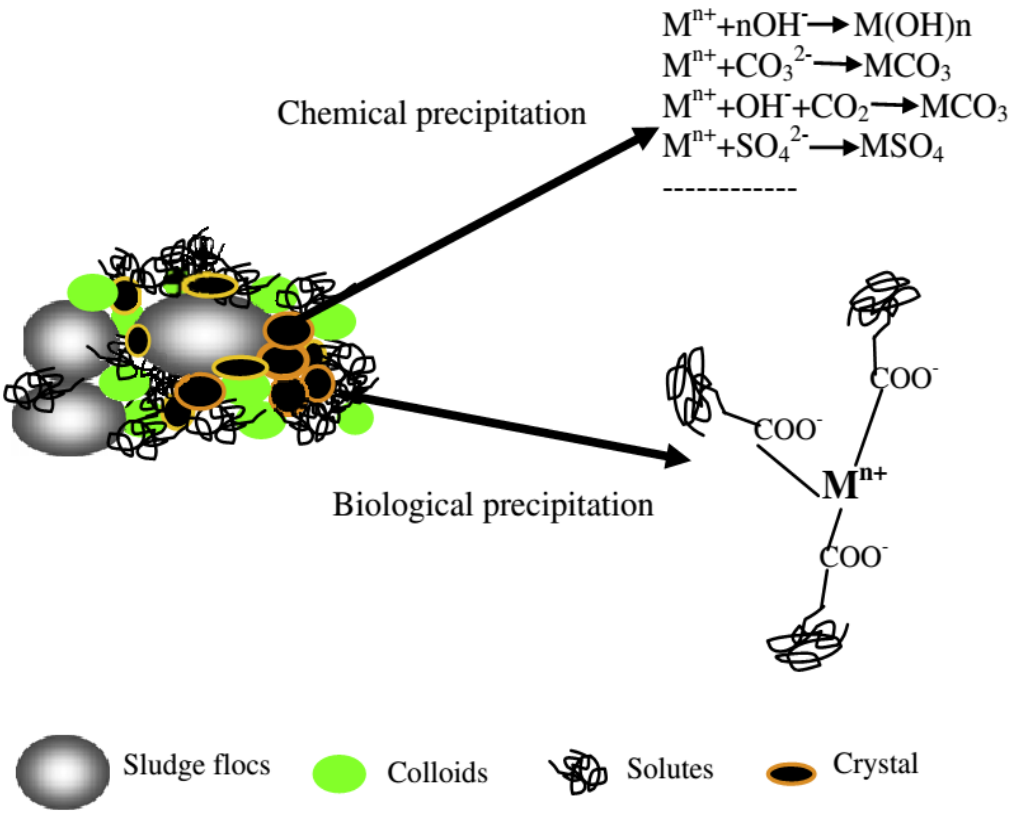

Figure 2.2 Schematics of inorganic fouling formation in MBR (Meng et al. 2009).

In MBR, organic fouling arises from deposition of biopolymers on membrane surface. Typical biopolymers usually include proteins, polysaccharides as well as humic acids. In comparison with colloids or cell clusters, biopolymers with smaller sizes could more easily accumulate on membrane surface and present lower back transport velocity, which largely increases their possibility to form organic fouling. Metzger et al. (2007) revealed a spatial distribution of organic foulants on membrane surface in MBR via fractionation and characterization of fouling layers. The results illustrated that the top membrane fouling layer was made up of porous and loosely bound matters, which is similar to activated sludge flocs. The constituent components of intermediate layer were mainly soluble microbial products (SMP) and microorganisms, with a relative higher concentration of polysaccharides. However, the bottom layer was predominated by SMP with a high concentration of proteins. Up to date, the primary

constituents of biopolymers on membrane surface have been identified to be polysaccharides and protein-like substances in MBR (Kimura et al. 2005, Rosenberger et al. 2006, Teychene et al. 2008, Zhou et al. 2007).

Biofouling is related to the formation of biofilm caused by the interactions between microorganisms with membrane surface. Since biofouling is difficult to be removed even with chemical cleaning, it has raised wide concerns in the field of membrane filtration, especially for microfiltration and ultrafiltration (Pang et al. 2005, Wang et al. 2005). In MBR, individual cells or flocs first attach or deposit on membrane surface, followed by the development of a cake layer via the growth and reproduction of viable fixed cells. Extracellular polymeric substances (EPS) and soluble microbial products (SMP) secreted by microorganisms also contribute to biofouling. It is widely accepted that the accumulation of EPS and SMP facilitates the formation of biological foulants and cake layer on membrane surface (Cogan and Chellam 2009, Flemming et al. 1997, Kim et al. 2006, Ramesh et al. 2007). Meanwhile, some studies had investigated microbial community structure on membrane in MBR, and concluded that the microbial communities living on membrane surfaces were different from those in suspended sludge, suggesting bacteria selectively adhere and deposit on membrane surface (Gao et al. 2010, Miura et al. 2007).

Although there are significant differences among inorganic fouling, organic fouling and biofouling from the perspectives of fouling components, formation mechanisms and impacts on flux decline, three types of fouling processes indeed may occur simultaneously, and interactions among them usually lead to a higher filtration resistance (Choo and Lee 1996). In general, membrane fouling starts from pore clogging followed by cake layer formation in MBR. However, the characteristics and forms of fouling in various systems could be of great differences (Meng and Yang 2007, Sipma et al. 2010, Sun et al. 2007).

Removable and irremovable fouling

Based on the cleaning protocols, membrane fouling can be classified into reversible fouling and irreversible fouling. As various definitions of irreversible and reversible fouling exist in the literature, Meng et al. (2009) further proposed that reversible and irreversible fouling should be replaced by removable and irremovable fouling. In general, removable fouling can be readily eliminated via various physical cleaning methods (e.g. backwash, air scouring or relaxation), while irremovable fouling normally can be removed by chemical cleaning. In general, removable fouling is the result of loose external deposition of substances, and irremovable fouling is formed due to pore clogging and strongly bound foulants deposited on membrane surface. However, in some cases, removable fouling can be transformed to irremovable fouling after a continuous long-term filtration. As such, in MBR, removable fouling is often referred to as cake layer formation, and irremovable fouling is due to pore clogging (Gao et al. 2011, Jeison and van Lier 2007).

So far, evidence suggests that the main contributor to MBR fouling is cake layer formation on membrane surface. Li and Chu (2003) reported that a sludge cake on membrane surface with a thickness less than 1 mm could generate a fouling resistance of 1.7×10^{13} m^{-1}, suggesting a great contribution of cake layer to the total membrane resistance. The effects of cake layer on membrane fouling in MBR are summarized in **Table 2.1.** In contrast, some reports, however, illustrated the positive role of cake layer towards filtration (Giraldo and LeChevallier 2007, Kuberkar and Davis 2000, Lee et al. 2001). It was reported that cake layer with a pore-like structure could act as a secondary membrane layer to prevent small size foulants from contacting with membrane, and this function, to some degree, could hinder fouling formation (Giraldo and LeChevallier 2007). Therefore, it is necessary to conduct an overall analysis of the functions and characteristics of cake layer for effective control of membrane fouling in MBR.

Table 2.1 Role of cake layer on membrane fouling and MBR performance (Meng et al. 2009).

Effects of cake layer on membrane fouling	References
Cake layer resistance was the major resistance of membrane fouling.	(Chu and Li 2006)
The contribution of cake resistance, membrane intrinsic resistance, irreversible fouling resistance to the total resistance in a submerged MBR was 80%, 12%, and 8%, respectively.	(Lee et al. 2001)
The resistance of cake layer accounted for 95-98% of total filtration resistance.	(Ramesh et al. 2007)
The specific filtration resistance of cake sludge was about 258 times higher than that of bulk sludge.	(Wang et al. 2007)
Sludge cake resistance was the major contributor to membrane fouling, and the sludge cake formation on membrane surfaces was detrimental to the filtration performance.	(Chang and Lee 1998)
Cake layer formation governed the achievable permeate flux.	(Jeison and van Lier 2007)
The cake resistance was the dominant resistance and the bulking sludge could cause a severe cake fouling.	(Meng and Yang 2007)

2.1.3 Factors affecting membrane fouling in MBR

The factors affecting membrane fouling development in MBR can be categorized into the following four clusters: biomass characteristics, membrane characteristics, feed characteristics, and operation conditions (**Figure 2.3**). Among them, biomass and membrane properties can directly influence fouling development, while operation conditions and feed properties may indirectly act on membrane fouling via changing sludge characteristics.

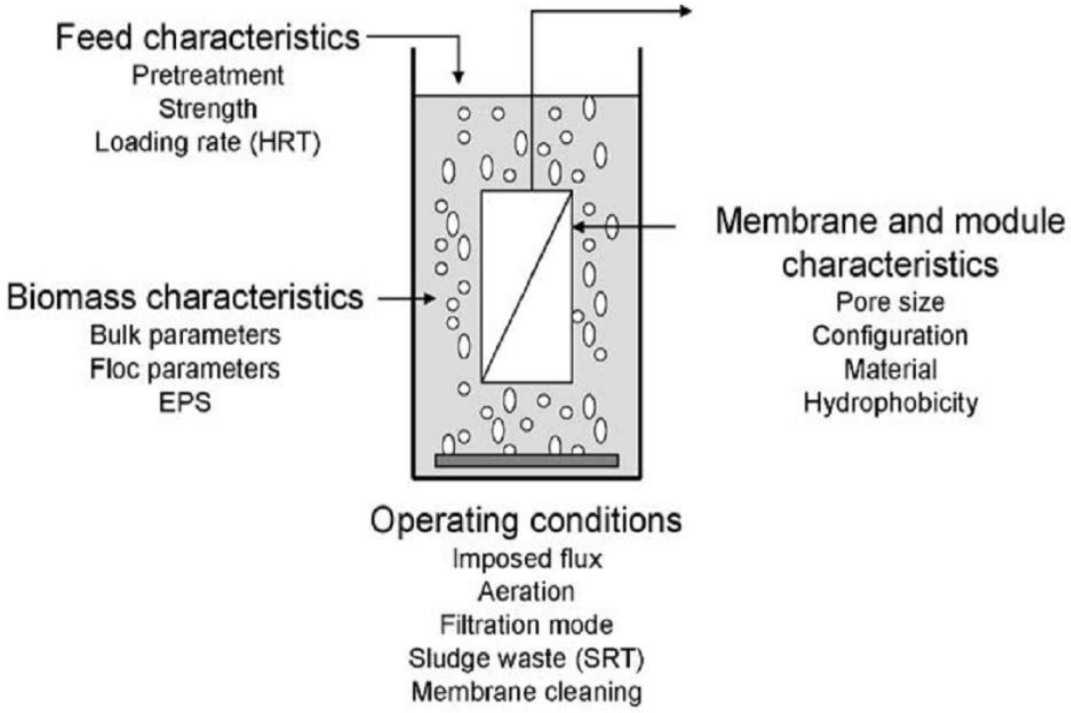

Figure 2.3 Factors affecting membrane fouling in submerged MBR (Le-Clech et al. 2006).

Biomass characteristics

Biomass contains a variety of complex components and it has been considered as a primary contributor to membrane fouling. In MBR, mixed liquor suspended solids (MLSS) have complicated interactions with membrane surface and then fouling formation. The controversial findings related to the impacts of MLSS on membrane fouling can be found in the literature. In cases where the influences of other parameters are neglected, the increase of MLSS concentration would lead to higher TMP or lower flux, suggesting a more severe fouling at high biomass concentration (Chang and Kim 2005, Çiçek et al. 1999). Meanwhile, some other findings argued that there were positive or insignificant impacts of MLSS concentration on membrane fouling (Le-Clech et al. 2003, Lesjean et al. 2005). For example, Rosenberger et al. (2005) observed that increasing MLSS concentration up to 6 g/L seemed to slow down fouling degree, while significant fouling could be expected at the MLSS concentration greater than 15 g/L. Moreover, the effect of MLSS in the concentration range of 8-12 g/L was found to be insignificant. Obviously, MLSS alone cannot provide a convincing

explanation of membrane fouling, simply due to the fact that membrane fouling in MBR is the result of combined interactions of various parameters.

In a MBR, EPS and SMP all play essential roles in membrane fouling formation. EPS is sticky secretions from microbial cells, composed of polysaccharides, proteins, humic acids, nucleic acids etc. They have been known to be important in maintaining the three-dimensional matrix of biofilms, which has a close relationship to cake layer formation on membrane surface. EPS structure with heterogeneous and varying nature tends to create a highly hydrated gel layer in which cells are embedded, resulting in the formation of a strong barrier to permeate flux during membrane filtration. After this, some organics deposited on the membrane surface can serve as nutrient source to facilitate the biofilm growth and enlargement. Many investigations have been conducted to illustrate the significant role of EPS in membrane fouling (Ahmed et al. 2007, Jinhua et al. 2006). The SMP have been described as soluble cellular components that are released during cell lysis, diffuse through cell membrane, are lost during synthesis or excretion (Laspidou and Rittmann 2002, Li et al. 2004). In MBR, substrates in feed also account for SMP formation. During membrane filtration, SMP could block the membrane pores, and also contribute to the formation of gel layer structure, and provide nutrients for further biofilm growth (Rosenberger et al. 2005). These imply that SMP may be involved in membrane fouling development (Lyko et al. 2007, Lyko et al. 2008).

Operating conditions

Aeration in an aerobic MBR can generate scouring force that may slow down the development of membrane fouling. High aeration intensity is useful for removing foulants from membrane surface, but it may also result in deflocculation microbial flocs and more SMP produced. At vigorous aeration, fouling formation would be predominated by the deposition of colloids and solutes (Fan and Zhou 2007). Therefore, in MBR, aeration rate has complicated influences on system operation and fouling control. On the other hand, solid retention time (SRT) also play an important role controlling fouling propensity in MBR. In general, higher

MLSS concentration can be achieved at longer SRT, leading to lower food to microorganisms (F/M) ratio, though it is not necessary to enhance fouling. However, extreme low SRT was found to reduce the MBR performance. It was reported that when SRT was shortened from 10 days to 2 days, fouling rate was found to increase by 10 times (Trussell et al. 2006).

Feed characteristics

Feed characteristics also exert impacts on fouling formation. The minerals, such as Mg, Al, Ca and Fe, were found to be enriched in membrane fouling layer, which originated from influent wastewater, and their interactions with biopolymers would significantly affect the characteristics of fouling layer (Choo and Lee 1996, Lin et al. 2011). Additionally, hydraulic retention time (HRT) not only dominates microbial growth and decay via changing F/M value, but also affects bound EPS production. Thus, its effect on membrane fouling development could not be ignored as well.

Membrane characteristics

Membrane characteristics including membrane materials, membrane configuration, membrane pore size, and hydrophobicity all affect membrane fouling development by the direct interactions with various types of foulants. For example, if the pore size is smaller than typical biomass filtrated, microbial deposition on membrane and subsequent cake layer formation would be expected. Hydrophobic membrane could cause server fouling than hydrophilic membrane due to the strong attractive interaction between biomass, membrane and solutes in MBR. Extensive research had been focused on potential impacts of membrane characteristics on fouling development (Chang et al. 2002, Le-Clech et al. 2005, Madaeni et al. 1999, Scott et al. 1998), but it appears that membrane characteristics would not be considered as the major fouling contributor in MBR.

2.2 MEMBRANE CLEANING IN MBR

2.2.1 Physical cleaning

As illustrated in **Figure 2.4**, physical cleaning has been commonly applied for eliminating removable fouling, whereas chemical cleaning has been shown to be effective in removing colloids, solutes and cells on membrane surfaces and embedded in membrane pores. In general, physical cleaning methods include air scouring, membrane backwashing (i.e. permeate pumped back into membrane in the reverse to filtration direction) and membrane relaxation (i.e. intermittent filtration). These, as standard maintenance strategies for fouling control, have been widely practiced in large-scale MBR operation.

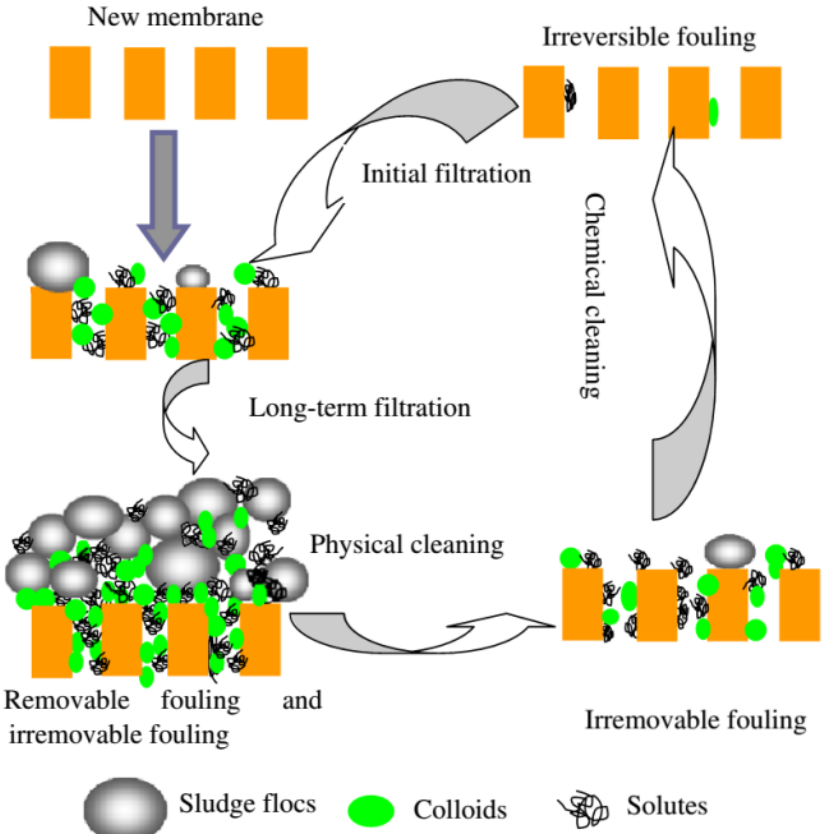

Figure 2.4 Schematics illustration of physical and chemical cleaning in MBR (Meng et al. 2009).

Physical cleaning via aeration has been widely employed in MBR. Aeration can serve as source of dissolved oxygen for microbial growth, mixing power and

scouring force along the membrane surface. Obviously, increasing aeration intensity is better for membrane cleaning, but at the cost of high energy consumption in MBR. For example, membrane cleaning efficiency was significantly improved by increasing biogas sparing intensity from 0.17 to 0.4 $m^3/(m^2h)$ in MBR (Robles et al. 2013). Meanwhile, the properties of air bubbles from aeration may also influence physical cleaning efficiency. During membrane cleaning of hollow fibre membranes in MBR, Çulfaz et al. (2011) observed that large and cap-shaped bubbles were more efficient than small ones. Similarly, Yamanoi and Kageyama (2010) reported that compared with smaller bubbles, higher shear stress was produced by larger bubbles with two-dimensional amorphous shapes between the membranes. On the contrary, an investigation by Sofia et al. (2004) showed that aeration with smaller bubbles seemed more effective in cleaning membrane in comparison to coarse bubbles in MBR. These results indicate that cleaning efficiency is only determined by bubble-size or bubble-shape, which is also influenced by many other factors, such as the geometry of membrane module, sludge concentration, bubble flow velocity, aeration diffuser etc. It should be noted that computational fluid dynamics (CFD) modelling has been employed to optimize aeration-based physical cleaning in MBR (Wang et al. 2014b, Wei et al. 2013).

It is well accepted that membrane backwashing can effectively wipe out foulants blocking pores and partially dislodge cake layer from membrane surface, while it is worth noting that backwashing is not applicable for commercialized flat-sheet membranes in view of membrane structures, except for several backwashable types, such as ceramic membrane and A3 Water Solutions FS membrane (Alnaizy et al. 2012, Doyen et al. 2010, Grélot et al. 2009). The key parameters in the design of backwashing include frequency, duration and flux of backwash. Robles et al. (2012) reported that the backwash frequency was affected by MLSS, whereas Hashino et al. (2011) showed that membrane with larger surface roughness had higher flux recovery after backwashing. Monitoring TMP change can provide useful information for optimizing backwashing process. The backwash initiation could be automatically adjusted based on the real-time

TMP values. In this case, the pre-set TMP point would be crucial for determining backwash efficiency. It had been suggested that the best TMP set-point should be 28-36 kPa at a constant flux of 35 L/(m^2h) and MLSS concentration of 10.1 g/L. When this point was reached, the backwashing should be conducted in order to keep both backwashing and filtration processes efficient (Villarroel et al. 2013). Similarly, backwash duration also can be optimized via TMP control. A generic control approach has been developed for determining when to stop backwashing process, i.e. when the TMP value does not further decrease within 5 s, backwashing should be finally ceased, which led to 25% of water saving (Smith et al. 2005). Generally, backwash flux is preset according to operation experience. The common backwash flux adopted is around 1-3 times higher than permeability flux for hollow fibre membranes. For example, the backwash flux may range from 25 L/(m^2 h) to 40 L/(m^2 h) at the permeate flux of 10-30 L/(m^2 h) (Jiang et al. 2005, Metzger et al. 2007, Wu et al. 2008b, Zsirai et al. 2012), even though much higher backwash flux was also applied in several cleaning scenarios (Hwang et al. 2009, Ivanovic and Leiknes 2008, Smith et al. 2005).

Membrane relaxation refers to a non-continuous operation during membrane filtration. Under relaxation, foulants attached on membrane would diffuse and be transported away from membrane surface through the existing concentration gradient. Obviously, such an intermittent operation can help to reduce membrane fouling and improve filtration performance with the benefits of water saving, less bakwashing frequency etc (Le-Clech et al. 2006, Wu et al. 2008a). Various relaxation/filtration durations had been applied in MBR systems (**Table 2.2)**. In general, it can be seen that after every 7-15 min filtration, 0.5-5 min relaxation should be initiated for aerobic MBR (AeMBR), whereas 0.5-2 min relaxation for anaerobic MBR (AnMBR) after 4-10 min filtration. More frequent relaxation adopted in AnMBR is the result of different fouling structures developed on membrane under anaerobic condition. Moreover, the fouling removal can be significantly enhanced if relaxation is combined with backwashing, e.g. the effective membrane cleaning was achieved in AnMBR operated at a 0.5 min relaxation/1 min backwahing after every 10 min filtration (Martinez-Sosa et al.

2011). Although detailed investigations involved in relaxaion demonstrated the fouling rate of intermitent filtraion was generally higher than continuous operation mode, relaxation could only allow filtraion to be stable for a longer operational period before cleaning conducted (Ng et al. 2005). There were also some reports to demonstrate this kind of operation was not ecomonically feasible for large-scale MBR (Hong et al. 2002), annd further cost analysis is also required to obtain a optimum method for fouling mitigation.

Table 2.2 Summary of filtration/relaxation duration applied in MBR (Wang et al. 2014b).

MBR type	Filtration duration (min)	Relaxation duration (min)	Scale	Reference
AeMBR	7-12	0.63-3	Full-scale	(Zsirai et al. 2012)
AeMBR	3.7-7.3	0.33-0.67	Lab-scale	(Wu et al. 2008a)
AeMBR	45	15	Lab-scale	(Hong et al. 2002)
AeMBR	10-15	5	Lab-scale	(Albasi et al. 2002)
AeMBR	8-15	1-8	Pilot-scale	(Gui et al. 2003)
AeMBR	4	1	Pilot-scale	(Santasmasas et al. 2013)
AeMBR	8	4	Lab-scale	(Chua et al. 2002)
AeMBR	10	2	Pilot-scale	(Ma et al. 2013)
AeMBR	8	2	Pilot-scale	(Santasmasas et al. 2013)
AeMBR	9	1.5	Full-scale	(Itokawa et al. 2008)
AnMBR	8	2	Lab-scale	(Huang et al. 2008)
AnMBR	4	1	Lab-scale	(Lin et al. 2010)
AnMBR	10	0.5	Pilot-scale	(Martinez-Sosa et al. 2011)
AnMBR	4.2	0.83	Pilot-scale	(Robles et al. 2013)
AnMBR	7	0.33	Lab-scale	(Tran et al. 2013)
AnMBR	4	1	Lab-scale	(Wen et al. 1999)
AnMBR	4	1	Lab-scale	(Ceron-Vivas et al. 2012)

2.2.2 Chemical cleaning

After a long-term operation of MBR, the efficacy of physical cleaning may become ineffective since more irremovable foulants were accumulated on membrane surface. In this case, chemical cleaning with various regents has been adopted to clean membrane by removing foulants which cannot be eliminated by physical cleaning alone. According to Porcelli and Judd (2010), traditional off-line chemical cleaning of membrane is a six-step process: (i) bulk reaction; (ii) bulk transport to fouling layer; (iii) transport into fouling layer; (iv) reaction with foulants; (v) transfer of modified foulants to solution and (vi) transport of waste foulants to bulk solution (**Figure 2.5**). Obviously, membrane cleaning efficacy is dependent on reagent reaction rate, back transport rate, reaction rate between foulants and reagent, etc.

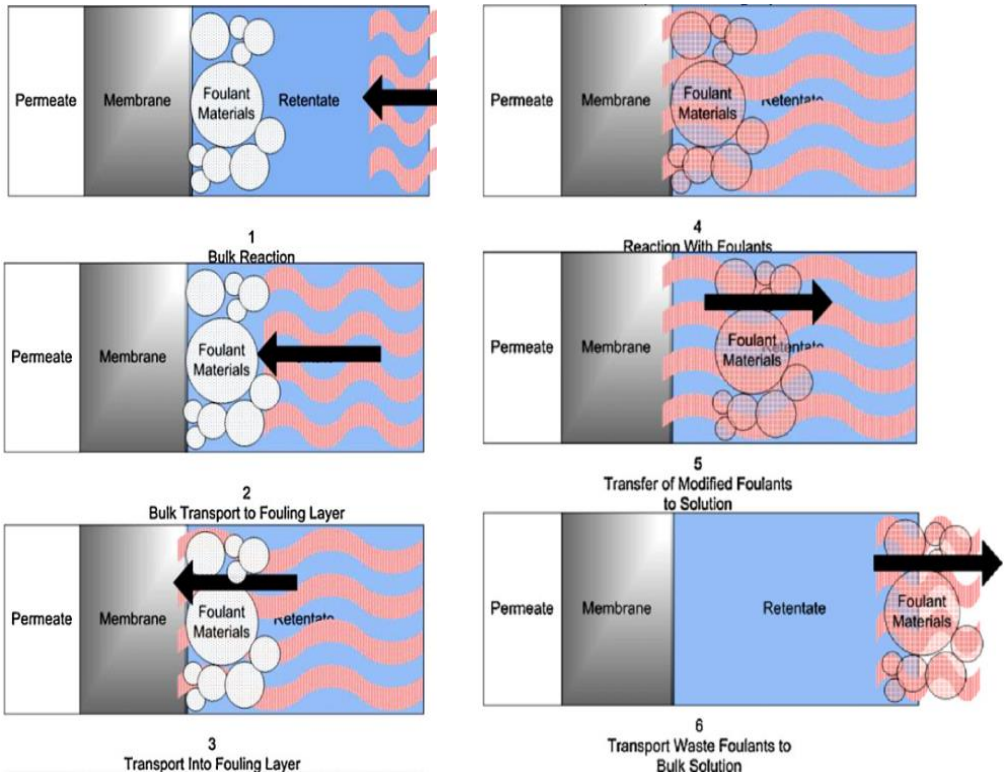

Figure 2.5 Schematics of off-line membrane chemical cleaning steps (Porcelli and Judd 2010).

In general, chemical cleaning regents can be classified as acid, base, oxidant and others. In practice, several chemical have often been jointly utilized to remove the complex fouling constituents including inorganic, organic and microbial species. Detail chemical cleaning mechanisms with four types of reagents are illustrated in **Figure 2.6**.

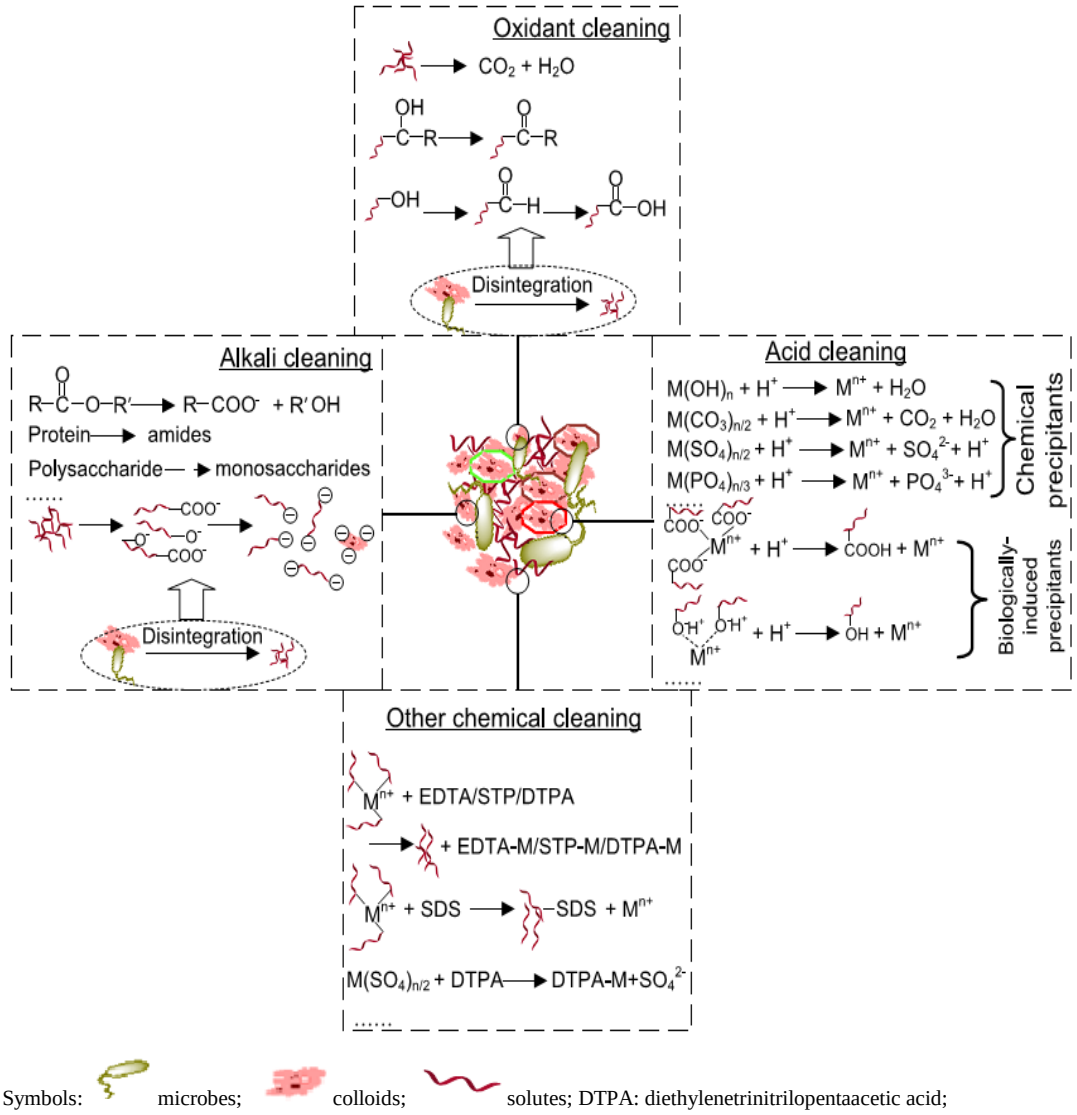

Figure 2.6 Mechanisms of chemical cleaning with acids, bases, oxidants and other chemicals (Wang et al. 2014b).

Acid Cleaning

Acids can remove inorganic foulants caused by chemical and biological precipitation, and acid cleaning is often achieved by neutralization and double degradation of foulants, such as metal hydroxides and hardness salts. The widely used acids for membrane cleaning include hydrochloric acid (HCl), sulfuric acid (H_2SO_4), oxalic acid, citric acid, nitric acid, and phosphoric acid (H_3PO_4). Among which, both HCl and H_2SO_4 have been most commonly used due to their low cost and strong functions to solubilize deposits, while use of citric acid with buffering and chelation abilities, can avoid the membrane damage associated with sudden pH change. Combined with NaClO, citric acid has been considered as the most widely used cleaning reagent for microfiltration (MF) and ultrafiltration (UF) membranes. Although H_3PO_4 also possesses buffering and chelating functions for eliminating inorganic scale, use of H_3PO_4 in MF and UF membrane systems were not commonly reported except for several industrial membrane systems (Al-Amoudi and Lovitt 2007).

Alkali Cleaning

Caustic conditions have been known to be necessary for removing organic foulants from membrane surface. As illustrated in **Figure 2.6**, large organic particles can be disintegrated into small size or soluble matters under strong alkaline condition. More importantly, proteins and polysaccharides deposited on membrane surface can be decomposed by alkaline to small molecules like amides and monosaccharides, while oils and fats may be saponified to soluble soap micelles. For example, at pH 11, the functional groups of organic substances were deprotonated and became negatively charged (Ang et al. 2011, Lee and Elimelech 2006). To a certain degree, the repulsive forces among organic foulants eventually leads to a loosen cake layer which can be easily removed from membrane surface. In practice, sodium hydroxide (NaOH) is the most commonly used alkaline for membrane cleaning, which is capable of removing more protein-related foulants than carbohydrates (Kimura et al. 2013). It should be noted that NaOH is not helpful for mitigating metals-associated membrane fouling, like inorganic fouling (Mo et al. 2010).

Oxidant Cleaning

During MBR cleaning, oxidants are commonly applied to oxidize organic and biological foulants. The primary mechanism of oxidant cleaning is to convert functional groups of organic matters into ketonic, aldehydic, and carboxylic groups with high hydrophilicity, which allows them to mitigate away from membrane surface. Oxidants are also able to disassemble sludge flocs and colloids into fine particles or soluble matters (Lee et al. 2013). After membrane cleaning by oxidant, organic matters on membrane surface tend to be more susceptible to further hydrolysis at high pH. This suggest the efficacy of combined membrane cleaning by mixed oxidant and base. Evidence shows that alkali could loosen the structure of fouling layer, and further facilitate the penetration of oxidant to membrane surface, such as chlorine (Liu et al. 2001). The widely used oxidants for membrane cleaning include sodium hypochlorite (NaClO) and hydrogen peroxide (H_2O_2), while the former is by far the most commonly used in industrial practice. Compared to H_2O_2, NaClO is able to more efficiently remove organic matters from NOM-fouled PES membrane (Strugholtz et al. 2005). Nevertheless, membrane cleaning with NaClO also has the following drawbacks: (i) some types membranes are not chlorine-tolerant and frequent contact with NaClO causes membrane surface/structure swelling and damage (Cheryan 1998, Zeman and Zydney 1996); (ii) many chlorinated organics like organic halogen (AOX) and trihalomethanes (THMs) may be generated, which in turn pose serious concerns on their potential impacts on the environment and public health (Grelot et al. 2008, Krause et al. 2010).

Other chemical cleaning

Other cleaning chemicals basically include surfactants and metal chelating agents. Surfactants (e.g. sodium dodecyl sulfate) as well as other detergents with amphiphilic property exhibit both hydrophilic and hydrophobic characteristics which favour fouling removal from membrane surface in MBR. The hydrophobic tails of surfactants tend to adsorb onto organic foulants, while hydrophilic heads to bind with water. As a result, the foulant-metal ion binding can be weakened or

even broken up. The metal chelating cleaning chemicals, such as ethylene diamine tetraacetic acid (EDTA), diethylenetrinitrilopentaacetic acid (DTPA), sodium tripolyphosphate (STP) have a strong ability of binding with metal ions, while displacing organics in metal-biopolymer complex through a ligand exchange reaction. In this way, the bonding bridges in organics and between membrane and organics could be weaken or even broken-up, leading to loosen cake layer structures (Li and Elimelech 2004).

2.2.3 Biological cleaning

Biological antifouling agents have been explored for membrane fouling control, but still at the developmental stage. Biological cleaning technologies, such as enzymatic cleaning, energy uncoupling, quorum quenching and bacteriophage have been investigated for biofilm control, which also have potential for cleaning of biologically fouled membrane, or as a preventive approach.

Enzymatic cleaning

Among the existing biological cleaning approaches, enzymatic cleaning is the most commonly used (Chen and Columbia 2011, Petrus et al. 2008, Yu et al. 2010). Enzyme with high specificity for a certain type of biopolymer generally exhibits extremely high degradation efficacy, e.g. protein-like organics can be disintegrated by proteases, and humic acid-associated foulants often catalysed by amylase (Yu et al. 2010). Moreover, alginate as a typical polysaccharide can be depolymerized by a specific alginate lyase (Chen and Columbia 2011). Proteins have been identified as a major constituent in most membrane biofouling. As such, protease has been extensively explored for biofouling control (Allie et al. 2003, Argüello et al. 2003, 2005, Te Poele and Van der Graaf 2005). It is obvious that enzymatic cleaning has the advantages over chemical cleaning, such as reduced usage of strong chemicals, no generation of secondary pollutants etc., all of which triggered an interest in investigating enzymatic agents as substituents for traditional chemical cleaner. However, it should be realized that application

of enzymatic cleaning at large scale is still limited by its high cost, low activity and inefficiency in removing mixed-culture microbes.

Energy uncoupling

Energy uncoupling has been proposed as a novel antifouling method to inhibit biofilm formation on membrane. Many compounds known as uncouplers may inhibit ATP synthesis via carrying protons through cellular membrane and dissipating proton gradient. They are commonly weak organic acids and are permeable to cellular membrane. Xu and Liu (2010) reported that uncouplers could effectively affect the biofilm stability and potentially led to disintegration of biofilm by disrupting microbial energy metabolism. In addition, it is worth noting that the microbial activities such as EPS secretion also require ATP synthesis (Wang et al. 2013b), which indicates disruption of cellular energy balance should perform as an effective way to mitigate biofouling.

Quorum quenching

Quorum sensing has been known to coordinate biofilm formation on a solid surface, including membrane (Khor et al. 2007, Yeon et al. 2008). Quorum quenching is a process where production of signalling molecules are inhibited, by which the formation of biofilm could be prevented. This sugests that quorun quencing offers another biological mean for mitigating membrane fouling. However, it should be noted that this approach is ineffective when inorganic foulants or biopolymers-associated organic fouling are concerned in MBR.

Bacteriophage

Bacteriophage are able to destroy bacteria and has been shown to be effective in removing biofilms (Lu and Collins 2007). By operation an ultrafiltration continuous recycled system with three species of *Pseudomonas aeruginosa*, *Acinetobacter johnsonii* and *Bacillus subtilis* with addition of phages, Goldman et al. (2009) found membrane fouling was reduced by more than 40% due to the seeded phages lytic activity. However, probably due to the safety concern, application of *bacteriophage* for membrane biofouling control is still very limited.

2.3 ON-LINE CHEMICAL CLEANING IN MBR

2.3.1 On-line and off-line cleaning

On-line (in-situ) and off-line (ex-situ) cleaning describe whether or not membrane module remains in MBR during cleaning process. As illustrated in **Figure 2.7**, on-line cleaning includes various cleaning methods, e.g., backwashing, chemical enhanced backwash (CEB), cleaning in place (CIP), cleaning in air (CIA) and recovery cleaning, among which CEB and CIP are considered in situ membrane cleaning without draining the bioreactor tank, whereas CIA needs to be done in a drained tank. Moreover, off-line cleaning is designated to take membrane modules out of the bioreactor for deep washing via a series of physical and chemical cleanings. Compared with off-line mode, on-line cleaning is generally preferred due to its relatively lower cost and much simpler operation. However, the cleaning interval for on-line cleaning is normally much shorter than that of off-line mode, e.g. several weeks to months for on-line cleaning and one to three years for off-line cleaning (Brepols et al. 2008, Judd 2010).

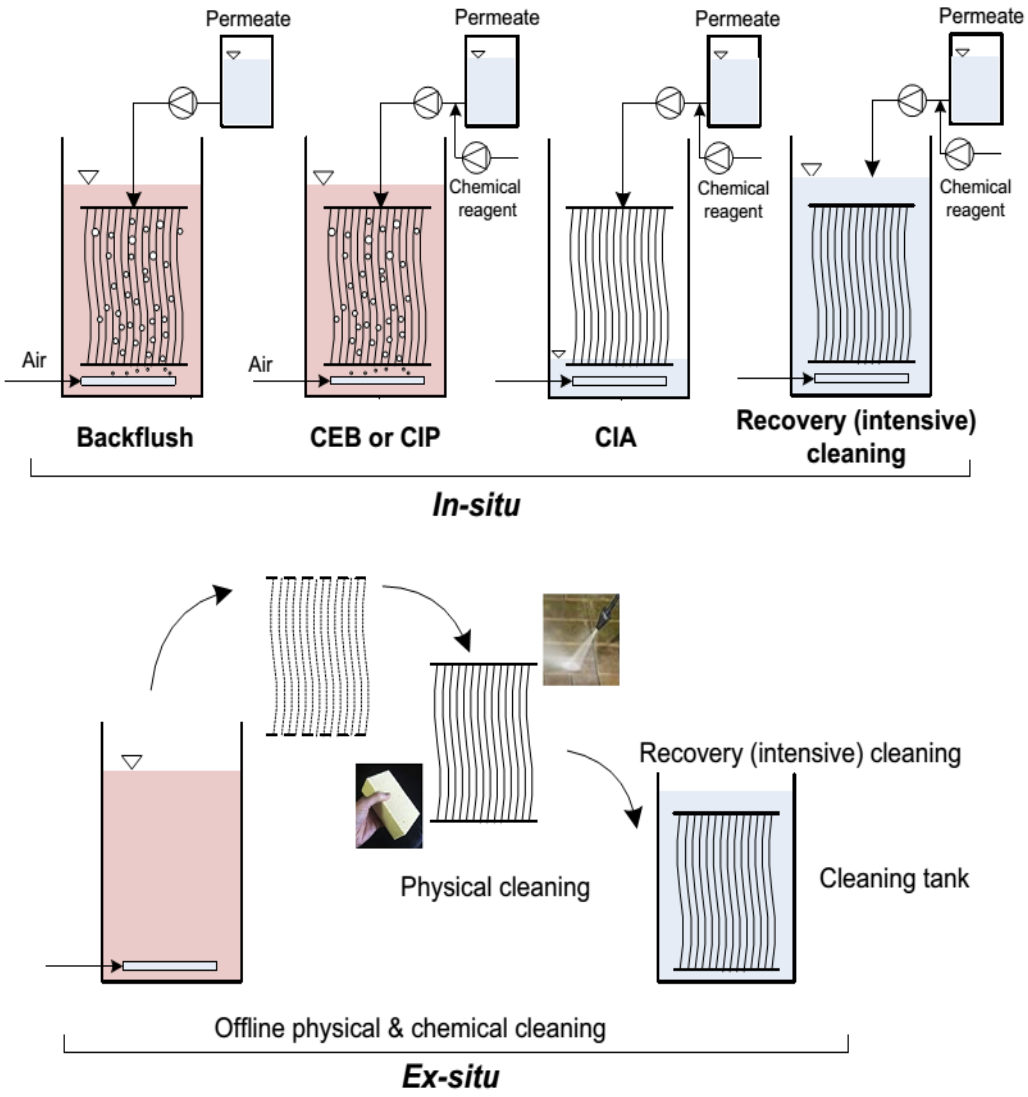

Figure 2.7 Schematic illustration of on-line and off-line membrane cleaning process in MBR (Wang et al. 2014b).

2.3.2 On-line chemical cleaning operation

Based on different cleaning intensities, on-line chemical cleaning protocol involves CEB, CIP and recovery cleaning. CEB is usually carried out if the physical cleaning is no longer effective for eliminating membrane fouling. During CEB, a relative lower concentration of chemical reagents is added into backwash water to flush the membrane in the reverse direction to filtration on a daily basis. CIP refers to on-line membrane cleaning by using higher concentration reagent without draining the bioreactor. Both CEB and CIP have

been recognized as a maintenance cleaning process. On the other hand, recovery cleaning allows soaking of membrane modules in a drained reactor filled with an extremely high concentration of cleaning agents, in on-line or off-line mode. It needs to be conducted when membrane filtration can no longer continue due to the decreased permeability.

CIP and CEB are often conducted to maintain a constant permeate flux and reduce the frequency of recovery cleaning. However, on-line chemical cleaning similar to physical backwashing cannot be employed for most commercialized flat-sheet membranes due to the membrane structures (Judd 2010), while in some cases CIP or CEB have also been applied for flat-sheet membranes as illustrated in **Figure 2.8**. Different from hollow fibre membrane, during on-line cleaning of flat-sheet membrane, the cleaning chemical is fed into membrane for a period of time (1-2 h) via a relatively low water head (Wang et al. 2014b). After soaking, the MBR operation restarts again and the residual chemical reagents can be flushed out together with the filtrated effluent. However, with the rapid development of membrane fabrication, many backwashable flat-sheet membranes are available in the market and have been successfully applied in MBR systems that could be cleaned with the same protocol as hollow fibre membrane (Alnaizy et al. 2012, Doyen et al. 2010, Grélot et al. 2009).

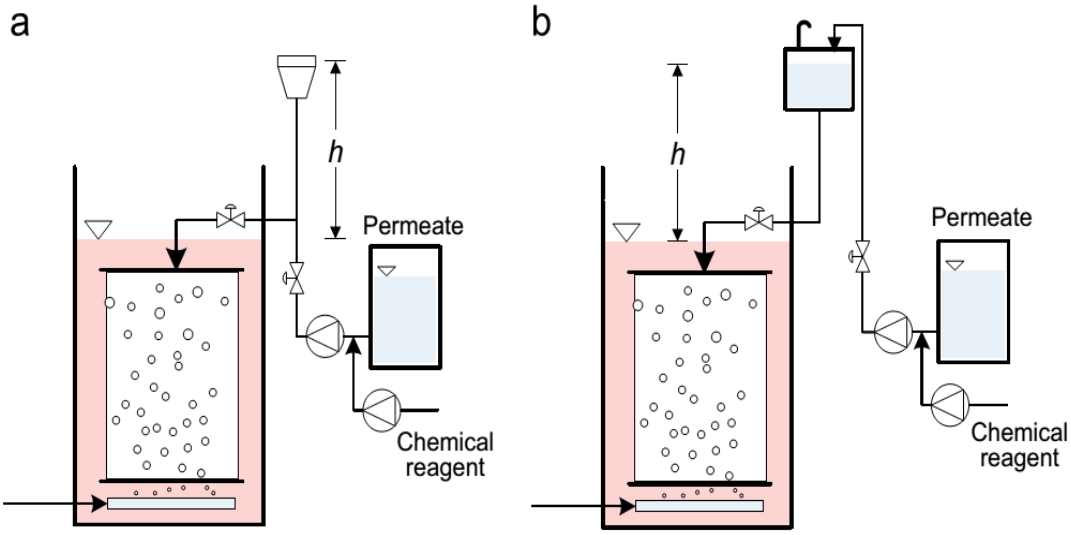

Figure 2.8 Schematics of on-line chemical cleaning for non-backwashable flat-sheet membranes. (a) pumping system with cleaning pipe open to air; (b) cleaning system with elevated tank. (Wang et al. 2014b).

So far, more and more full-scale MBRs have adopted on-line chemical cleaning as an effective method to maintain the system operation. As summarized in **Table 2.3**, on-line chemical cleaning primarily requires frequent cleaning and short cleaning intervals (approximately 3-120 d) compared with the off-line mode. The membrane soaking duration largely ranges from 0.5-4.5 h. In terms of the chemical reagents, NaClO combined with critic acid or NaOH has been commonly used in most cleaning systems. **Table 2.3** shows that various chemical reagent concentrations used in maintenance cleaning of membrane. It can be seen that the concentration of NaClO normally is in the range of 200-2000 mg/L, and the commonly applied concentrations for NaOH and citric acid are 0.1-2 wt% and 0.2-1.5 wt%, respectively. In fact, chemical concentration, reaction time as well as cleaning frequency should be adjusted and recombined according to the practical fouling conditions in order to achieve an optimal cleaning performance. Furthermore, it is worth pointing out that different membranes may require different chemical concentrations. As shown in **Table 2.3**, cleaning of flat sheet membranes seems to need higher NaClO concentration of 2000-5000 mg/L compared with 100-3000 mg/L NaClO for hollow fibre membranes, whereas the cleaning interval of flat sheet membrane (e.g. 60-120 d) is much longer than that of hollow fibre membranes (e.g. 3-30 d).

Table 2.3 On-line chemical cleaning protocols applied in MBR (Itokawa et al. 2008, Judd 2010, Wang et al. 2014b).

Membrane type	Maintenance cleaning protocol
Flat Sheet	5000 mg/L NaClO every 2-4 months for 2 h followed by 300 mg/L acid soaking in some plants
Flat Sheet	Maintenance cleaning performed every 3–4 months and dilute HCl every 2–3 months for struvite removal
Flat Sheet	0.5 wt% NaClO 6 times a month for 3 h supplemented with 0.1 wt% NaOH twice a year

Flat Sheet	2000-5000 mg/L NaClO and 5000 mg/L citric acid for 4-5 times every year
Hollow Fibre	1000-1500 mg/L NaClO every 3-7 d and 3000 mg/L NaClO every month for 0.5-2 h (supplemented with a quarterly 1-1.5 wt% citric acid cleaning in some plants)
Hollow Fibre	A weekly 500 mg/L hypochlorite and 0.2 wt% citric acid each for 0.75-1 h
Hollow Fibre	200 mg/L hypochlorite every 10 d supplemented by 2000 mg/L citric acid every 20 d
Hollow Fibre	100-200 mg/L NaClO every 3-7 d for 1 h
Hollow Fibre	200-800 mg/L NaClO with 2500-3200 mg/L citric acid once a week or two weeks
Hollow Fibre	500 mg/L NaClO weekly, 3000 mg/L NaClO monthly and a quarterly 1.5 wt% citric acid cleaning (each for 2-3 h)
Hollow Fibre	3000 mg/L NaClO for 1.5 h
Hollow Fibre	200-500 mg/L NaClO for 1.5-3 h every 10-30 d
Hollow Fibre	A weekly 500-3000 mg/L NaClO for 2 h supplemented by a quarterly cleaning with 1 wt% citric acid for 2 h
Hollow Fibre	2 wt% NaOH and 3000 mg/L NaClO for 2 h monthly
Hollow Fibre	2000 mg/L NaClO for 2 h every 2 weeks
Hollow Fibre	2500 mg/L H_2O_2 and 2000 mg/L citric acid/phosphoric acid every 2 weeks
Hollow Fibre	A weekly 1000 mg/L NaClO for 4.5 h supplemented with citric acid cleaning at pH=3
Hollow Fibre	300 mg/L NaClO for 0.5-1 h twice a month
Hollow Fibre	1000 mg/L NaClO for 1.5 h once every two weeks

2.3.3 Impacts of on-line chemical cleaning with NaClO on MBR system

At present, NaClO has been considered as the most extensively used cleaning chemical for mitigating removable and irremovable fouling in MBR. And the effectiveness of other reagents is always examined by comparing with that of NaClO. The primary advantage of NaClO is its excellent cleaning effectiveness with low cost, and NaClO also can be easily combined with other reagent to achieve better cleaning performance. For example, NaClO can effectively remove biofilms from various solid surfaces, which consist of proteins,

polysaccharides, microbial cells etc (Fukuzaki 2006). However, during on-line chemical cleaning, inevitable contact of NaClO with membranes and microorganisms may also lead to various impacts on MBR system.

Impacts on membrane integrity

Inevitable contact between membrane and chemical agents occur during on-line or off-line cleaning. Numerous investigations have been conducted to explore the potential impacts of NaClO on different types of membranes (Abdullah and Berube 2013, Arkhangelsky et al. 2007, Do et al. 2012a, b, Regula et al. 2013, Rouaix et al. 2006, Vanysacker et al. 2014, Wang et al. 2010). Abdullah and Berube (2013) conducted an investigation to assess the effects of NaClO on polyvinylidene fluoride (PVDF) based membrane, and showed that NaClO was significantly detrimental to membrane structure. As shown in **Figure 2.9**, increased porosity and nominal pore size were observed after the exposure of commercial PVDF membranes to NaClO with various dosages, which in turn would affect membrane yield and strength as well. Similarly, Vanysacker et al. (2014) found that the membrane pore size and surface porosity were increased in three kinds of membranes (PVDF, polyethylene, polysulfone) treated by 1% NaClO and 2% citric acid, whereas membrane hydrophobicity and membrane surface chemistry remained unaffected. Arkhangelsky et al. (2007) reported that the mechanical strength of ultrafiltration membrane in terms of elongation and elasticity could be damaged upon NaClO cleaning via gradual breaking-up of O-C-O and C-S bonds, and more deterioration was observed in cellulose acetate (CA) membranes compared with polyethersulfone (PES) membranes (**Figure 2.10**). However, Wang et al. (2010) did not observe apparent changes to the chemical structure of PVDF membranes except for the surface properties during chemical cleaning of a pilot-scale MBR.

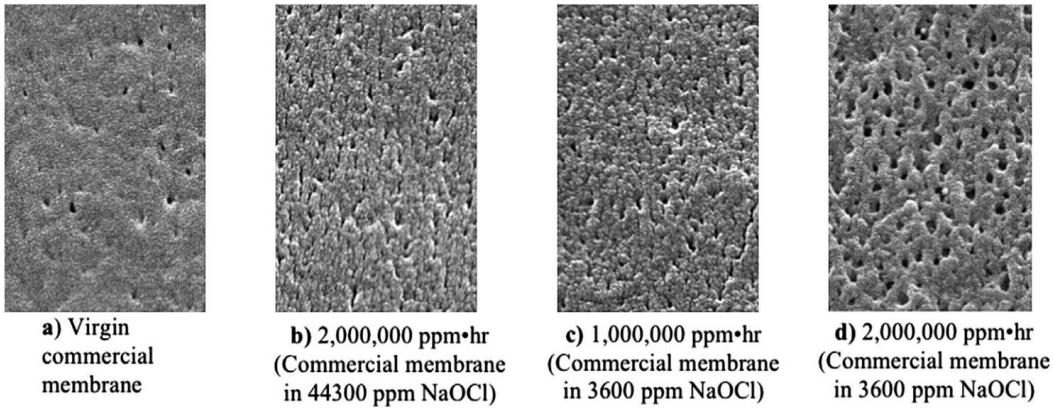

Figure 2.9 SEM images of (a) virgin PVDF membrane and (b, c, d) treated PVDF membranes after exposure to various NaClO dosages (Abdullah and Berube 2013).

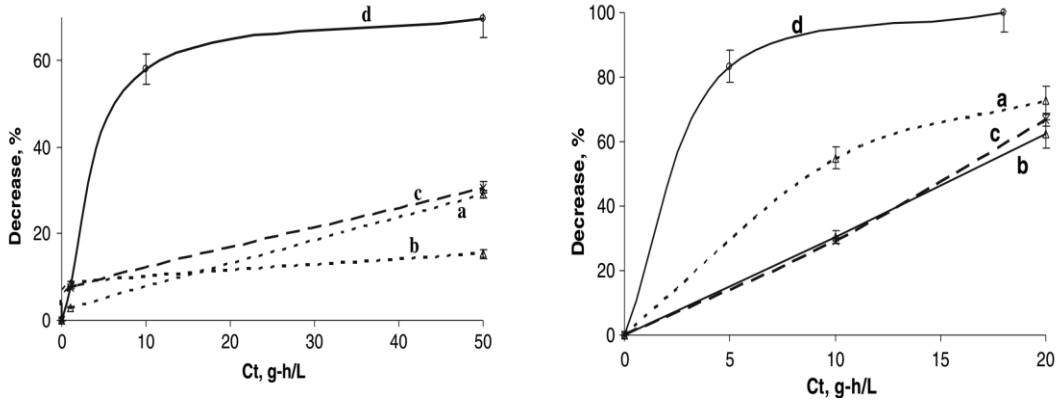

Figure 2.10 Decrease in mechanical strengths of (a) PES membrane and (b) CA membrane. a, b, c represents ultimate tensile strength, elongation and Young's modulus, respectively; d stands for (a) C-S and (b) O-C-O absorbance peak intensities (Arkhangelsky et al. 2007).

Furthermore, both chemical dose and cleaning duration significantly affect membrane integrity, and a higher reagent concentration and a longer reaction duration would eventually aggravate membrane damage. However, Regula et al. (2013) argued that the commonly used applied concentration × time (*Ct*) relationship could not reasonably predict the imposed damages on membrane by chemical cleaning, while it had been suggested that the impact of chemical cleaning with NaClO on membrane was correlated to $C^n t$ instead of *Ct* (Abdullah

and Berube, 2013). If the power *n* is smaller than 1, the effect of chemical concentration on membrane characteristics is less than the exposure duration (i.e. t).

Impacts on microbial characteristics

During on-line chemical cleaning, NaClO is brought into membrane from the permeate side and subsequently into the suspended mixed liquor in MBR. Therefore, the effect of residual NaClO on microorganisms cannot be ignored. However, up to date, little information is currently available on microbial responses to on-line chemical cleaning with NaClO in the literature.

Lee et al. (2013) carried out batch experiments to evaluate the effect of NaClO on activated sludge and found that the average floc size decreased from 43.6 μm to 26.7 μm at 5 mg NaClO/g MLSS, and the produced polysaccharides in EPS was increased by 1.5 times compared with that observed at 1 mg NaClO/g MLSS. Moreover, serious foaming and cellular lysis occurred at the NaClO dosage of 55 mg NaClO/g MLSS, while organic removal and nitrification were negatively affected. In addition, Wu et al. (2007) also reported that CIP with 0.5% NaClO for 2 h soaking significantly influenced the microbial activity in terms of specific dehydrogenases activity (SDA) in MBR, which in turn affected organic removal. After CIP, it took 5 days before SDA restored to normal value. It had been found that the dominant microbial species in biofilms were greatly affected after chemical cleaning with NaClO, and most survived bacteria in treated biofilms were found to belong to the relatives of extremophiles, especially halotolerant or halophilic species (Navarro et al. 2016).

Impacts on membrane performance

So far, little attention has been paid to the re-development of membrane fouling after chemical cleaning, and only some hints can be found after the analysis of literature data. After a consecutive CEB with NaClO, NaOH and citric acid in a lab-scale MBR, as shown in **Figure 2.11,** the gradual decreases of recovered flux and cleaning interval between were observed, suggesting that chemical cleaning

seemed to enhance the fouling re-development probably due to the changes of membrane surface properties after chemical cleaning (Kweon et al. 2012). Moreover, Kuzmenko et al. (2005) also observed that cleaning with higher dosage of free chlorine could firstly result in complete restoration of membrane permeability, but subsequently led to more severe fouling formation by BSA in a long-term operation (**Figure 2.12**).

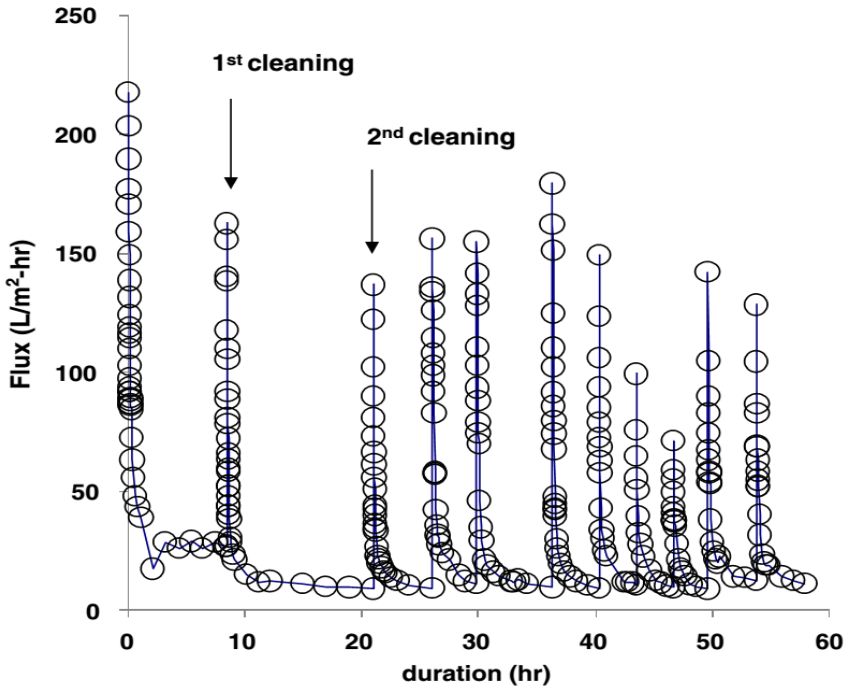

Figure 2.11 Flux decline behaviours in MBR (Kweon et al. 2012).

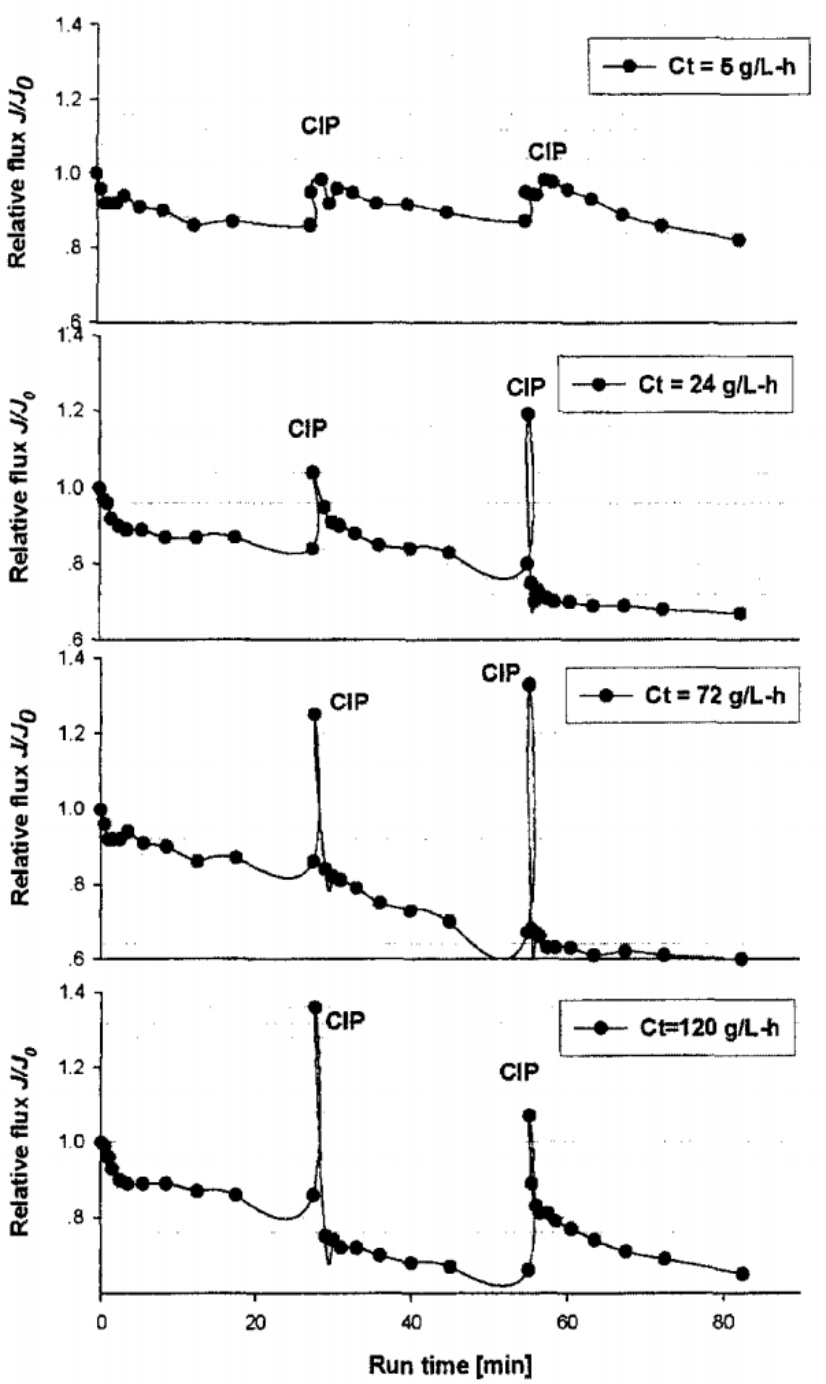

Figure 2.12 Relative flux of PES membranes cleaned by free chlorine at the dosages of 5 g h/L, 24 g h/L, 72 g h/L and 120 g h/L (Kuzmenko et al. 2005).

In a study of optimizing the NaClO-assisted CEB for controlling membrane fouling in a long-term operation of MBR, two identical lab-scale aerobic MBRs were operated with a pure water backwashing (MBR-A) and low-concentration NaClO backwashing (MBR-B), respectively (Wang et al. 2014c). The NaClO

concentrations of 0.5 ppm, 1.5 ppm, 0.05 ppm and 0.2 ppm were applied in sequential four runs, and the backwashing intervals for run II was 72 h, and 12 h for other three runs. As shown in **Figure 2.13**, in run II and run III, the MBR-B with NaClO backwashing had higher TMP increasing rate than MBR-A with water backwashing. The average TMP increase rates were 0.125 kPa/h for MBR-B and 0.055 kPa/h for MBR-A in run II, and 0.136 kPa/h for MBR-B and 0.102 kPa/h for MBR-A in run III. According to Wang et al. (2014c), the relatively low NaClO concentration (0.05 ppm) used in run III could kill some living bacteria, but was not able to effectively detach them from membrane surface, leading to the decrease in the ratio of living to dead cells with more production of biopolymers. This explained the higher fouling potential observed. However, these researchers failed to explain the similar fouling behaviors in run II with highest NaClO concentration. Similarily, Lee et al. (2013) als observed in a dead-end membrane system that the rising rate of membrane resistance was two-time higher at 5 mg NaClO/g MLSS than at 1 mg NaClO/g SS. Consequently, it is reasonable to consider that on-line chemical cleaning with NaClO in MBR may seriously influence membrane performance, and there is an urgent need to look into this issue in a more holistic manner.

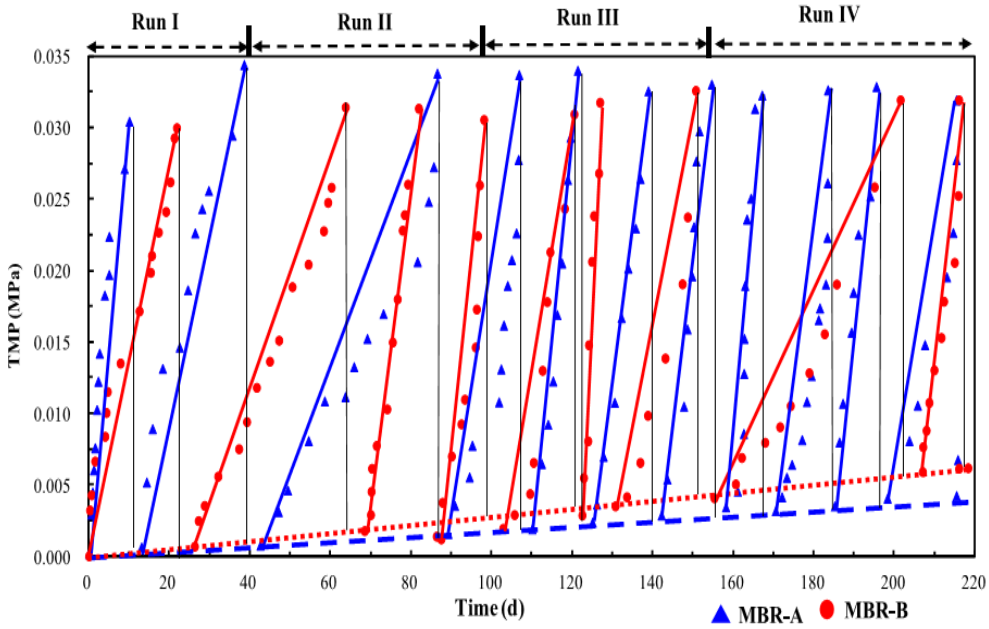

Figure 2.13 TMP profiles for two MBR systems during the long-term operation (Wang et al. 2014c).

2.4 SUMMARY

This review highlights the basic principles of membrane fouling and cleaning methods in MBR. Among the various cleaning approaches, on-line chemical cleaning with sodium hypochlorite is generally preferred due to its high effectiveness, simple operation and low cost. However, it can be expected that NaClO usage during on-line chemical cleaning may seriously influence microorganisms as well as membrane performance. This may open up a window to systemically explore the potential impacts of such prevalent practice on MBR operation.

CHAPTER 3 ENHANCED MEMBRANE BIOFOULING POTENTIAL BY ON-LINE CHEMICAL CLEANING WITH SODIUM HYPOCHLORITE IN MBR

3.1 INTRODUCTION

Membrane bioreactor (MBR) has gained increasing popularity in wastewater reclamation and reuse worldwide. However, the inherent membrane biofouling is the biggest challenge encountered in the operation of MBR, resulting in a significant flux decline and increased operation cost (Lee et al. 2012, Meng et al. 2009). Although several operation strategies including relaxation, backwashing, enzyme cleaning, etc. have been developed to mitigate or prevent membrane biofouling, chemical cleaning by sodium hypochlorite (NaClO) is still a major effective method for removing both reversible and irreversible membrane fouling in MBR process (Lee et al. 2013, Porcelli and Judd 2010, Wei et al. 2011). During the on-line chemical cleaning, cleaning agent, e.g. NaClO, is injected into membrane from the permeate side, while membrane modules are still soaking in bioreactor (Wang et al. 2014b). Compared to off-line cleaning, on-line cleaning is generally preferable due to its simplicity, low cost and effectiveness. Wei et al. (2011) found that on-line chemical cleaning with a combination of NaClO, NaOH and HCl could achieve nearly 100% permeability recovery rate during first several runs in a pilot-scale MBR. Kweon et al. (2012) also suggested water flux recovery could reach to approximately 100% during the first two cleaning in-place (CIP) runs when low turbidity feed water was used.

The content in this chapter has been published as: Cai, W. and Liu, Y. (2016). Enhanced membrane biofouling potential by on-line chemical cleaning in membrane bioreactor. J. Membr. Sci. 511, 84-91.

The principle of on-line chemical cleaning with NaClO is illustrated in **Figure 3.1**. When NaClO solution is fed into membrane, it firstly passes through membrane pores and reacts with the foulants on membrane surface. The residual effective NaClO ends up in bioreactor and tends to oxidize soluble organic matters and microorganisms presented in MBR. After cleaning finished, membrane filtration restarts accompanied by fouling development again. This suggests that membrane and microorganisms in MBR are both exposed to cleaning chemical (e.g. NaClO) in the course of on-line chemical cleaning. In fact, it has been well known that NaClO may impair the surface integrity of various types of polymeric membranes. For example, Puspitasari et al. (2010) conducted a series of continuous membrane cleaning studies and revealed that the surface modification substance on polyvinylidene fluoride (PVDF) membrane could be removed by NaClO, followed by membrane hydrophobicity increase and hydraulic resistance decline. Abdullah and Berube (2013) also showed exposure to NaClO could increase the porosity and nominal pore size of commercial membrane, while significantly reduced its yield strength and intrinsic resistance. Comparatively, the effects of NaClO on microbial properties were less reported. Lee et al. (2013) found the organic removal and nitrification performance in MBR were negatively affected by NaClO exposure, and serious foaming happened when 55 mg NaClO/g MLSS was applied in chemical enhanced backwashing (CEB). Moreover, the reduced microbial activity, degradation inhibition and cell lysis were also reported to occur during on-line chemical cleaning with various NaClO concentrations (Lim et al. 2005, Wu et al. 2007).

According to **Figure 3.1**, it is known that the bulk suspension in MBR is exposed to the residual NaClO during on-line chemical cleaning of membrane, and several studies described above suggested this exposure could affect microbial properties. However, little information has been currently available about possible responses of microorganisms to NaClO especially from the perspective of membrane biofouling re-development after cleaning since activated sludge exposed to chemical agent can partially revert back onto membrane surface as foulants when

membrane filtration restarts. Therefore, this study aims to investigate the impacts of on-line chemical cleaning with NaClO on microbial oxidation and subsequent biofouling behaviours. The results presented may offer different insights into the current practice of on-line chemical cleaning of membranes in MBR.

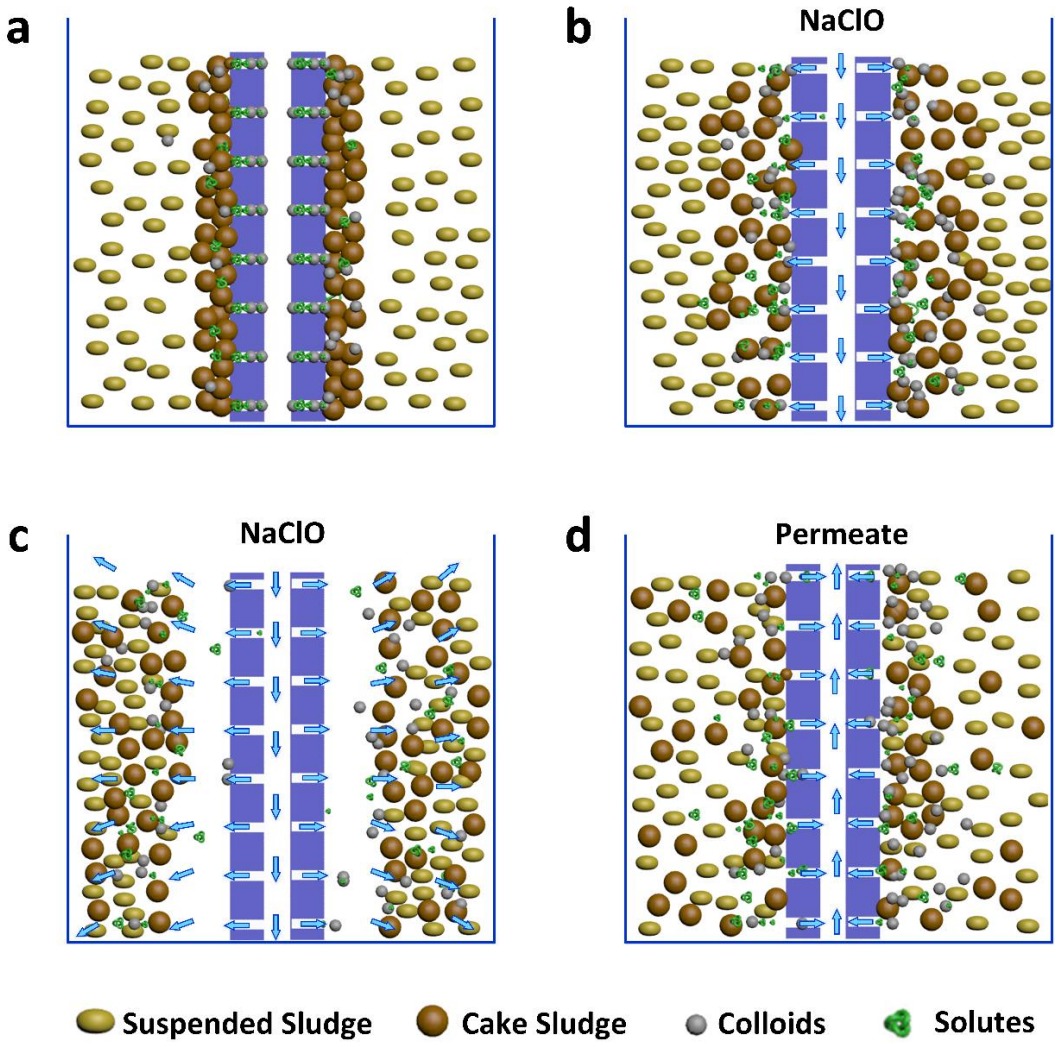

Figure 3.1 Schematic illustration of on-line chemical cleaning with NaClO.

3.2 MATERIALS AND METHODS

3.2.1 Sludge treatment assay

Activated sludge collected from a local wastewater treatment plant was acclimatized in a chemostat cultured with a synthetic substrate consisted of 690

mg/L of CH_3COOH, 313 mg/L glucose, 200 mg/L NH_4Cl, 60 mg/L K_2HPO_4 and other trace minerals for one month. The acclimated activated sludge was washed thrice with 10 mM phosphate buffered saline (PBS) solution before use. Different amounts of NaClO (Sigma-Aldrich) were added to a series of 1 L bioreactors with initial biomass concentration of 1000 mg/L for having the initial NaClO concentrations of 0 mg/L, 2 mg/L, 5 mg/L, 10 mg/L, 20 mg/L. Dissolved oxygen concentration in the bioreactors were kept at quasi-saturation level through air aeration. The contact between activated sludge and NaClO in each bioreactor was controlled at 30 min, after which sludge samples were collected for further analysis.

3.2.2 Cross-flow microfiltration test

A standard crossflow microfiltration module was employed to evaluate the fouling potentials of activated sludge after exposed to NaClO with various dosages. Flat-sheet hydrophilic PVDF membrane (GVWP2932A, Merck Millipore, Singapore) with nominal pore size of 0.22 μm and effective surface area of 42 cm^2 were embedded in the crossflow cell (CF042 Membrane Cell, Sterlitech). TMP changes during membrane filtration were monitored by two pressure sensors installed on both inlet and outlet of the filtration module, and readings were recorded with Labview software at the time intervals of 10 s (**Figure 3.2)**. A constant permeate flux of 30 L/(m^2h) was maintained through automatic adjustment of peristaltic pump (Cole-Parmer, USA), which was also confirmed by measured permeate volume using a digital balance (Mettler Toledo, Switzerland). The circulation flowrate in the feed chamber was controlled at 0.2 L/min by a digital gear pump. After exposed to NaClO with various concentrations for 30 min, activated sludge was harvested by centrifugation at 3000 rpm and resuspended in PBS solution at a MLSS concentration of 1000 mg/L for subsequent membrane filtration experiments.

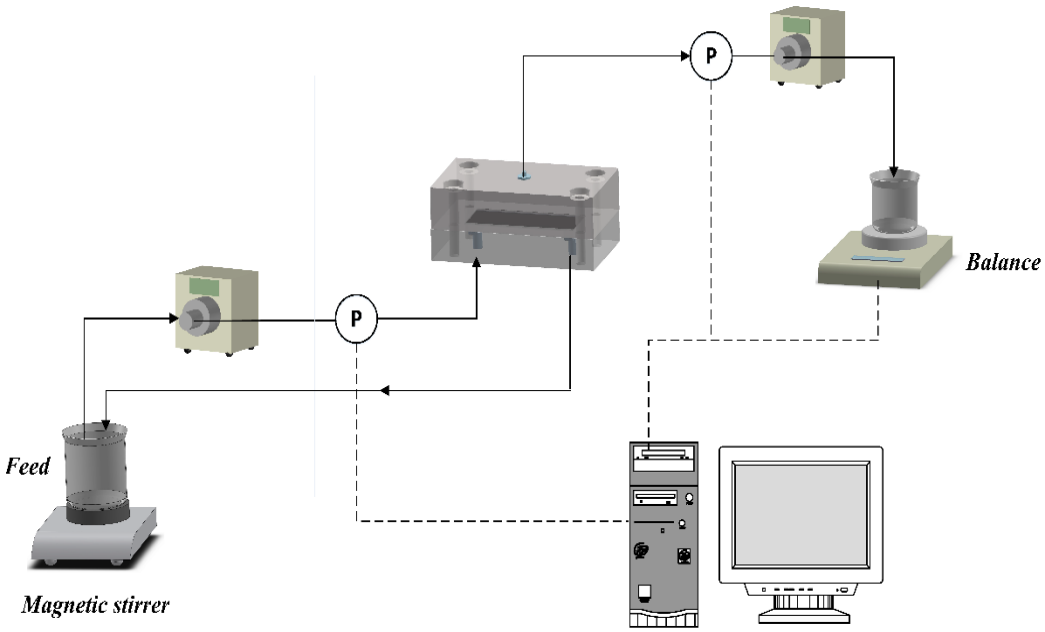

Figure 3.2 The crossflow membrane filtration system.

3.2.3 Determination of tight bound EPS

The method by Morgan et al. (1990) was modified for extraction of extracellular polysaccharides (PS) and proteins (PN) from biosamples. A 20 mL of sludge suspension was centrifuged at 4000 rpm for 5 min. The harvested sludge was then resuspended in 0.85% NaCl solution to its original volume. The mixture was kept at 80 °C in a water bath for 30 min, followed by 1 min vortex. The biomass and supernatant were separated through centrifugation at 10,000 rpm for 10 min. The harvested supernatant was further filtered through 0.45 mm membrane for PS and PN measurement. PS was determined by the phenol-sulfuric acid method (Dubois et al. 1956), whereas PN was analysed by modified Lowry method (Lowry et al. 1951). Glucose and bovine serum albumin were used as the standards, respectively. Each measurement was repeated three times.

3.2.4 Determination of autoinducer-2

The content of autoinducer-2 (AI-2) was measured based on the method by Xu and Liu (2011). Briefly, harvested activated sludge was resuspended in 20 mL of

fresh autoinducer bioassay (AB) medium, then chilled in an ice-water bath and homogenized for 1 min. The suspension was further centrifuged at 10,000 rpm for 10 min, and subsequently filtered through 0.2 mm syringe filter. The collected filtrate was stored at -20 °C for use. The reporter strain Vibrio harveyi BB170 (ATCC BAA 1117) was incubated aerobically in fresh AB medium for 16 h with shaking at 30 °C, followed by a dilution of 1/5000 (v/v) into AB medium. 180 mL of the diluted cells was added to 96-well plate containing 20 mL of cell-free samples. The 96-well plate was incubated in a rotary shaker at 150 rpm and 30 °C. The intensity of luminescence was measured hourly using a microplate reader (Tecan, infinite 200 PRO). Fold induction was calculated from bioluminescence relative to sterile AB medium. The concentration of AI-2 was obtained by comparing the peak fold induction with the calibration standard DPD (Omm Scientific, Dallas, USA). Each cell-free sample was assayed six times in parallel.

3.2.5 Determination of live/dead cell ratio

The ratio of live/dead cells was measured with Live/Dead BacLight Bacterial Viability Kits (L7012, Molecular Probes), which consists of two nucleic acid dyes: SYTO 9 and propidium iodide (PI). With an appropriate mixture of the SYTO 9 and PI stains, live cell with intact cell membranes stains fluorescent green, whereas dead cell with damaged membranes stains fluorescent red. The ratio of green to red fluorescence emission is proportional to the relative numbers of viable cells. Briefly, the biomass concentration of each mixture was adjusted to 400–500 mg/L. 100 µL of diluted dye mixture was pipetted into 96-well flat-bottom plate containing 100 µL sample. After mixing thoroughly, the plate was incubated at room temperature in the dark for 15 min and subsequently fluorescence intensity was measured with microplate reader (Tecan, infinite 200 PRO). A series of prepared live/dead cell mixtures were used as calibration standards. Each sample was tested six times in parallel.

3.2.6 Visualization of microorganism

Live/Dead BacLight Bacterial Viability Kits (Molecular Probes) were used to visualize microbial viability according to the protocol provided by the kits.

Firstly, 200 mL of SYTO 9 and PI mixture (1000 times dilution from stock solution) was added into the collected sludge, and the stained sample was then incubated in the dark for 15 min. After that, the stained biomass was gently rinsed several times with deionized water to remove unbound dyes, and then covered with a slip for further observation by confocal laser scanning microscopy (Nikon eclipse 90i, part of the A1R hybrid confocal spectral imaging system) with a 20 × objective. At least 5 images were randomly taken for each sample.

3.2.7 Determination of surface property and floc size in activated sludge

The relative hydrophobicity of activated sludge was measured by microbial adhesion assay to hydrocarbons with n-hexadecane as organic phase in this study. After exposure to NaClO, sludge was collected and resuspended in PBS solution. 5 mL of sample was then mixed with 1.5 mL hexadecane and agitated for 10 min at 30 °C in an orbital shaker. After 2 min vortex, followed by 30 min settling, the absorbance of the aqueous phase was measured with a UV spectrophotometer (Shimadzu, UV-1800) at 600 nm. The percentage of cells adhering to hexadecane is calculated based on equation (3.1).

$$\text{Relative hydrophobicity} = (1- B/A) \times 100\% \quad (3.1)$$

where A is the absorbance of initial sludge suspension, B is the absorbance of the aqueous phase.

Moreover, zeta potential values of activated sludge and membrane surface were respectively analyzed by Zetasizer (Malvern) and SurPASS (Anton Paar). The particle sizes of activated sludge were measured by a Mastersizer (Malvern Mastersizer 2000). Each measurement was repeated at least three times.

3.3 RESULTS AND DISCUSSION

3.3.1 Characteristics of activated sludge after exposure to NaClO

3.3.1.1 NaClO-triggered bacterial lysis and sludge surface change

Figure 3.3 showed the respective biomass concentration after exposed to NaClO at various dosages for 30 min, based on which bacterial lysis was calculated. It can be seen that the biomass concentration was reduced from 1000 mg/L to 973.3-784.8 mg/L after 30 min exposure to 0-20 mg/L NaClO. These results suggested that a substantial amount of biomass was chemically solubilized to dissolved matters by a strong oxidation of NaClO, e.g. a maximum of 21.5% of bacterial lysis was achieved at 20 mg/L NaClO. In fact, it has been well recognized that NaClO especially at high concentration can kill bacteria and solubilize cells accompanied by serious foaming. Liao et al. (2004) found 0.3 wt% free chlorine caused a decline of biomass concentration from 4.0 g/dm^3 to approximate 3.0 g/dm^3, indicating a 25% cell lysis occurred after 1 h oxidation. Lee et al. (2013) reported that soluble COD was increased by about 180 mg/L in MBR during 30 min exposure to 55 mg NaClO/g MLSS. It was also worth noting that the released organic substances caused by bacterial lysis would bring in significant negative impacts on current practice of long-term MBR operation including poor permeate quality (Liang et al. 2007), severe membrane fouling (Paul and Hartung 2008, Rosenberger et al. 2005) and variation of biomass properties (Barker and Stuckey 1999).

Moreover, sludge hydrophobicity is one of the main surface properties that are regularly monitored, which is essential for the formation and stability of sludge flocs (Chen et al. 2014, Van den Broeck et al. 2011). Evidence shows surface hydrophobicity also presents significant influence on membrane fouling development (Meng et al. 2006). It appears from **Figure 3.4** that sludge surface became less hydrophobic after exposure to NaClO. This is probably due to the fact that NaClO may oxidize functional groups of organic components of sludge into ketonic, carboxylic and aldehydic groups, consequently improving the

hydrophilicity of floc surface (Wang et al. 2014b). In addition, the respective zeta potential of treated sludge after exposed to 0, 2, 5, 10, 20 mg/L NaClO was -13.6 ± 1.25, -10.80 ± 0.20, -13.86 ± 1.10, -13.93 ± 0.75, -14.18 ± 0.52 mV (**Figure 3.4**). Since PVDF membrane surface had a zeta potential of -22 mV, the repulsive electrostatic forces between treated sludge and membrane surface would be expected. However, the tiny changes of zeta potential observed could not distinctly influence subsequent biofouling performance. Moreover, the sludge floc size did not significantly change after NaClO exposure (**Figure 3.5**).

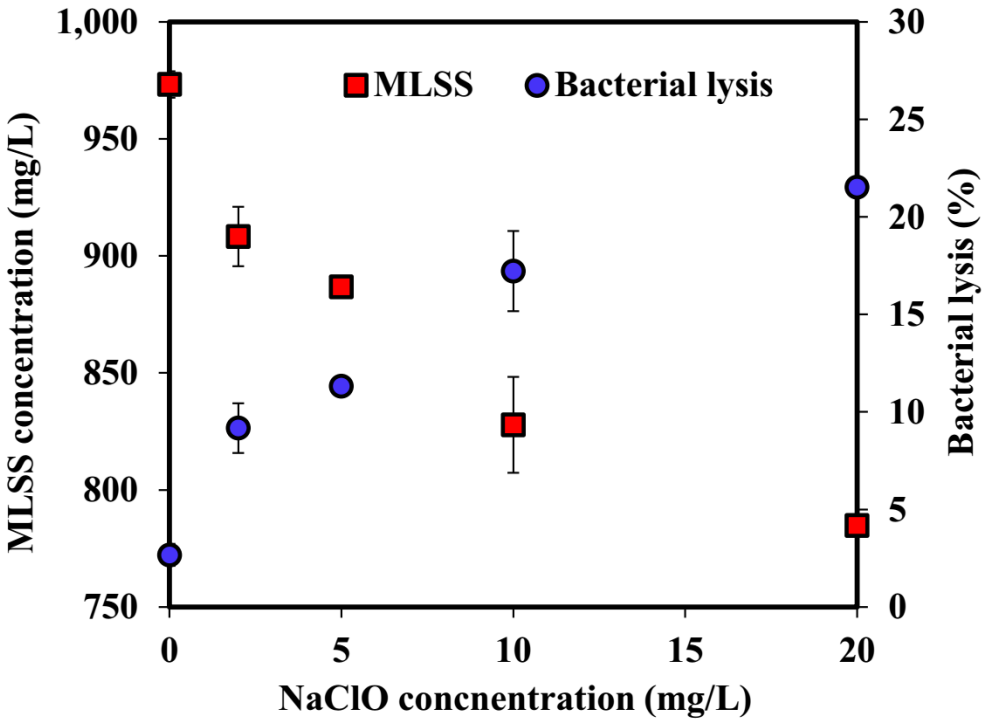

Figure 3.3 Bacterial lysis after 30-min exposure to NaClO.

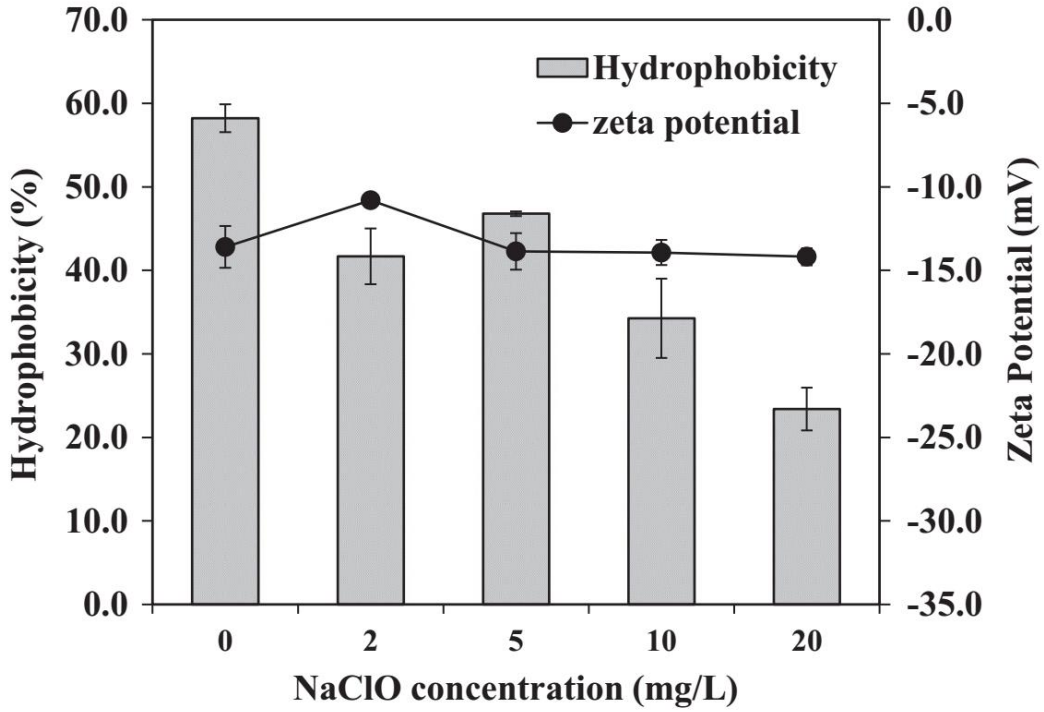

Figure 3.4 Surface properties of activated sludge after 30-min exposure to NaClO.

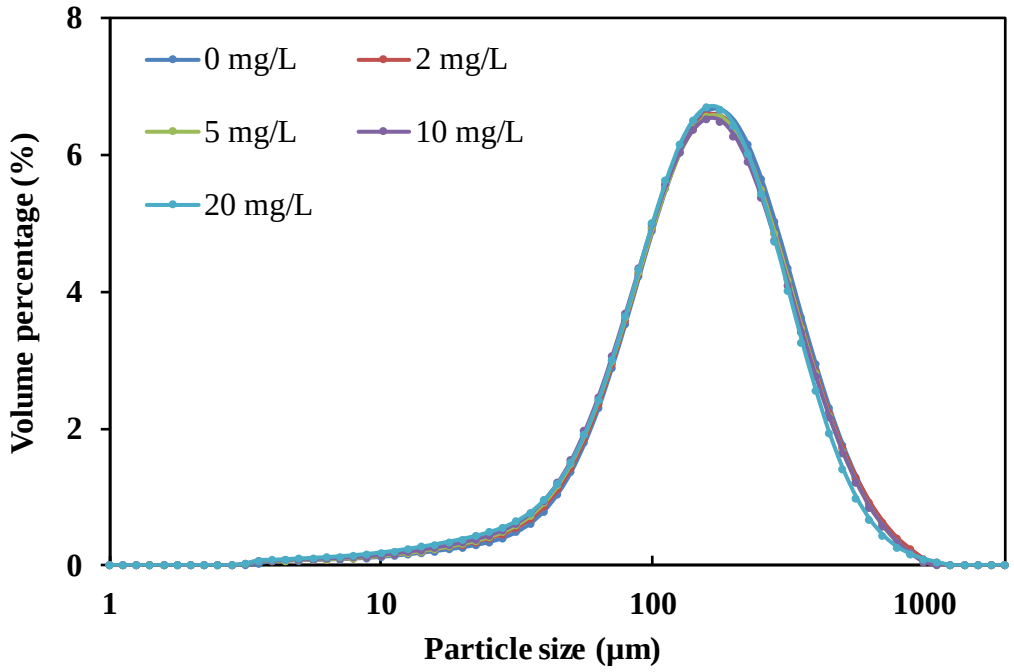

Figure 3.5 Particle size of activated sludge after 30-min exposure to NaClO.

3.3.1.2 NaClO triggered EPS and AI-2 production

EPS comprises of a series of organic substances, during which polysaccharides (PS) and proteins (PN) are known as two primary components. The role of EPS on biofilm formation has been well documented for more than a decade (Flemming and Wingender 2010). **Figure 3.6a** showed the EPS contents in terms of PS and PN in activated sludge after exposure to NaClO with various dosages. The total EPS concentration ranged from 119.68 mg/g MLSS to 158.59 mg/g MLSS. Among them, PN accounted for a great part of EPS and was more markedly affected by NaClO than polysaccharides. As compared to the control free of NaClO exposure, the PN content in activated sludge was increased by 9%, 11%, 19% and 39%, whereas 4%, 4%, 11% and 17% of increase for PS observed after 30-min exposure to 2, 5, 10 and 20 mg/L NaClO, respectively. AI-2 has been known as a universal inter-species signal molecule for both Gram-negative and Gram positive bacteria, which could coordinate biofilm formation by a mixture of species (McNab et al. 2003). **Figure 3.6b** further revealed that AI-2 content of sludge tended to increase from 0.258 μmol/g MLSS to 1.042 μmol/g MLSS, indicating a 4-fold rise with exposure to 20 mg/L NaClO. It seems that under oxidative stress imposed by NaClO, microorganisms can be stimulated to produce more signal molecules, which may further boost cell-to-cell communication between interspecies and favour subsequent biofilm formation.

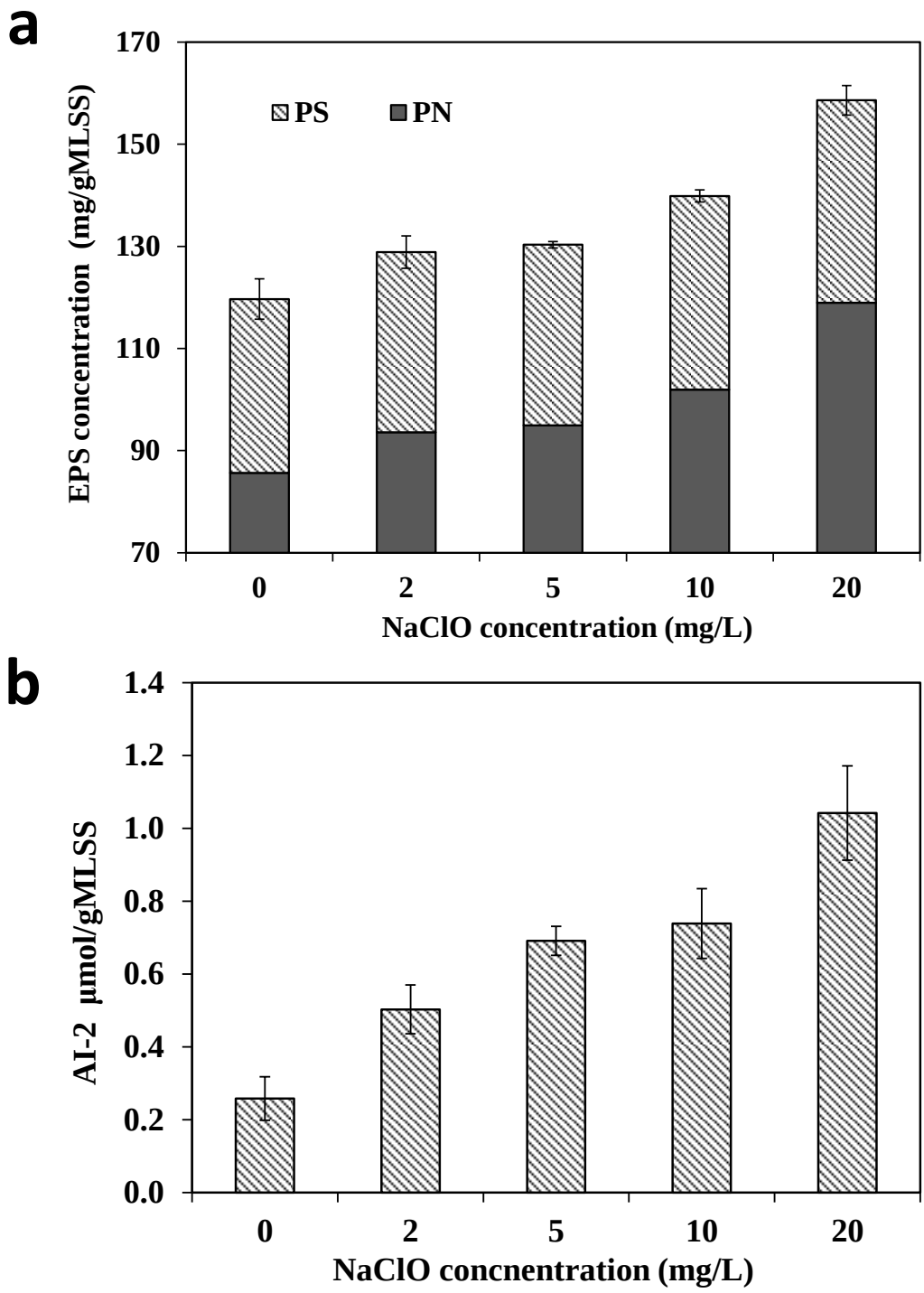

Figure 3.6 Contents of (a) EPS and (b) AI-2 in activated sludge after 30-min exposure to NaClO.

3.3.2 Membrane fouling potentials of activated sludge after exposure to NaClO

Figure 3.7a showed the respective TMP profiles observed in the filtration of the suspension of activated sludge after exposed to 0, 2, 5, 10, and 20 mg/L NaClO for 30 min respectively. Obviously, the TMP jump was positively related to the NaClO dosage applied for the sludge treatment. In the first 20-min filtration, the TMP nearly remained unchanged, e.g. dTMP/dt was found to be smaller than 0.092 kPa/min. These in turn suggested that the development of cake layer on the membrane surface was insignificant due to the high shear force induced by the circulation flow. Along with the formation cake and pore blocking, a sharp increase in TMP was observed in **Figure 3.7a**. **Figure 3.7b** further showed the respective average membrane fouling rate of activated sludge treated with different NaClO concentrations, and a quasi-linear correlation to the NaClO concentration was obtained. For example, sludge exposed to 20 mg/L NaClO feathered the highest membrane fouling rate at 2.02 ± 0.05 kPa/min, while control the lowest at 1.08 ± 0.03 kPa/min, indicating a nearly 2-fold faster fouling development on membrane surface appeared with exposure to NaClO.

It appears from these results that NaClO as a membrane cleaning agent commonly used in on-line chemical cleaning could impose remarkable negative impacts on microorganisms and post-development of membrane biofouling in MBR. In fact, on-line chemical cleaning with NaClO for the membrane fouling control in MBR should be regarded as a double-edged sword, i.e. NaClO may help to clean membrane fouling, but also accelerates the post membrane fouling rate. Despite limited available studies focusing on microbial responses to on-line chemical cleaning especially from membrane fouling perspective, several hints can still be found from the literature. By operating two identical aerobic MBRs with NaClO-assisted maintenance cleaning, Wang et al. (2014c) found backflush with a low concentration of NaClO seemed to present higher TMP increasing rate than pure water backwashing during several periods. In the study of consecutive CEB with NaClO, NaOH and citric acid in MBR, Kweon et al. (2012) found a decline in recovered flux appeared and the chemical cleaning intervals were

gradually shortened. As a microbial response to oxidative stress imposed by NaClO, suspended bacteria in MBR after chemical cleaning were stimulated to move onto membrane surface, and such a movement may be facilitated by AI-2 and EPS release (**Figure 3.8**).

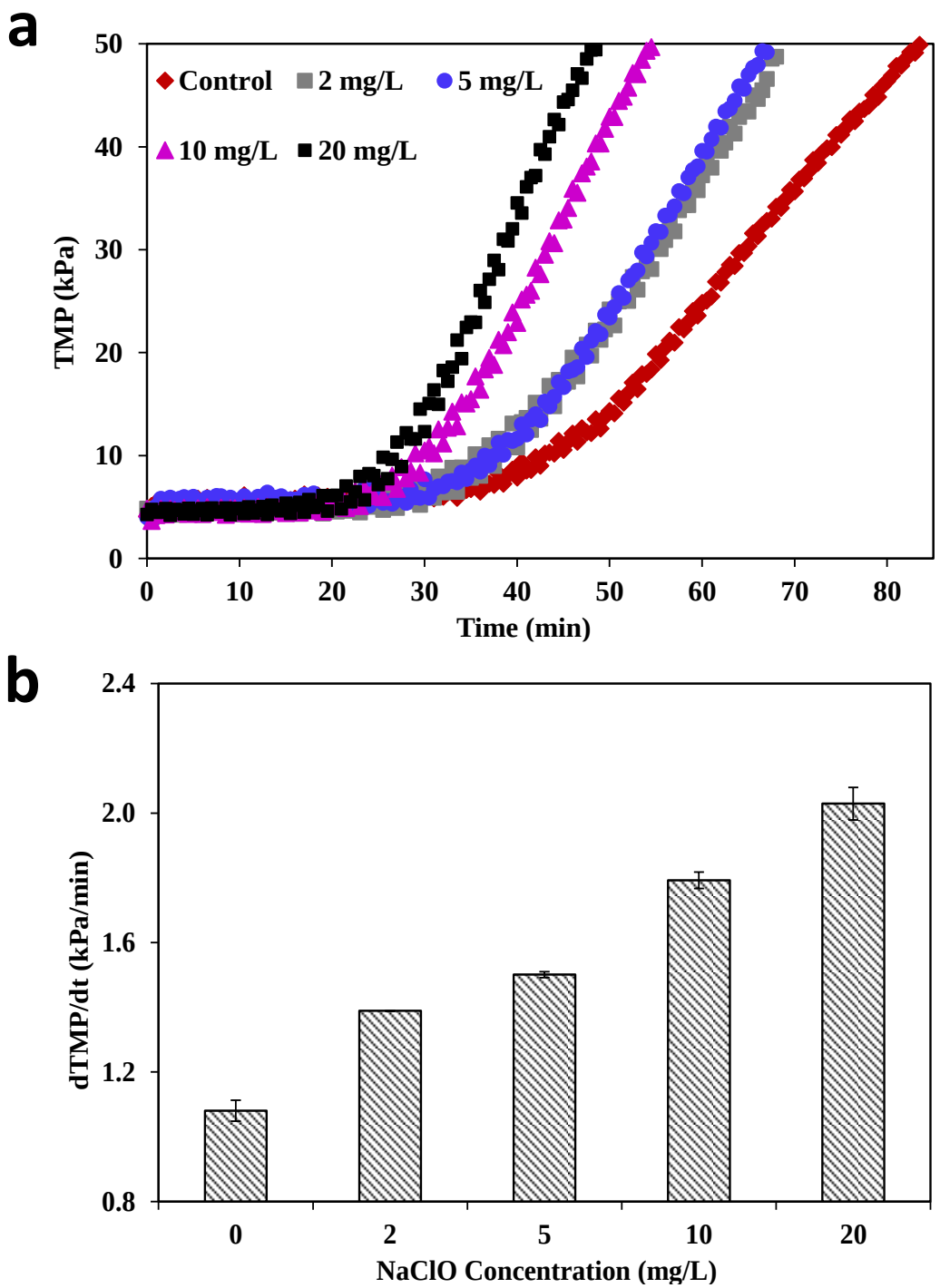

Figure 3.7 (a) TMP profiles and (b) fouling rates of the activated sludge suspension after 30-min exposure to NaClO.

Quorum sensing has been known to coordinate genes expression and ameliorate phenotypic adaptation of bacteria which is crucial for bacterial survival, especially under stressful conditions (Fuqua et al. 1994, Pereira et al. 2013, Vendeville et al. 2005). As observed in **Figure 3.8a**, NaClO-triggered AI-2 may be responsible for enhanced attachment of live bacteria on membrane surface after exposed to NaClO. In fact, evidence shows that AI-2 as an interspecies communication molecule plays an essential role in biofilm formation, e.g. the inter-species communication through AI-2 was found to be crucial for the pure and mixed culture biofilm formation (McNab et al. 2003). Furthermore, in the study of membrane fouling control by cellular communication, Xu and Liu (2010) also observed that AI-2 content was positively correlated to membrane fouling development. Indeed, cell-to-cell communication has been shown as predominant mechanism to control biofilm development in a variety of species (Bridier et al. 2011). **Figure 3.6b** suggested quorum sensing via AI-2 secretion was enhanced under external oxidative stress imposed by NaClO. As a matter of fact, it has been known that quorum sensing in diverse species may regulate genes expression in a way to ameliorate the deleterious effects of oxidative stress. For example, AHL-dependent quorum sensing has been reported to protect cell DNA from damage by oxidative stress via regulating non-specific protein *DpsA* expression in *Burkholderia pseudomallei* (Lumjiaktase et al. 2006). Quorum sensing in *Pseudomonas aeruginosa* may control the genes responsible for relieving oxidative stress caused by hydrogen peroxide (Hassett et al. 1999). Similarly, quorum sensing in *Vibrio cholera* positively affected the cell response to oxidative stresses and improved the bacterial survival (Joelsson et al. 2007, Joelsson et al. 2006). It seems that that quorum sensing in diverse species may positively regulate bacterial response to oxidative stresses, likely through attachment onto a solid surface as evidenced by enhanced biofouling development on membrane surface (**Figure 3.7**). Lastly, it should be noted that biofilm formation has been known as a defensive response that protects bacteria

against the adverse effects of various stresses (Shemesh et al. 2010, Zhang et al. 2007).

As shown in **Figure 3.8b**, NaClO-triggered EPS production also contributed to enhanced biofouling development on membrane surface. Generally, it is well accepted that EPS plays a key role in cell attachment and biofilm formation. By strengthening polymeric matrix structure, it serves as glue to favour microbial attachment and maintain the stability and integrity of biofilm (Oliveira et al. 1994, Xavier et al. 2005). The enhanced EPS production in current study shown in **Figure 3.6a** seems to be a trait expressed under oxidative stress, and the consistent results were also obtained by some other studies (Lee et al. 2013, Wu et al. 2007). Indeed, EPS secretion has been recognized as an inherent or adapted resistance mechanism that aids in bacterial survival under adverse environmental stresses. For instance, Chen et al. (2004) reported the secreted exopolysaccharide in terms of colanic acid provided defense against hydrogen peroxide in Escherichia coli, and the strain deficient in colanic acid production presented more susceptibility to hydrogen peroxide than its wild-type parent. Similarly, Helbling and VanBriesen (2007) also suggested EPS produced by *S. epidermidis* afforded additional protection that helped in resistance to free chlorine. This can be possibly explained by the fact that secreted EPS consumes invading oxidants by adsorption or reaction, effectively minimizing its available concentration diffused to cell wall or cell membrane where initially oxidative reactions can occur (Helbling and VanBriesen 2007, Samrakandi et al. 1997). The enhanced EPS secretion induced by oxidative environment may in turn facilitate post membrane fouling formation as shown in **Figure 3.7**. Moreover, EPS synthesis seems at least partially regulated by quorum sensing via modulating the expression of genes related to EPS biosynthesis (De Araujo et al. 2010, Quinones et al. 2005). Therefore, most likely quorum sensing works as an internal controlling mechanism that coordinates population behaviours (e.g. EPS production) in order to confer a survival superiority to microorganisms under oxidative stress.

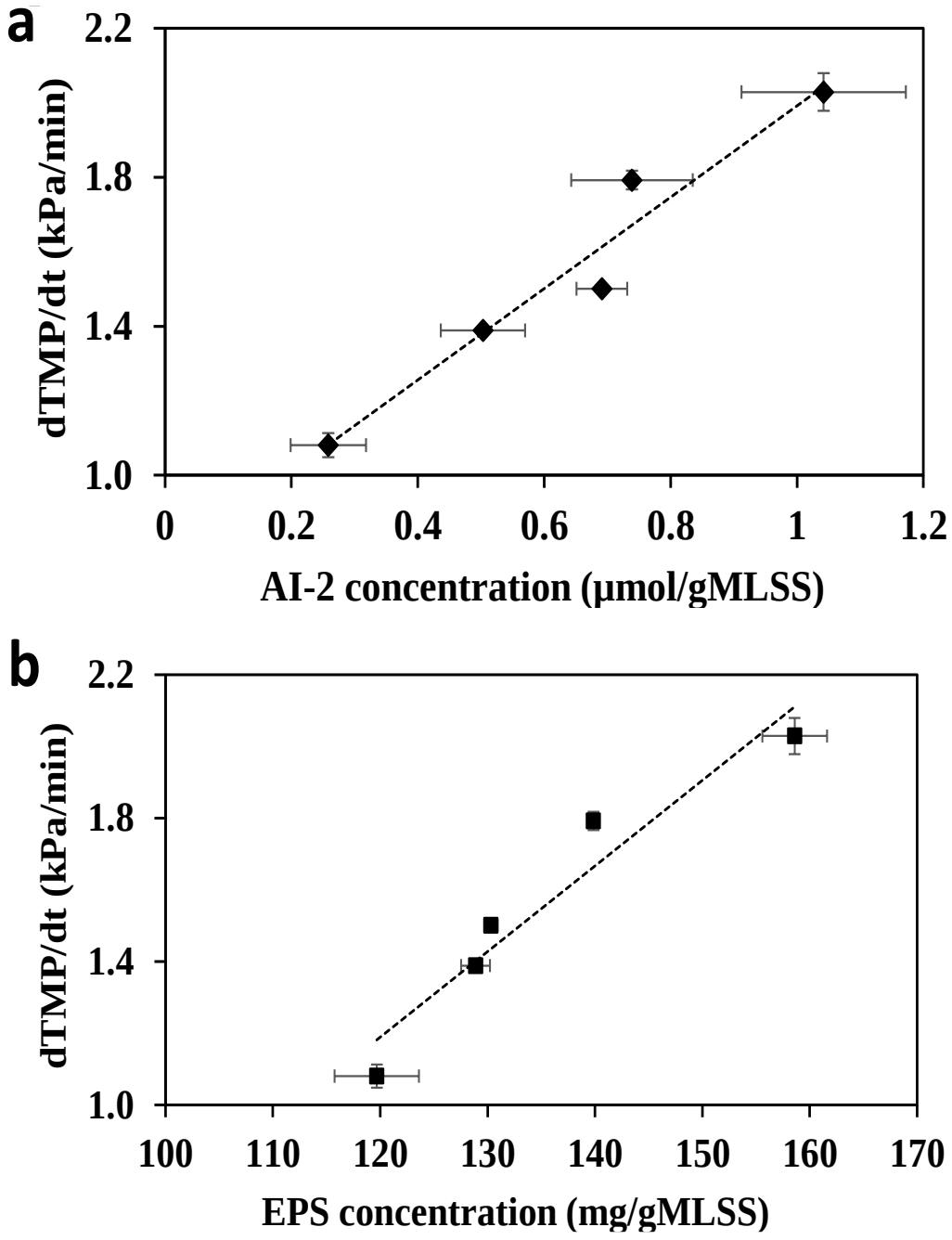

Figure 3.8 Relationship between AI-2, EPS content and membrane fouling rate (a) AI-2 (b) EPS.

3.3.3 Live/dead ratios in activated sludge and cake layer

In general, NaClO as a strong disinfectant could oxidize organics and kill microorganisms in order to control bacterial growth on membrane surface. Therefore, both live and dead bacteria existed together after treated with a

specific concentration of NaClO. In this part, cell viabilities in suspended sludge after exposure to NaClO (before membrane filtration) as well as in cake layer on membrane surface (after membrane filtration) were determined (**Figure 3.9**). Compared to the control without exposure to NaClO, the number of live bacteria in the activated sludge exposed to 20 mg/L NaClO was reduced from 97.3% (control) to 77.6%. In contrast, the number of live bacteria in the cake formed during the filtration of the suspension of activated sludge exposed to 20 mg/L NaClO was increased from 75.1% (control) to 90.6%. These results were further confirmed by CLSM images (**Figure 3.10**). It appears that bacteria survived after exposed to NaClO exhibited a greater tendency than dead bacteria to attach onto membrane surface. It has been known that oxidative stress may promote microbial attachment onto a solid surface, which is considered as a protective strategy of survived microorganisms. In addition, enhanced production of EPS and AI-2 after exposure to NaClO in turn may facilitate microbial attachment on membrane surface. These results indeed provide microbiological evidence further supporting the observed TMP changes as shown in **Figure 3.7.**

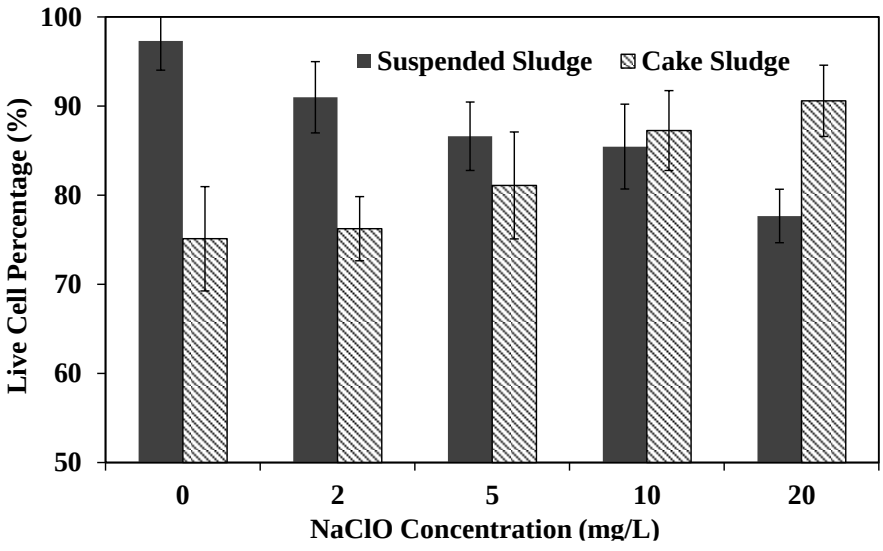

Figure 3.9 Percentages of live bacteria in suspended activated sludge as well as in membrane cake layer.

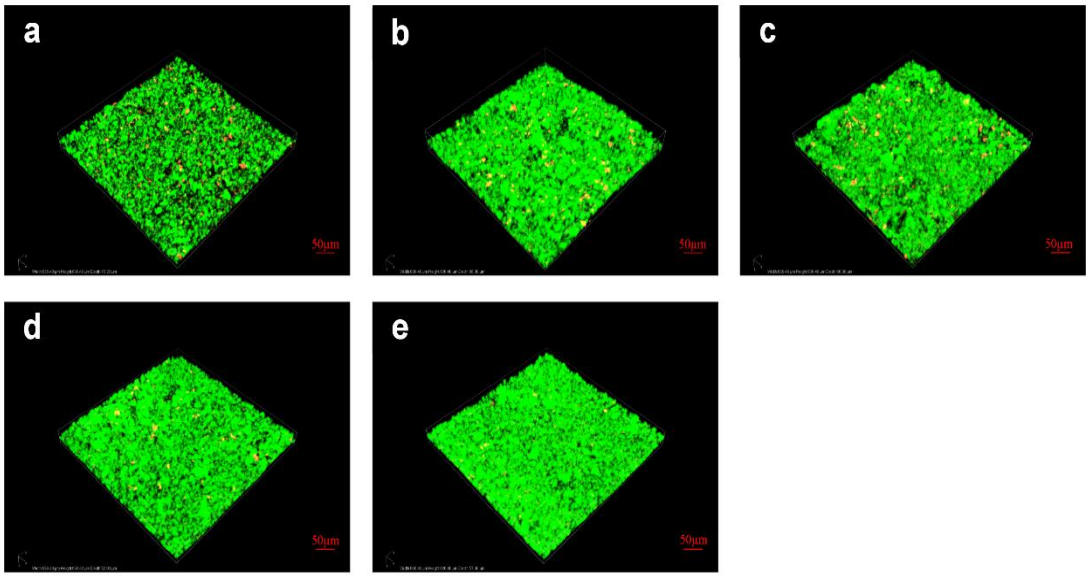

Figure 3.10 CLSM images of fouling layer on membrane surface developed from activated sludge exposed to (a) 0 mg/L, (b) 2 mg/L, (c) 5 mg/L, (d) 10 mg/L and (e) 20 mg/L NaClO. Green color: live bacteria; Orange color: dead bacteria.

Based on the experimental observations, **Figure 3.11** further illustrates the possible effects of NaClO on the development of membrane biofouling. After exposed to NaClO, survived cells tended to excreted more AI-2 and EPS to promote microbial attachment on the membrane surface, which has been known as an effective strategy to mitigate oxidative stress imposed by NaClO. This may also explain why the fouling layers developed at different NaClO dosages were primarily composed of live instead of dead cells (**Figure 3.9** and **Figure 3.10**). As a result, enhanced membrane fouling was observed (**Figure 3.7**). Consistent with these results, it was shown that chlorine dioxide at the sublethal level stimulated the formation of polymeric matrix in *Bacillus subtilis* due to the activation of a membrane-bound kinase KinC via sensing membrane potential decrease caused by chlorine dioxide. The activated KinC could further induced expression of major genes (*epsA-epsO* and *yqxM-sipW-tasA*) which were responsible for biofilm matrix formation (Shemesh et al. 2010). In *E. coli*, biofilm induction in response to several stresses including oxidative stress (H_2O_2), pH, heavy metal and temperature also has been observed, which appeared related to the decline in the synthesis of indole (an interspecies extracellular signal that

suppresses biofilm formation) (Zhang et al. 2007). Moreover, subinhibitory concentration of antibiotics can also trigger the production of biofilm matrix for both Gram-negative and Gram-positive bacteria (Hoffman et al. 2005, Rachid et al. 2000b). Actually, biofilm development is a complicated and dynamic process involved in a series of microbial responses to various signals (Zhang et al. 2007), and microorganisms can greatly benefit from this coordinated biofilm community, e.g. improved ability to retain extracellular enzymes nearby, control competition relationship as well as resist desiccation (Costerton et al. 1995, LaPaglia and Hartzell 1997). Moreover, biofilm-forming phenotype also confers protective barrier against bacterial damage from a harsh microenvironment (Rachid et al. 2000a, Shemesh et al. 2010). For example, the development of biofilm successfully provided protective environment for *Pseudomonas aeruginosa* against invasive heavy metals like copper and lead due to the fact that EPS minimized their diffusion into biofilm (Teitzel and Parsek 2003). Similarly, LaPaglia and Hartzell (1997) reported the survival rate of *Archaeoglobus fulgidus* greatly depended on the microbial ability to produce biofilm which may serve as a protective barrier for bacteria to reserve nutrient and avoid contact to toxic agents. They also found gradually applied stress induced the biofilm formation with fibrous structures and fast acting stress triggered much denser biofilm matrix produced. The explanations for the protective function of biofilm or microbial resistance to stresses have been primarily concluded as (1) limitation of biocides transport in the biofilm structure; (2) heterogeneous nature of biofilm (e.g. stratified pattern of microbial growth and activity) better adaptive to adverse conditions; (3) phenotypic adaptions due to accumulation of regulatory mechanisms (e.g. quorum sensing, *rpoS*-mediated stress response) (Bridier et al. 2011, Mah and O'Toole 2001). Owing to the biofilm matrix or induced microbial resistance, biocides, antibiotics and detergents used often present less effective against microorganisms (Helbling and VanBriesen 2007, Lisle et al. 1998). In addition, it should be noticed that bacteria embedded in biofilms matrix present phenotypes that differ from their planktonic counterparts, e.g. attachment of *Klebsiella pneumoniae* to glass slides increased disinfection resistance by nearly 150-fold than the planktonic bacteria (Lechevallier et al. 1988). Furthermore,

bacterial cells grown in biofilm were found to better resist various stresses derived from antibiotics (Desai et al. 1998), oxidant (Zhang et al. 2007) and heavy metals (Lisle et al. 1998). This may raise another potential concern on fouling removal efficiency due to microbial resistance to disinfectants.

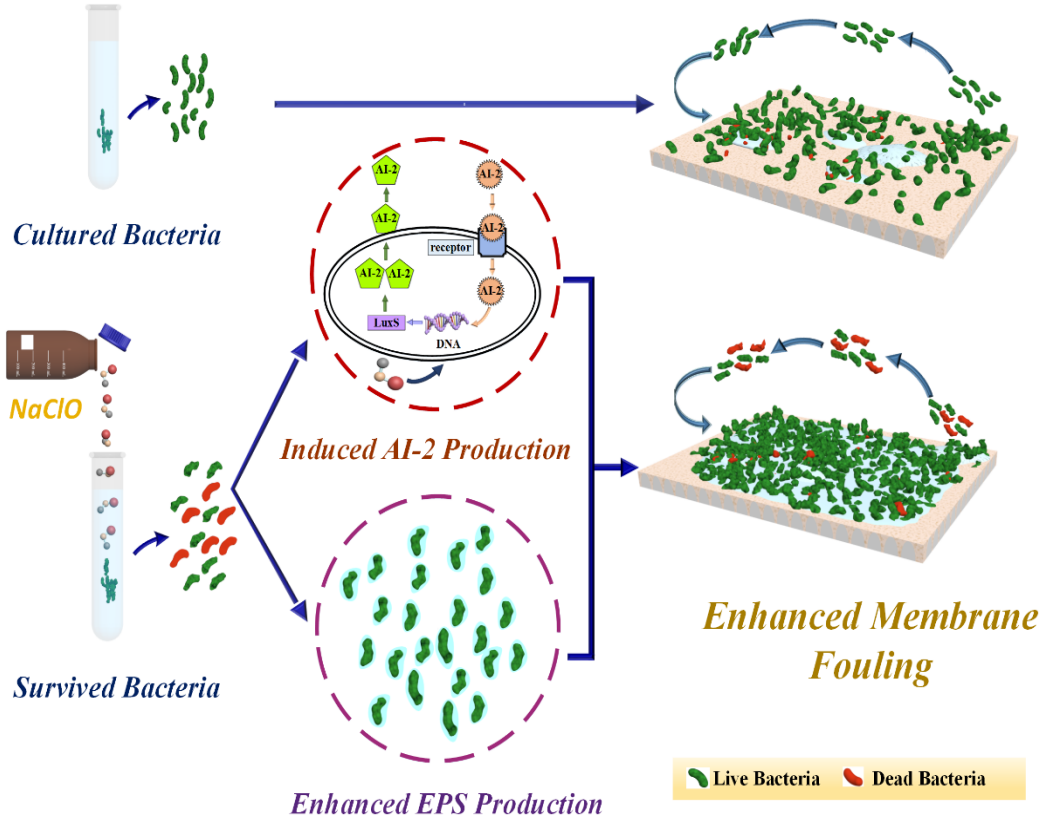

Figure 3.11 Possible effects of NaClO on microorganisms and membrane fouling development.

3.4 CONCLUSIONS

This study sheds light into the double-side effects of on-line chemical cleaning with NaClO on the membrane fouling control and redevelopment in MBR. The results clearly indicated the NaClO-triggered bacterial lysis and enhanced production of EPS and AI-2 in activated sludge. More importantly, survived

bacteria after exposure to NaClO exhibited a greater tendency than dead bacteria to adhere onto membrane surface, leading to a faster re-development of membrane biofouling. The observed fouling behaviours of activated sludge exposed NaClO may be explained by the defensive response of microorganisms to the oxidative stress exerted by NaClO, accompanied with the over-production of AI-2 and EPS which in turn favoured the fast microbial colonization onto membrane surface. Consequently, the dark side of on-line chemical cleaning as revealed in this study should be taken into consideration in practical operation of large-scale MBR, meanwhile novel environmentally friendly membrane cleaning strategy should also be explored.

CHAPTER 4 OXIDATIVE STRESS INDUCED MEMBRANE BIOFOULING BY ON-LINE CHEMICAL CLEANING WITH SODIUM HYPOCHLORITE IN MBR

4.1 INTRODUCTION

Upon exposure to NaClO, substantial oxidative stress in the form of reactive oxygen species (ROS) can be generated in microorganism. It has been reported that the elevated levels of ROS could damage DNA, RNA, membrane lipids and proteins, potentially leading to cell death (Arts et al. 2015, Cabiscol et al. 2010). Therefore, most living microorganisms are equipped with internal defensive systems to prevent the harmful effects of ROS. Increasing evidence also showed that diverse stresses (e.g. oxidative stress, heavy metal, antibiotics etc) at sublethal levels could induce the production of polymeric matrix in various strains (Hoffman et al. 2005, Rachid et al. 2000, Shemesh et al. 2010, Zhang et al. 2007). These should shed lights on the prevalent practice of on-line chemical cleaning of MBR, i.e. NaClO exposure may induce oxidative stress through generation of ROS, which may in turn facilitate the membrane biofouling re-development on membrane surface when normal membrane filtration restarts in MBR. In fact, it had been recently demonstrated in chapter 3 that the membrane fouling potential was significantly increased after the exposure of activated sludge microorganisms to NaClO with various dosages, which was related to the overproduction of extracellular polymeric substances (EPS) and autoinducer-2 (AI-2). However, the role of oxidative stress induced by chemical cleaning with NaClO in the development of membrane biofouling in MBR has not yet clearly understood. Hence, there is an urgent need to systematically explore the linkage between intracellular oxidative stress and biofouling formation, and further elucidate possible structure of fouling layer formed by these stressed bacteria.

NaClO as a strong oxidant, can cause bacterial death, leading to the co-existence of both live and dead bacteria within a certain range of dosage. Meanwhile, bacterial death was found to affect the membrane permeability of activated sludge due to changes in EPS production, floc size and surface hydrophobicity (Azami et al. 2011). Therefore, this study aims to explore the potential impacts of oxidative stress induced by NaClO on membrane fouling by examining the biofouling behaviours of a serious of stressed biomass in comparison to respective control at the same bacterial viability. For this purpose, stressed biomass was prepared upon the exposure to NaClO at different dosages, while non-stressed biomass as control was obtained by mixing live and dead bacteria at various ratios. It is expected that this study can offer better understanding of membrane biofouling in the presence of oxidative stress, and such information is useful for future development of on-line chemical cleaning methods for MBR.

4.2 MATERIALS AND METHODS

4.2.1 Preparation of stressed and non-stressed biomass

Activated sludge collected from a local wastewater treatment plant in Singapore was acclimatized in a chemostat cultured with a synthetic wastewater containing 690 mg/L CH_3COONa, 313 mg/L glucose, 200 mg/L NH_4Cl, 60 mg/L K_2HPO_4 and other trace minerals. The acclimatized sludge was washed thrice with 10 mM phosphate buffered saline (PBS) solution to remove the contaminants prior to usage. NaClO stock solution purchased from Sigma-Aldrich was standardized by N, N-diethyl-p-phenylenediamine (Hach, USA). To obtain the stressed biomass, 1000 mg/L of acclimated activated sludge was exposed to NaClO at different dosages for 30 min during which dissolved oxygen was kept at nearly saturation level. After this, almost all of the chlorine was consumed and residual free chlorine was undetectable. The harvested sludges with various survivability were then washed and resuspended in 10 mM PBS solution. The sludge concentration was then re-adjusted to 1000 mg/L for further analysis. For the non-stressed biomass as control, dead cells were prepared by autoclaving the acclimatized sludge at 121 ˚C for 20 min and then washed thrice with 10 mM PBS solution.

Afterwards, live/dead mixtures were prepared by proportionally mixing live sludge with autoclaved sludge, both of which concentrations were previously adjusted to 1000 mg/L. In this way, the stressed and non-stressed biomass were obtained for further analysis.

4.2.2 Crossflow microfiltration test

Membrane fouling behaviours of biomass in the presence and absence of induced oxidative stress were examined in a standard crossflow microfiltration system at a constant permeate flux of 30 L/(m^2h). Similar with the method described in chapter 3, a commercial flat-sheet hydrophilic PVDF membrane (GVWP2932A, Merck Millipore) with nominal pore size of 0.22 μm and effective surface area of 42 cm^2 was embedded in a crossflow module (CF042 Membrane Cell, Sterlitech) and soaked in Milli-Q water for 24 h before usage. All the filtration operation conditions were the same with the above experiments described in the section of 3.2.2 of chapter 3. The microfiltration test will be terminated when TMP reached up to 50 kPa, and membrane fouling rate will be further calculated based on the liner part in the plot of TMP against filtration duration.

4.2.3 Intracellular ROS determination

The ROS quantity was measured by using 2',7'-dichlorodihydrofluorescein diacetate (H2DCFDA) (Sigma-Aldrich), which was commonly used as an indicator of ROS in cells. Upon cleavage of the acetate groups by intracellular ROS, the nonfluorescent H2DCFDA was converted to the highly fluorescent 2',7'-dichlorofluorescein (DCF) for further detection. According to the protocol provided by the kit, the H2DCFDA was added into a series of prepared biomass suspensions for providing a final H2DCFDA working concentration of 10 μM. After incubation at 37ºC for 30 min in dark, the residual probes outside cells were washed off with 10 mM PBS solution. After this, 200 μL of the cell suspension was pipetted into a 96-well flat bottom plate for fluorescence measurement at the excitation wavelength of 488 nm and emission wavelength of 525 nm using a microplate reader (Tecan, infinite 200 PRO). The production of ROS was directly

proportional to the detected fluorescence intensity. Each sample was tested six times in parallel.

4.2.4 Determination of bacterial viability and cell visualization

Similar with the method described in chapter 3, the bacterial viability was measured with the Live/Dead BacLight Bacterial Viability Kits (L7012, Molecular Probes) according to the protocol provided by the kits. Briefly, 100 µL of 100 mg/L of biomass suspension was mixed thoroughly with 100 µL of the diluted SYTO 9 and PI solution in a 96-well flat-bottom plate. After dark incubation at room temperature for 15 min, the fluorescence intensity was determined with a microplate reader (Tecan, infinite 200 PRO). The ratio of green to red fluorescence intensity is proportional to the relative numbers of viable cells. A series of prepared live/dead cell mixtures were used as calibration standards. Each observation was done at least six times in parallel.

The microbial viability was further visualized with the Live/Dead BacLight Bacterial Viability Kits (L7012, Molecular Probes). For suspended biomass, 3 µL of the SYTO 9 and PI dye mixture was added into 1 ml of sludge suspension and mixed thoroughly. For the attached biomass, 200 µL of diluted SYTO 9 and PI mixture was uniformly added into the collected biofilm. Afterwards, the stained samples were incubated in dark for 15 min, and then transferred to a glass slide with coverslip for further observation by confocal laser scanning microscopy (Zeiss, LSM 880 Airyscan) with a 63× objective. For each observation, at least 10 pictures were randomly taken.

4.3 RESULUTS AND DISCUSSION

4.3.1 NaClO triggered bacterial lethality and ROS production

Figure 4.1 showed the bacterial survival rates of activated sludge after exposure to NaClO with various dosages. It can be seen that the number of viable cells almost linearly decreased with the increase in the NaClO dosage from 0 to 30 mg/L, and 58.1% of microbial death was achieved at the NaClO dosage of 30

mg/L. 100%, 90%, 70% and 50% of bacteria still remained alive in sludge after exposure of biomass to 0 mg/L, 3.2 mg/L, 12.1 mg/L, 23.2 mg/L NaClO, respectively, which were further confirmed by CLSM images in **Figure 4.2**. Although NaClO has been well known as a strong and effective disinfectant, the mechanism of its germicidal activity has not yet been fully understood thus far. The possible killing mechanisms of NaClO may include inhibition of enzyme activity essential for the growth, impairment of cell respiration, damage to membrane transport capacity, disruption of protein synthesis, or injury to cell membrane and DNA (Benarde et al. 1967, Fukuzaki 2006, Haas and Engelbrecht 1980). However, an investigation by Cho et al. (2010) proposed that free chlorine tended to attack cell inner components such as intracellular enzymes instead of damages to cell surface due to its more retarded reaction during diffusive transport through the cell barrier.

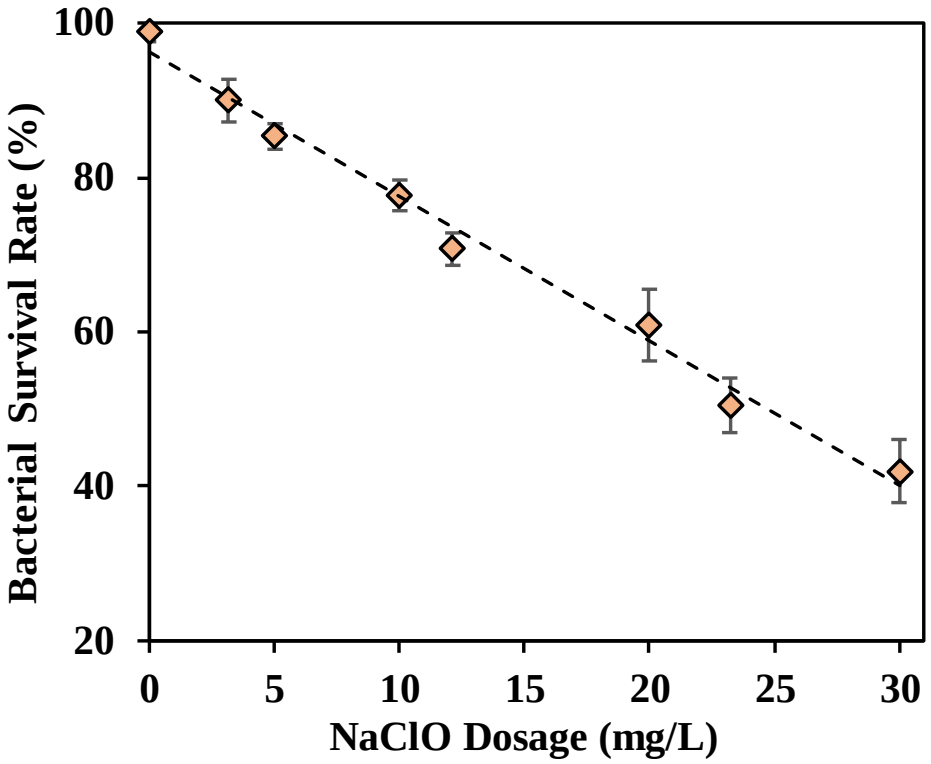

Figure 4.1 Bacterial survival rate after 30-min exposure to NaClO with various dosages.

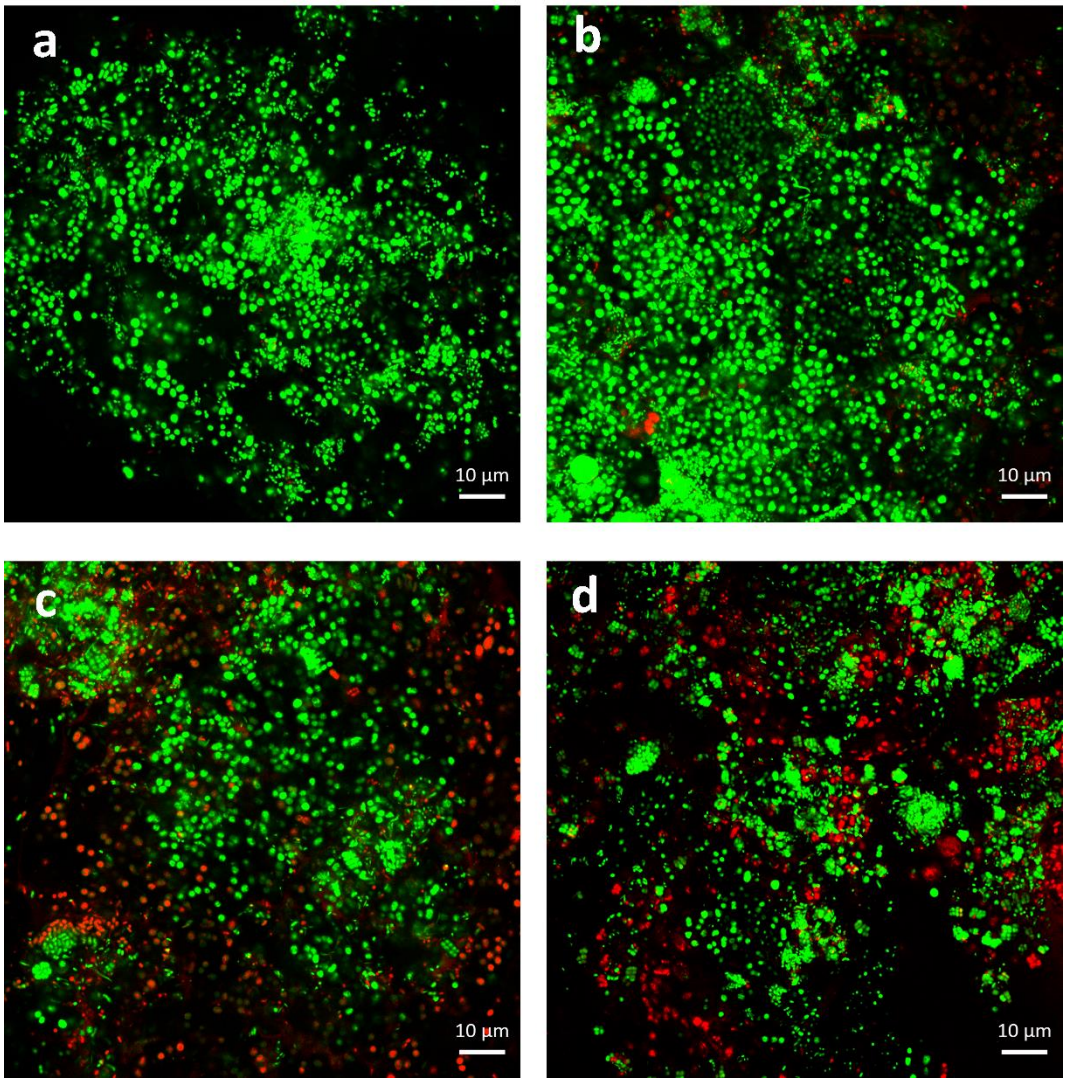

Figure 4.2 CLSM images of microorganisms after 30-min exposure to (a) 0 mg/L, (b) 3.18 mg/L, (c) 12.12 mg/L, (d) 23.23 mg/L NaClO. Green colour: live bacteria; Red colour: dead bacteria.

Figure 4.3a further exhibited the fluorescence intensity of intracellular ROS in microorganisms after exposure to NaClO at various dosages, which was further compared with the corresponding control free of NaClO exposure at the same cell viability. Upon the exposure to NaClO, more ROS was generated with increasing NaClO dosage, while the ROS intensity in the control biomass remained relatively low. Specifically, the respective ROS production of stressed biomass after exposed to 3.2, 12.1 and 23.2 mg/L NaClO was found to be 226%, 531% and 891% higher than the corresponding control (**Figure 4.3b**). These

results clearly suggested that NaClO could trigger the significant overproduction of oxidative stress in the survived bacteria. Consistent with this study, Han et al. (2016) also observed that the ROS generated at 50 mg NaClO/g SS was 180% more than that in the control free of NaClO exposure, which may further cause cell membrane damage or enzyme inhibition. In fact, aerobic microorganisms are generally equipped with enzyme defensive systems (e.g. catalases, peroxidases and superoxide dismutases) to respond to or prevent the unfavourable effects of ROS (Dukan et al. 1999, Fukuzaki 2006). However, upon the exposure to aggressive NaClO at relatively high dosage, these defensive enzymes might be exhausted or inactivated quickly, resulting in the substantial accumulation of ROS within cells. Meanwhile, some evidence shows that NaClO can also trigger production of intracellular ROS in the form of highly reactive hydroxyl radicals (•OH) through the Fenton-like reaction with iron ion released from damaged enzymes as described in equation (4.1) (Dukan and Touati 1996, Han et al. 2016). And hydroxyl radicals (•OH) can also be generated in the presence of superoxide anions (O2•-) via the reaction shown in equation (4.2) (Dukan and Touati 1996, Han et al. 2016).

$$NaClO + Fe^{2+} + H^{+} \rightarrow {}^{\bullet}OH + Cl^{-} + Fe^{3+} + Na^{+} \quad (4.1)$$

$$NaClO + O_2^{\bullet -} + H^{+} \rightarrow {}^{\bullet}OH + Cl^{-} + O_2 + Na^{+} \quad (4.2)$$

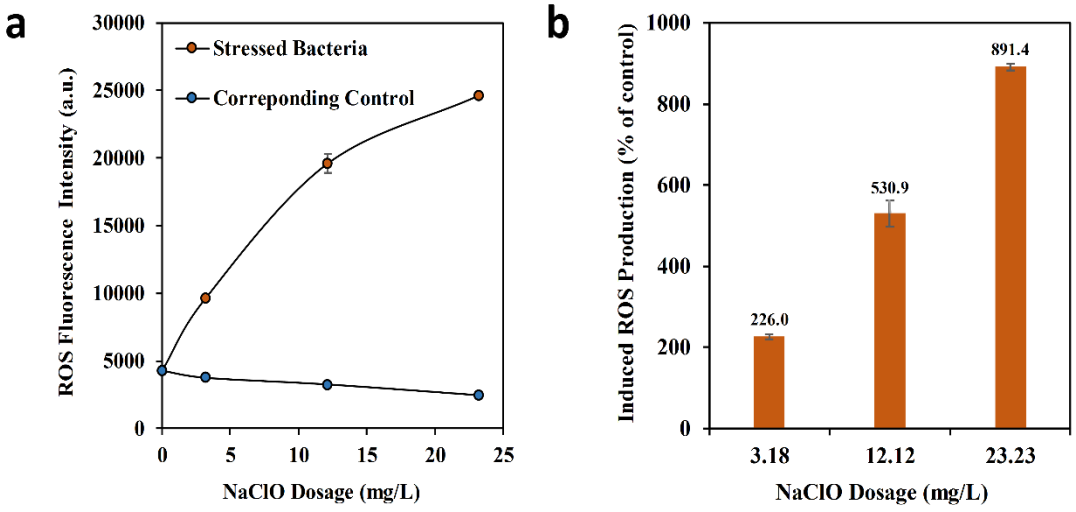

Figure 4.3 (a) ROS fluorescence intensity of microorganisms after exposure to NaClO at various dosages in comparison to corresponding control at the same cell viability; (b) the increased ROS production by NaClO exposure.

4.3.2 Oxidative stress-induced membrane fouling formation

To explore the role of oxidation stress in biofouling formation, membrane fouling potentials of the stressed biomass with various levels of ROS were further investigated in a standard crossflow microfiltration system. **Figure 4.4** showed the filtration profiles of these stressed biomass and their corresponding control at the same cell viability. After the oxidative stress had been induced, a sharp increase in TMP was observed during the initial filtration period, while no apparent TMP rise was found within the first 40-min membrane filtration of the control non-stressed suspension. Moreover, it was found that the rate of membrane fouling development was positively related to the relative ROS level, e.g. TMP reached 50 kPa in 33.7 min under 226% ROS, in contrast to 25.8 min for bacteria at 891% ROS. **Figure 4.5** further revealed a quasi-linear correlation between the membrane fouling rate and relative ROS level induced by NaClO. For example, the biomass with 891% ROS feathered the highest membrane fouling rate of 2.7 kPa/min, while the lowest of 2.2 kPa/min with 226% ROS. Comparatively, the membrane fouling rates maintained a much lower range of 1.7-1.8 kPa/min for all of the corresponding control biomass. Such observation was consistent with the previous study in chapter 3 showing the accelerated formation of membrane fouling in the presence of NaClO. Consequently, it appears that NaClO commonly used for on-line chemical cleaning imposes remarkable negative impacts on microorganisms under oxidative stress condition, which may in turn enhance the post-development of membrane biofouling in MBR.

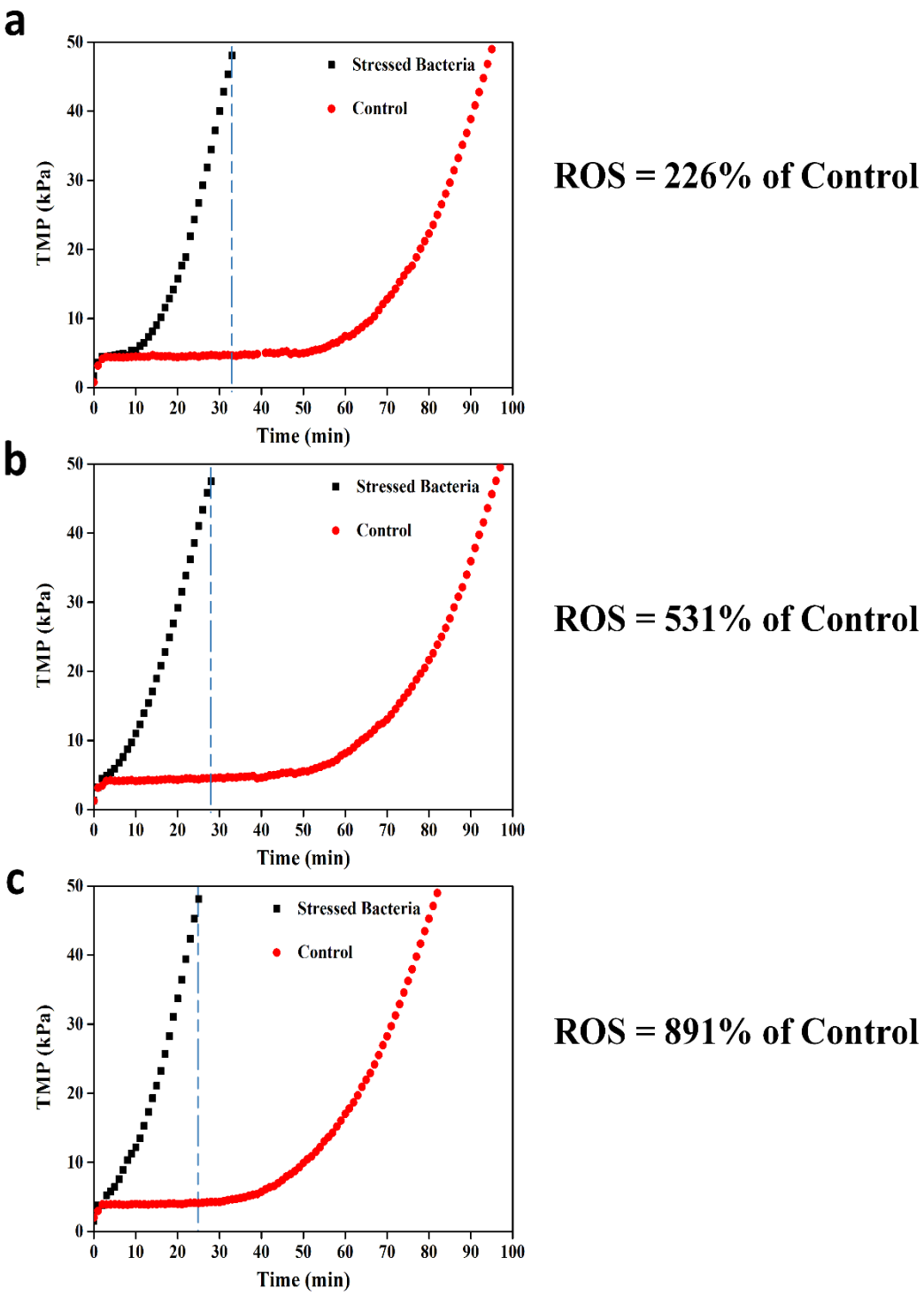

Figure 4.4 TMP profiles of stressed microorganisms at various ROS levels in comparison to corresponding control at the same viability.

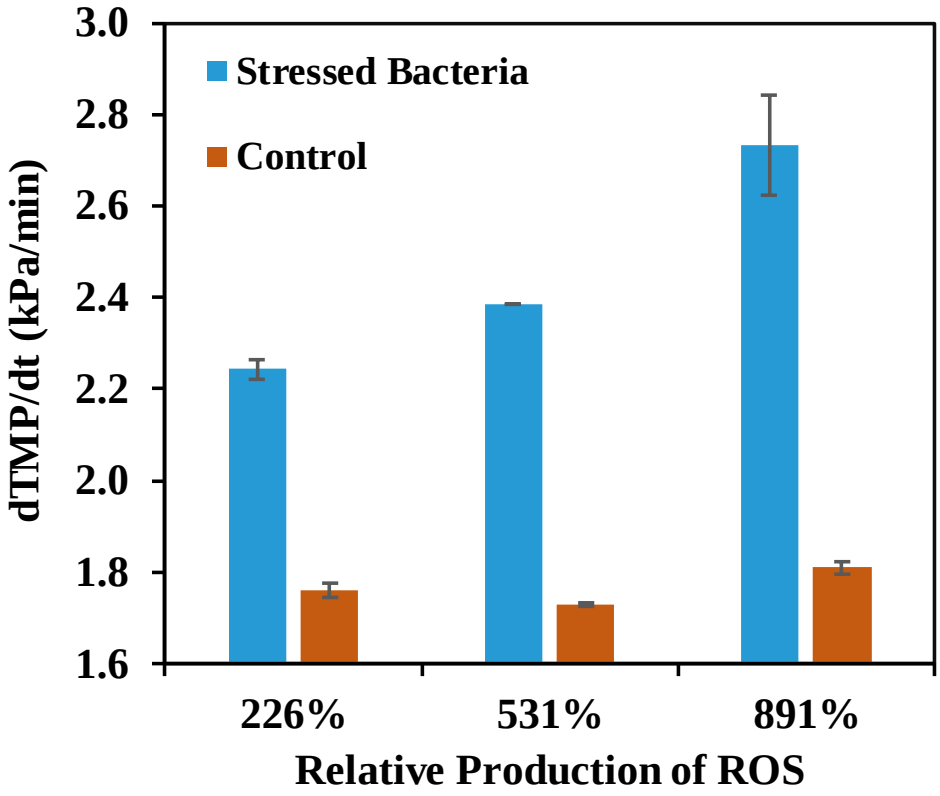

Figure 4.5 Membrane fouling rates of stressed microorganisms at various ROS levels in comparison to corresponding control at the same viability.

Furthermore, the relationship between absolute ROS fluorescence intensity and membrane fouling rate was presented in **Figure 4.6**. It showed that the NaClO-triggered oxidative stress appeared to be responsible for the faster microbial colonization on the membrane surface. Consistent with this observation, it had been reported that chlorine dioxide at its sublethal concentration could also stimulate the formation of polymeric matrix in *Bacillus subtilis*, and the expression of major genes regulating biofilm matrix formation was enhanced in the presence of chlorine dioxide via the activation of membrane-bound kinase Kin C (Shemesh et al. 2010). In fact, the oxidative stress-triggered formation of membrane fouling can be regarded as a widely conserved response of microorganisms to various stressful conditions, e.g. Hoffman et al. (2005) showed that aminoglycoside antibiotics at subinhibitory concentration could also induce biofilm formation in the species of *P. aeruginosa* and *Escherichia coli*.

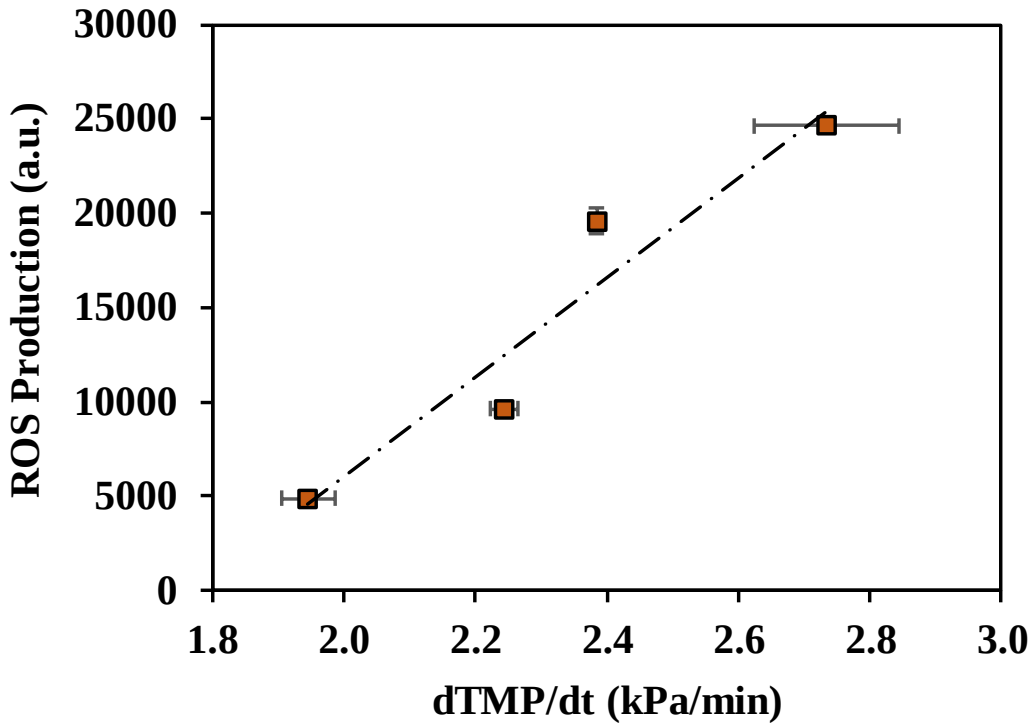

Figure 4.6 Relationship between ROS level and membrane fouling rate.

4.3.3 Structure of biofouling layer formed by stressed and non-stressed biomass

As discussed above, the induced production of oxidative stress had profound effects on the biofilm formation. Furthermore, CLSM was employed to visualize the structure of biofouling layer formed by stressed and non-stressed biomass at the initial cell viability of 50% in sludge suspension. **Figure 4.7** illustrated the trends of cell viability in biomass attached onto membrane versus filtration time. It should be noted that membrane filtration experiments for stressed and non-stressed bacteria were terminated when TMP reached 50 kPa. Since the fouling formation was accelerated by the induced oxidative stress (**Figure 4.4**), this is why the measurements for stressed bacteria stopped at around 30 min in contrast to nearly 80 min for the non-stressed bacteria. In the presence of oxidative stress, the percentage of viable cells in developed fouling layer rapidly increased from 51.3% after 5 min filtration to 84.4% after 30 min filtration. In the absence of

oxidative stress, attachment of live cells onto membrane surfaces remained insignificant at the level of 27-28% within the first 30 min filtration due to no apparent membrane fouling formation, however it gradually reached up to 58.5% after 80 min filtration. These seem to suggest that live bacteria were mainly found to the biofouling layer in the presence of oxidative stress, while dead bacteria primarily constituted biofilm in the absence of oxidative stress. Consistent with this observation, the three dimensional CLSM images (**Figure 4.8**) also revealed the similar phenomena with visualized fouling patterns. It can be seen clearly that without oxidative stress, dead bacteria preferentially adhered onto membrane surface, followed by the attachment of live cells. As for stressed microorganisms, on the contrary, more viable bacteria tended to adhere onto the membrane surface, supported by a layer of live bacteria at the membrane surface, while the top layer of biofilm predominantly consisted of dead bacteria. After 30 min membrane filtration, the stratification phenotype became more pronounced and a thick green layer (representing live bacteria) in the bottom can be observed. These indeed provide direct evidence showing oxidative stress promoted live bacteria to closely attach onto membrane, which in fact can be seen as a protective strategy for bacteria to survive under unfavourable environment.

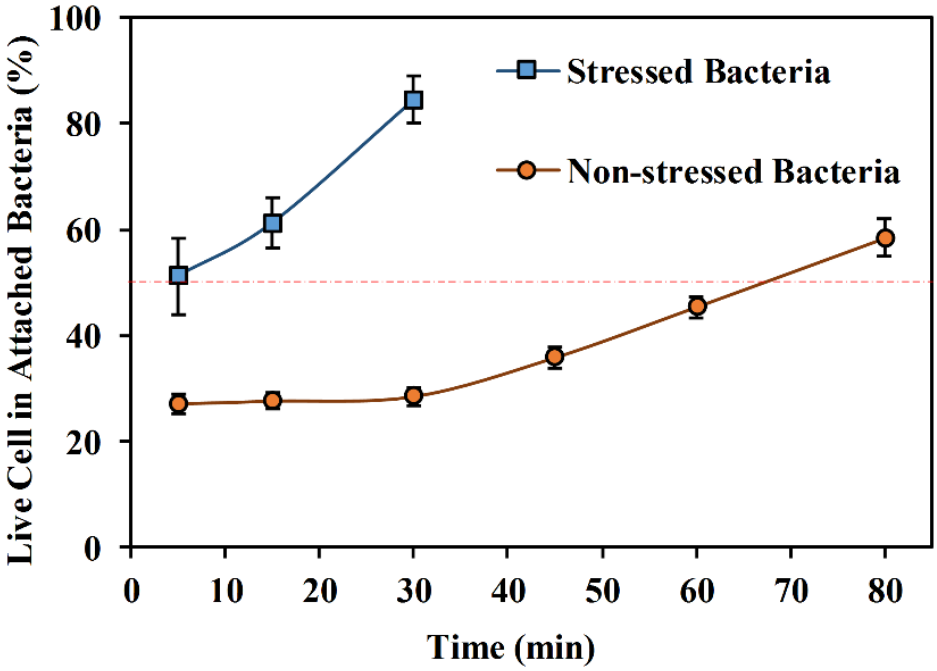

Figure 4.7 Live cell percentages of stressed and non-stress bacteria attached on membranes surface at the initial cell viability of 50%.

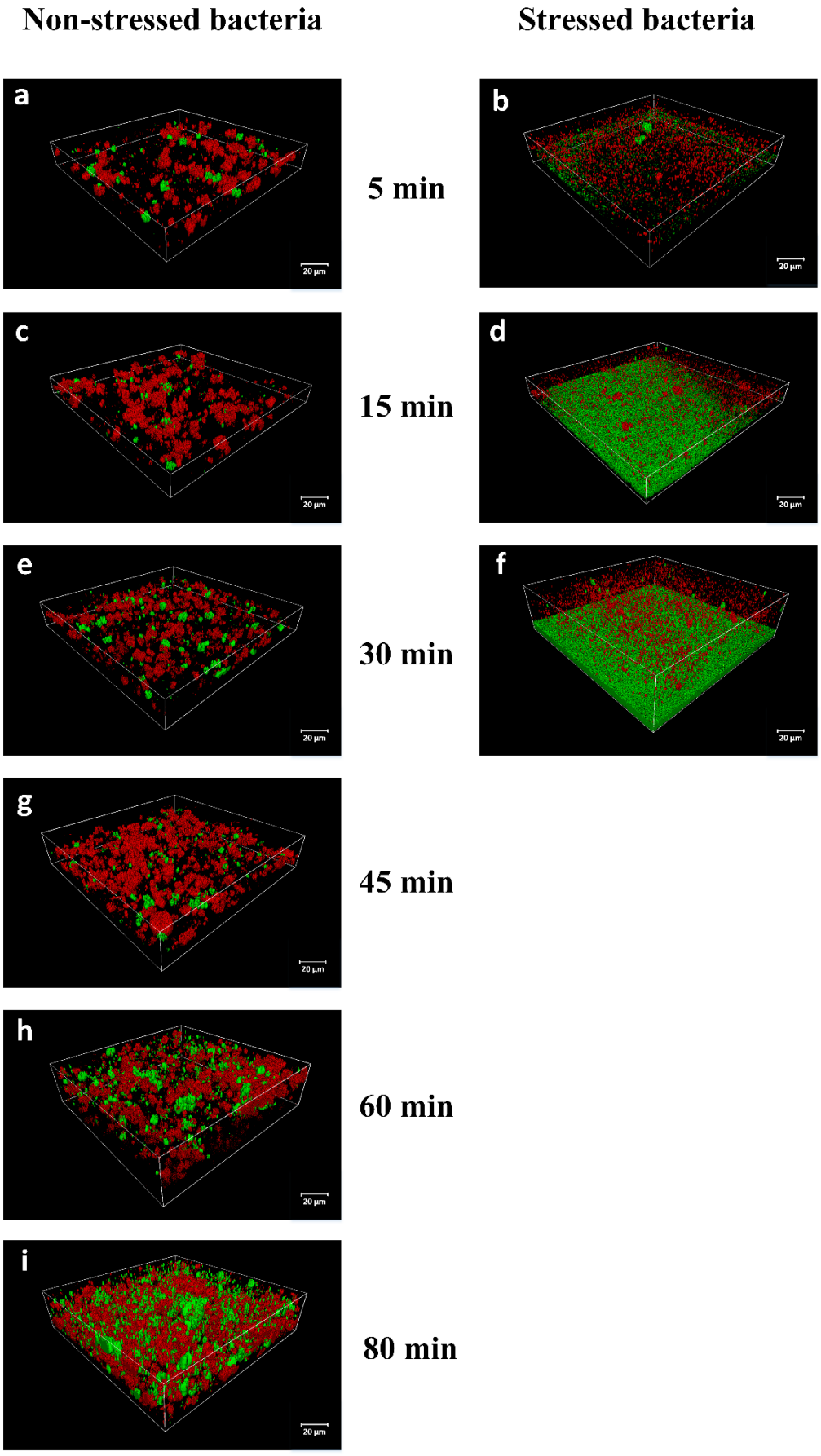
Non-stressed bacteria
Stressed bacteria
a
b
5 min
c
d
15 min
e
f
30 min
g
45 min
h
60 min
i
80 min
20 µm

Figure 4.8 Visualization of biofouling layer formed by stressed and non-stressed bacteria at the initial cell viability of 50%. Green color: live bacteria; Red color: dead bacteria.

It has been known that microorganisms tend to attach onto solid surfaces when they are subject to harsh conditions such as oxidative stress, heat shock etc. In fact, microorganisms seem to greatly benefit from the formation of aggregative community, due to the fact that biofilm-forming phenotype can protect themselves against deleterious conditions encountered (Cai and Liu 2016, Zhang et al. 2007). The underlying reasons are worth highlighting from two points. Firstly, the presence of multi-layer structure and EPS matrix of biofilm can hinder the penetration and reaction of disinfectants (Bridier et al. 2011). Secondly, microorganisms embedded in biofilm can develop numerous phenotypic adaptations via gene expression, gene transfer or gene mutation, which was devoted to their better antimicrobial protection (Bridier et al. 2011, Conibear et al. 2009, Maeda et al. 2006, Nguyen et al. 2010). This may also explain why microorganisms living in biofilm differ from those in planktonic culture. For example, *Klebsiella pneumoniae* attached on glass slides expressed an increased resistance to hypochlorous acid by 150-fold (Lechevallier et al. 1988). Similarly, *Pseudomonas aeruginosa* embedded in biofilm exhibited 2-600 times more resistant to heavy metal than their free-swimming counterparts (Teitzel and Parsek 2003). Due to the protective roles of biofilm, in this study, survived bacteria under oxidative stress tended to rapidly and predominately attach onto the membrane surface in order to mitigate damage (**Figures 4 and 7**). Meanwhile, the stratified biofilm structure (i.e. live bacteria in bottom layer and dead bacteria in top layer) appeared **(Figure 8**). It has been known that the basal layer of biofilm was generally characterized by stronger cohesion strengths than the outer layer (Derlon et al. 2008). Besides, the outer layer may also provide another barrier to protect inner bacteria. Therefore, the appearance of stratified biofilm architecture in this study indeed confers a much better survival superiority for microorganisms against unfavourable conditions.

Based on this study, it should be expected that during practical chemical cleaning of MBR, the unavoidable exposure of microorganisms to NaClO may trigger the overproduction of oxidative stress, which can subsequently enhance membrane fouling development during the next-round operation. Meanwhile, the structure of fouling layer may be changed as well, which exhibits better resistance to harsh conditions. Therefore, in the long-term operation of MBR with frequent chemical cleaning, it can be anticipated that microorganisms have a tendency to develop much stronger adaptation and resistance phenotype, leading to the less and less effectiveness of antifouling agents (e.g. NaClO). For instance, by cleaning fouled membrane from MBR with NaClO, Navarro et al. (2016) found a great fraction of survived bacteria remained on cleaned membrane belonged to close relatives of extremophiles, e.g. halotolerant bacteria, and apparent proliferation of these bacteria was observed on the membrane surface in the subsequent operation of MBR, indicative of developed resistance of these bacteria to NaClO. To overcome such developed microbial resistance while achieve sustainable permeability, the usage of high-dosage disinfectant is inevitable, which in turn may lead to more severe membrane biofouling at an accelerated pace. Given such vicious cycle, in a long-term, might gravely impair MBR performance and increase operational cost, it is necessary to explore novel environmentally friendly strategies for membrane cleaning in MBR.

4.4 CONCLUSIONS

This study probably for the first time investigated the potential impacts of NaClO-induced oxidative stress on the development of membrane biofouling. It was clearly shown that the stressed bacteria at various ROS levels exhibited higher membrane fouling tendency than the respective control at the same cell viability. In the presence of oxidative stress, more viable bacteria tended to rapidly migrate from the solution onto the membrane surface especially on the bottom layer of biofilm, and this can be regarded as an effective strategy protecting bacteria from the oxidative stress. On the contrary, in the absence of oxidative stress, dead bacteria preferentially adhered onto the membrane surface.

Consequently, this study provided new insights into the undesirable impacts of on-line chemical cleaning with NaClO on MBR operation, and novel membrane cleaning strategy with environmental friendly features should be explored.

CHAPTER 5 GENERATION OF DISSOLVED ORGANIC MATTER AND BYPRODUCTS FROM ON-LINE CHEMICAL CLEANING WITH SODIUM HYPOCHLORITE IN MBR

5.1 INTRODUCTION

As described above, during on-line chemical cleaning, NaClO solution is injected into the membrane in reverse to normal filtration, while the membrane module is still soaked in the bioreactor (Wang et al. 2014b, Wei et al. 2011). After passing through fouling layer accumulated on membrane surface, the residual effective NaClO is further diffused into bulk suspension, as a result of which microorganisms and soluble organic matter may be oxidized. These suggest that suspended activated sludge in MBR may also be oxidized by NaClO in the course of on-line chemical cleaning. As a consequence of such exposure, microbial lysis induced by NaClO may occur since NaClO, as a strong oxidant, has been known to break up sludge flocs or partially solubilize bacterial cells (Cai and Liu 2016, Lee et al. 2013, Lim et al. 2005).

In MBR, dissolved organic matter (DOM) generally originates from influent wastewater and microorganisms-associated soluble microbial products (SMP) (Wang et al. 2013a). As presented above, it is reasonable to consider that a wide variety of DOM may also be produced as a result of cell lysis triggered by NaClO. Meanwhile, the organic matter in MBR may further react with NaClO to generate a variety of byproducts, which may raise serious concerns if these byproducts are

---

The content in this chapter has been published as: Cai, W., Liu, J., Zhang, X., Ng, W.J. and Liu, Y., 2016. Generation of dissolved organic matter and byproducts from activated sludge during contact with sodium hypochlorite and its implications to on-line chemical cleaning in MBR. Water Res. 104, 44-52.

brought into effluent destined for receiving water bodies or even public water supplies (Doederer et al., 2014; Sedlak and von Gunten, 2011). However, little information is currently available for the DOM and byproducts produced in MBR, especially from the perspective of those triggered by on-line chemical cleaning. In chapter 3, we had reported that a substantial amount of bacterial cells were solubilized after exposure of biomass to NaClO. This study, therefore, aims to further characterize these DOM and subsequent byproducts produced. For this purpose, the composition of DOM released from activated sludge after exposure to NaClO was characterized by a three-dimensional excitation-emission matrix (EEM) fluorescence spectroscope, and the formation of halogenated byproducts was investigated by measuring total organic halogen (TOX) with a TOX analyser and by selectively detecting halogenated compounds with an ultra performance liquid chromatography/electrospray ionization-triple quadrupole mass spectrometer (UPLC/ESI-tqMS), which has been successful applied in detection, identification and quantification of halogenated byproducts in drinking water and wastewater (Yang and Zhang 2013, 2014, Zhai et al. 2014). This study may provide direct experimental evidence showing the generation of various DOM and byproducts, which also raises the concern about the current practice of on-line chemical cleaning of membranes in MBR.

5.2 MATERIALS AND METHODS

5.2.1 Chemicals and organic solvents

NaClO stock solution (4%-4.99%) was purchased from Sigma–Aldrich and standardized by N, N-diethyl-p-phenylenediamine (Hach, USA) before usage. Standard compounds including chlorobromoacetic acid (97%), dichloroacetic acid (>99%), trichloroacetic acid (>99%), 4-chlorophenol (>99%), 5-bromosalicylic acid (90%), 5-chlorosalicylic acid (98%), iodoacetic acid (>99%), 2,4,6-tribromophenol (99%), 2,4,6-trichlorophenol (98%), pyrrole (99%) were ordered from Sigma–Aldrich. Besides that, 3,5-dibromo-4-hydroxybenzaldehyde (98%) was purchase from Alfa Aesar, and tetrabromopyrrole was synthesized (based on the reaction of pyrrole with

bromine) in the laboratory according to the procedure by Yang and Zhang (2014) since it was not commercially available. Organic solvents (HPLC grade) including acetonitrile, methyl tert butyl ether (MtBE), ethanol and methanol, and all the other chemicals (reagent grade) were purchased form Sigma–Aldrich.

5.2.2 Sludge treatment assay

Activated sludge collected from a local wastewater treatment plant was acclimatized in a chemostat for one month with a synthetic substrate mainly consisting of CH_3COOH (690 mg/L), glucose (313 mg/L), NH_4Cl (200 mg/L), K_2HPO_4 (60 mg/L) and other trace minerals. The acclimatized activated sludge was washed thrice with a 10 mM phosphate buffered saline solution before use. NaClO stock solution was then dosed to a series of 1 L bioreactors for having respective initial NaClO concentration of 0, 2, 5, 10, and 20 mg/L, which was selected according to other relevant studies (Cai and Liu 2016, Han et al. 2016, Lee et al. 2013, Lim et al. 2005). The initial biomass concentration was maintained at around 1000 mg/L, and dissolved oxygen concentration in each bioreactor was kept at quasi-saturation level through aeration. The contact time between activated sludge and NaClO was 30 min, after which nearly all the chlorine was exhausted. The residual total chlorine was quenched with $NaAsO_2$ after the reaction according to the standard method (APHA, 2012). Thereafter, the supernatant was collected and filtered through 0.45 mm membrane for further analysis. In fact, the free chlorine residual was not detectable, whereas the combined chlorine was found to be in the range of 0-0.2 mg/L after 30-min exposure to 0-20 mg/L NaClO.

5.2.3 EEM analyses

A fluorescence spectrophotometer (LS55, Perkin Elmer Company, USA) was employed to obtain three dimensional EEM spectra. Excitation scans were performed from 200 to 500 nm at 5 nm intervals. For each excitation wavelength, emission wavelengths were scanned at 0.5 nm steps varying from 200 to 500 nm. A 10 nm band-pass of excitation and emission slits and 1200 nm/min of scanning speed were set in this study. The threshold of fluorescence emission intensity is

1000 a.u.. Since all of the EEM analyses were done on the same day with the same instrument. This offers a basis for data comparison, and data normalization and correction were not conducted as the fluorescence values obtained were expressed as fluorescence intensity unit (a.u.). The exported EEM data were processed with Origin 9.0 (OriginLab Inc., USA). The EEM spectra were plotted as elliptical shape of contours. The X and Y axis respectively represent the emission and excitation spectra, and the third dimension, which represents the contour lines, expresses the fluorescence intensity. The EEM data were further analysed using fluorescence regional integration (FRI) technique (Chen et al. 2003). In brief, volumetric integration beneath EEM was conducted within each selected region. The volume Φ_i beneath region "*i*", representing the fluorescence response of DOM with similar characteristics, was calculated based on equations (5.1) - (5.4):

$$\Phi_i = \sum_{ex} \sum_{em} I(\lambda_{ex}\lambda_{em})\Delta\lambda_{em}\Delta\lambda_{ex} \tag{5.1}$$

in which, $\Delta\lambda_{ex}$ is the excitation wavelength interval (taken as 5 nm), and $\Delta\lambda_{em}$ is the emission wavelength interval (taken as 0.5 nm). Normalized excitation–emission area volumes $(\Phi_{i,n}, \Phi_{T,n})$ and percent fluorescence response $P_{i,n}$ were calculated as follows:

$$\Phi_{i,n} = MF_i\Phi_i = MF_i \sum_{ex} \sum_{em} I(\lambda_{ex}\lambda_{em})\Delta\lambda_{em}\Delta\lambda_{ex} \tag{5.2}$$

$$\Phi_{T,n} = \sum \Phi_{i,n} \tag{5.3}$$

$$P_{i,n} = \frac{\Phi_{i,n}}{\Phi_{T,n}} \times 100\% \tag{5.4}$$

In order to avoid possible effect of Raleigh scattering, all the first- and second-order Raleigh scatterings were subtracted from accounting the peak area in each region by using Origin 9.0.

5.2.4 TOX measurement

TOX was measured according to Standard Method 5320B (APHA, 2012), except that an ion chromatograph was used for analysing Cl^- and Br^- (Li et al. 2011, Liu and Zhang 2013), and the Waters UPLC/ESI-tqMS was used for analysing I^- (Pan and Zhang 2013b). In brief, 400 mL of each produced DOM sample was adjusted to pH=2 with nitric acid. A 3-channel adsorption module (TXA03C, Mitsubishi Chemical Analytech) was used for activated carbon adsorption. Before adsorption of each sample, the sample reservoir in the adsorption module was pre-cleaned sequentially with 20 mL ultrapure water and 20 mL sample. Then 300 mL of the produced DOM sample was evenly divided into three aliquots (100 mL each), and each aliquot was passed through two consecutive prepacked activated carbon columns (Mitsubishi Chemical Analytech) at a flow rate of 3 mL/min. After adsorption, the activated carbon columns were rinsed with 30 mL of 5000 mg/L KNO_3 as NO_3^- to remove inorganic halides, and were subsequently subjected to pyrolysis at 1000 °C with an AQF-100 automatic quick furnace (Mitsubishi Chemical Analytech). The hydrogen halide and halogen gases produced from pyrolysis were absorbed in ultrapure water. Then the whole absorption solution (around 7 mL) was transferred to a 15 mL tube, and the final volume of the absorption solution was adjusted to 8 mL with ultrapure water. By doing these, the TOCl, TOBr and TOI in each 100 mL aliquot were converted and transferred into the 8 mL absorption solution in the form of Cl^-, Br^- and I^-, respectively.

1 mL of the absorption solution was analyzed by an ICS-3000 ion chromatography system (Dionex). A KOH eluent was generated by the EGC KOH cartridge (Dionex) at a flow rate of 1 mL/min. Chloride and bromide were separated with an isocratic eluent of 10 mM KOH from 0 to 10 min followed by a linear gradient eluent of 10−45 mM KOH from 10 to 25 min. The concentrations of the halides were quantified with a conductivity detector. The practical quantitation limits for TOCl and TOBr were 0.002 mg/L as Cl and 0.004 mg/L as Br, respectively. Calibrations of chloride and bromide ions in ion chromatograph measurement were conducted by injecting a series of NaCl and

NaBr aqueous solutions at different concentrations into the ion chromatograph. 2,4,6-trichlorophenol and 2,4,6-tribromophenol were the standard compounds for TOCl and TOBr according to the standard method (APHA, 2012). To determine the recoveries of TOCl and TOBr during TOX measurement, two 400 mL standard solutions were prepared. One solution contained 2,4,6-trichlorophenol at 0.01 mg/L as Cl, 2,4,6-tribromophenol at 0.005 mg/L as Br and NaCl at 8000 mg/L, and the other solution contained 2,4,6-trichlorophenol at 0.05 mg/L as Cl, 2,4,6-tribromophenol at 0.01 mg/L as Br and NaCl at 8000 mg/L. NaCl was added to both standard solutions to simulate the matrix (mainly chloride concentration) in each DOM sample. Both solutions were subjected to triplicate TOCl and TOBr measurements as aforementioned.

Another 3 mL of the absorption solution was first acidified to pH < 3 with formic acid, followed by nitrogen sparging at 150 mL/min for 2 min (Pan and Zhang 2013b), and then analysed by Waters UPLC/ESI-tqMS. 5 μL of a pretreated sample was injected into the UPLC. The operation parameters were set according to (Pan and Zhang 2013b) as follows: UPLC eluent, 0.5 mL/min of ultrapure water containing 0.3% (v/v) formic acid; run duration, 6 min; ESI negative mode; capillary voltage, 2.8 kV; cone voltage, 40 V; source temperature, 120 °C; desolvation temperature, 400 °C; desolvation gas flow, 800 L/h; cone gas flow, 50 L/h; low and high mass resolutions, 15 (1-unit resolution). Under these conditions, I^- in a pre-treated absorption solution can be selectively detected by the UPLC/ESI-tqMS selective ion recording scan of *m/z* 126.9, and the peak area of I^- was used to calculate the TOI concentration in the water sample, according to the calibration curve obtained by the measurement of iodoacetic acid standard solutions at 0, 5, 10, 20 and 50 μg/L as I. For the 100 mL adsorption volume, the practical quantitation limit for TOI was 2 μg/L as I.

5.2.5 (UPLC)/ ESI-tqMS analyses

Prior to (UPLC)/ ESI-tqMS analyses, each DOM sample was pre-treated according to (Zhang et al. 2008b). In brief, 1500 mL of each water sample was first acidified to pH < 0.5 with 70% (v/v) aqueous sulfuric acid, followed by the

addition of sodium sulfate to saturation. Then, the acidified sample was extracted with 150 mL MtBE, and 110 mL of the organic layer was transferred to a rotary evaporator and concentrated to 0.5 mL. This 0.5 mL solution in MtBE was mixed with 20 mL acetonitrile, and the mixture was concentrated back to 1 mL, and stored at 4 °C. Prior to UPLC/ESI-tqMS analyses, 0.5 mL of the acetonitrile solution was diluted to 1 mL with ultrapure water, and filtered with 0.45 μm membrane.

The operation parameters of ESI-tqMS were set according to previous studies (Yang and Zhang 2013, Zhai et al. 2014). ESI negative mode; desolvation temperature 350 ºC; source temperature 120 ºC; capillary voltage 2.8 kV; desolvation gas 650 L/h; cone gas 50 L/h; cone voltage 30 V for chlorinated byproducts and 15 V for brominated byproducts; collision energy 30 eV for chlorinated byproducts and 20 eV for brominated byproducts; collision gas 0.25 mL/min. In UPLC/ESI-tqMS full scans, the operational parameters were set as the same as aforementioned for ESI-tqMS, except that desolvation gas flow 800 L/h, desolvation temperature 400 °C, cone voltage 20 V and scan time 0.06 s were applied. With the powerful of precursor ion scan (PIS) function, all electrospray-ionizable halogenated byproducts can be selectively detected (Pan and Zhang 2013b, Zhai and Zhang 2011). Multichannel analysis mode was used for data collection for all PISs, with a scan time of 0.3 s, run durations of 8 min for PISs m/z 35/37 (for chlorinated byproducts), and 6 min for PISs m/z 79/81 (for brominated byproducts). By doing this, precursor ion intensities were substantially enhanced by accumulating multiple scans (1600 scans for PISs m/z 35/37, and 1200 scans for PISs m/z 79/81), and intensity fluctuation in a single scan was effectively eliminated. Besides, UPLC/ESI-tqMS full scans at different m/z ranges (i.e. 100-210, 200-310 and 300-410) were conducted for each DOM sample. A 7.5 mL pretreated sample was injected into the UPLC. Water–methanol binary eluent at 0.4 mL/min was used at 35 ˚C column temperature. The eluent changed linearly from 90% water to 10% water in 0-7.50 min, and then returned to 90% water in 7.50-7.60 min, which was maintained in 7.60-

10.00 min. In UPLC/ESI-tqMS full scans, the operational parameters were also set per previous studies (Yang and Zhang 2013, Zhai et al. 2014).

5.2.6 Other measurements

The Quant-iT PicoGreen dsDNA Assay Kit (Molecular Probes) was used to measure soluble DNA concentration based on the protocol provided by the kit. The lambda DNA was used as the standard, and fluorescence intensity was recorded by a microplate reader (Tecan, infinite 200 PRO). Dissolved organic carbon (DOC) was analysed by a total organic carbon analyser (Shimadzu, Japan). Polysaccharide and protein contents were measured by the phenol-sulfuric acid method (Dubois et al. 1956) and Lowry method (Lowry et al. 1951) with glucose and bovine serum albumin as the standards, respectively.

5.3 RESULUTS AND DISCUSSION

5.3.1 NaClO-triggered DOM release

Figure 5.1a showed the release of DOM after exposure to various NaClO dosages of 0, 2, 5, 10 and 20 mg/L for 30 min, while the DOC concentration in liquid phase was found to increase from 2.7 to 24.7 mg/L. The concentration of each DOM component in terms of polysaccharides and proteins was summarized in **Table 5.1**, showing the presence of diverse organic matters after exposure of biomass to NaClO. According to the study in chapter 3 and 4, this observed bacterial lysis mainly resulted from strong oxidation by NaClO. Consequently, a substantial amount of present microorganisms was chemically solubilized to DOM. Furthermore, it was clearly observed in **Figure 5.1b** that the DNA level in water phase was increased from 0.02 to 0.54 mg/L, indicating a 27-fold rise, after 30 min exposure to a NaClO dose of 20 mg/L. This indeed provided evidence supporting the bacterial lysis. Moreover, it should be noted that the released DOM (up to 24.7 mg/L) may adversely affect permeate quality and membrane fouling during the long-term MBR operation. Similarly, Lee et al. (2013) found that soluble chemical oxygen demand (SCOD) was increased by roughly 180 mg/L in an MBR after 30 min exposure to NaClO dosage of 55 mg/g

MLVSS. According to Lim et al. (2005), around 250% increase in the COD concentration was also observed after 24 h oxidation with 50 mg NaClO/g SS as compared with control.

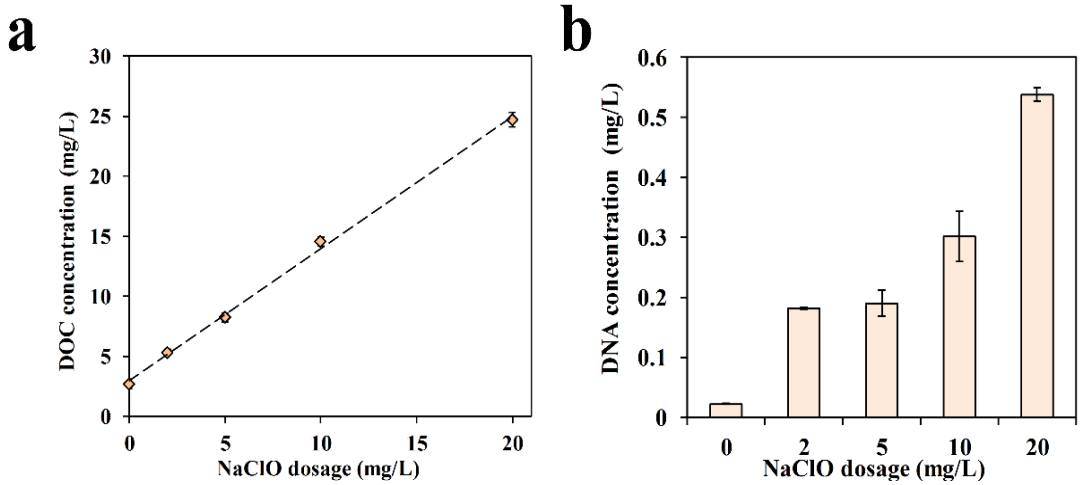

Figure 5.1 (a) Released DOC concentration and (b) DNA concentration in liquid phase after 30 min exposure to NaClO.

Table 5.1 Polysaccharide and protein concentrations in the released DOM from activated sludge after 30 min exposure to NaClO.

NaClO dosage (mg/L)	Polysaccharide concentration (mg/L)	Protein concentration (mg/L)
0	1.13	0.46
2	1.96	2.90
5	3.16	6.10
10	5.04	9.61
20	9.20	14.01

5.3.2 EEM fluorescence analysis of released DOM

Figure 5.2 shows the three-dimensional EEM spectra of DOM released from activated sludge after 30 min exposure to NaClO dosage of 0-20 mg/L. The four main peaks were gradually intensified with the increase of NaClO dosage, suggesting a wide variety of organic matters were released into the liquid phase after exposure of biomass to NaClO. Peak A and peak B were located at

excitation/emission wavelengths (Ex/Em) of 200-220/315-355 nm and 275/307-360 nm, which have been reported to be tyrosine-like substances and tryptophan protein-like substances, respectively (Baker 2001, Coble 1996, Xu and Jiang 2013, Yamashita and Tanoue 2003). Peak C and D detected with Ex/Em at 265-270/455 nm and 355-360/412-455 nm, respectively, were generally referred as humic acid-like substances (Baker 2001, Chen et al. 2003, Coble 1996). The fluorescence parameters including specific peak location and fluorescence intensity of the peaks are summarized in **Table 5.2**. Tyrosine protein-like substances appeared to be the principle component detected in the control DOM reflecting the background property. After exposure to NaClO, Peaks B to D gradually became predominant, indicating that a significant amount of tryptophan protein-like as well as humic acid-like materials were produced from cellular lysis of activated sludge induced by NaClO. For all the four peaks, the fluorescence intensities were positively related to the NaClO dosages, which suggested both protein-like (Peak A and B) and humic acid-like (Peak C and D) substances were significantly generated. It can be seen that more protein-like materials were released when low NaClO dosage (i.e. 0-10 mg/L) were used, while content of humic acid-like substances exceeded protein-like materials as NaClO dosage further increased (i.e. 20 mg/L). The fluorescence intensities of Peak A to D observed at NaClO dosage of 20 mg/L were 259%, 250%, 1525% and 875%, respectively, higher than those detected in control. The released DOM at NaClO dosage of 20 mg/L was mainly composed of humic acid-like substances (Peak C 523.3 a.u. and Peak D 299.4 a.u.), followed by tyrosine protein-like substances (Peak A 519.3 a.u.) and tryptophan protein-like substances (Peak B 172.0 a.u.). In addition to fluorescence intensity-based quantitative analysis, peak location is another characteristic indicator of organic substances. The locations of Peak A and peak B were gradually blue shifted in terms of emission wavelength, respectively, with increasing the NaClO dose from 0 to 20 mg/L. In fact, a blue shift in emission peak is generally associated with structural changes, including the fragmentation of large molecules, decrease of conjugated bonds in a chain structure or aromatic rings, or elimination of amine, hydroxyl and carbonyl groups (Coble 1996, Senesi 1990, Swietlik and Sikorska 2004). A

similar blue-shift trend was also observed at the result of decreased aromaticity and breakup of large molecules of natural organic matter during chlorine dioxide disinfection (Swietlik et al. 2004, Swietlik and Sikorska 2004).

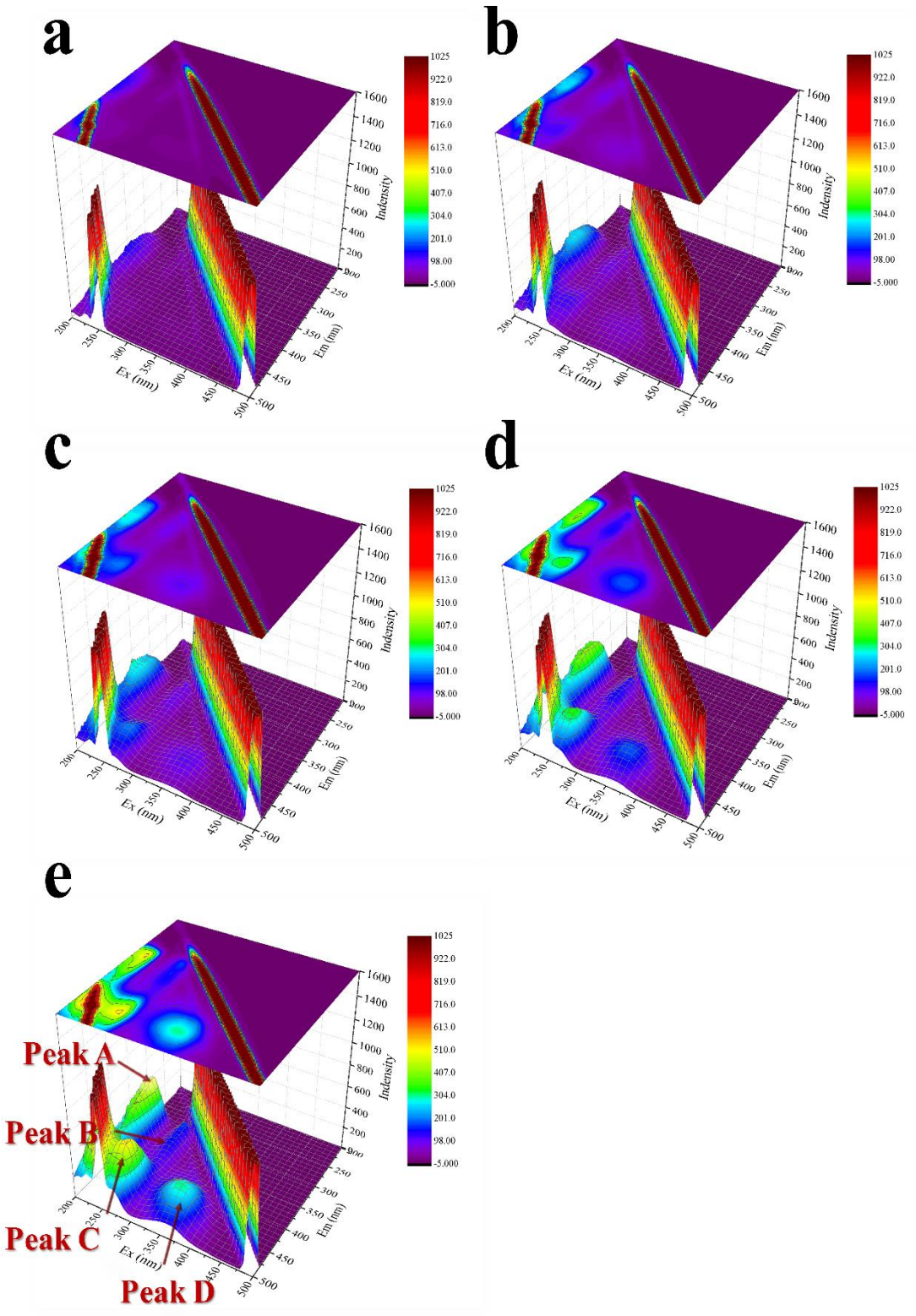

Figure 5.2 EEM fluorescence spectra of the DOM released from activated sludge after 30 min exposure to NaClO doses of (a) 0 mg/L, (b) 2 mg/L, (c) 5 mg/L, (d) 10 mg/L and (e) 20 mg/L.

Table 5.2 Fluorescence spectral parameters of released DOM from activated sludge after 30 min exposure to NaClO.

NaClO dose	Peak A		Peak B		Peak C		Peak D	
(mg/L)	Ex/Em	Intensity	Ex/Em	Intensity	Ex/Em	Intentisy	Ex/Em	Intensity
0	200/350	144.7	275/307	49.2	265/455	32.2	360/412	30.7
2	215/355	264.5	275/355	80.7	265/455	118.6	360/455	62.7
5	200/350	323.9	275/350	85.8	265/455	197.0	360/455	101.5
10	215/345	416.5	275/360	142.1	265/455	336.8	360/455	180.0
20	220/315	519.3	275/310	172.0	270/455	523.3	355/450	299.4

Since several fluorescence peaks with low intensities could not be clearly identified in **Figure 5.2**, the FRI technique was employed to further analyse and quantitatively assess the changes of componential structure in the released DOM. According to Chen et al. (2003), fluorescence peaks of respective substances with corresponding Ex and Em ranges are as follows: Regions I and II (Ex/Em = 200-250/200–380 nm, simple aromatic protein-like substances); Region III (Ex/Em = 200-250/380–500 nm, fulvic acid-like materials); Region IV (Ex/Em = 250-280/200–380 nm, soluble microbial byproduct-like materials); Region V (Ex/Em = 280-500/380–500 nm, humic acid-like organics). Based on the volumetric integration within each region, the FRI distribution of DOM released was calculated as shown in **Figure 5.3**. The chemical composition of released DOM varied greatly with different NaClO dosages applied. In the control free of NaClO treatment, Region I + II (protein-like substances) showed the highest $P_{i,n}$ (40.6%). However, the $P_{i,n}$ value of Region I + II was found to decline, while $P_{i,n}$ corresponding to Region V for humic acid-like substances appeared to rise up rapidly with increasing the NaClO dosage. As for DOM released at a NaClO dosage of 20 mg/L, the predominant compounds were humic acid-like materials (with $P_{i,n}$ of 48.3%), sequentially followed by fulvic acid-like materials with $P_{i,n}$ of 22.8%, protein-like substances with $P_{i,n}$ of 22.2%, and soluble microbial byproduct-like materials with $P_{i,n}$ of 6.7%. In addition, EEM may also offer indications of the biodegradability of DOM because of its capability to distinguish biodegradable substances (e.g. tyrosine protein-like and microbial byproduct-like compounds) and non-biodegradable materials (e.g. humic acid-, fulvic acid- and tryptophan protein-like compounds) (Guo et al. 2014, Jia et al. 2013). It appears that most of DOM released from activated sludge after exposure

to NaClO, e.g., humic acid-like substances, was not readily biodegradable, i.e. they could not be easily utilized by microorganisms in MBR. In addition, humic acid-like substances may easily pass through microfiltration membrane and end up in the permeate of MBR (Lee et al. 2003) which may cause a serious concern about the permeate quality and water reuse.

It should be noted that the origin of the produced humic acid-like substances deserves further investigation. It has been known that humic acids contain various functional groups including phenolic, carboxylic acid, enolic, quinone, ether etc., among which quinone moieties with the electron-shuttling ability are primarily responsible for the redox mediating property of humic acids (Gomes de Melo et al. 2016). Meanwhile, quinones also contribute greatly to the fluorescence of humic acid, while a positive link between the fluorophores and redox-active quinones has been reported (Yang et al. 2016). Based on these findings, it is reasonable to speculate the humic acid-like substances detected with EEM in this study might likely originate from quinones or their related analogues. Moreover, **Table 5.2** showed that peak C, the most intense peak of humic acid-like substances, appeared at the excitation location of 265-270 nm, which was consistent with the excitation maximum of a model dihydroquinone (Ex=267 nm) reported by and Cory and McKnight (2005). This in turn supports the above discussion. Obviously, further investigation should be needed to identify the detailed origins of the released humic acid-like substances.

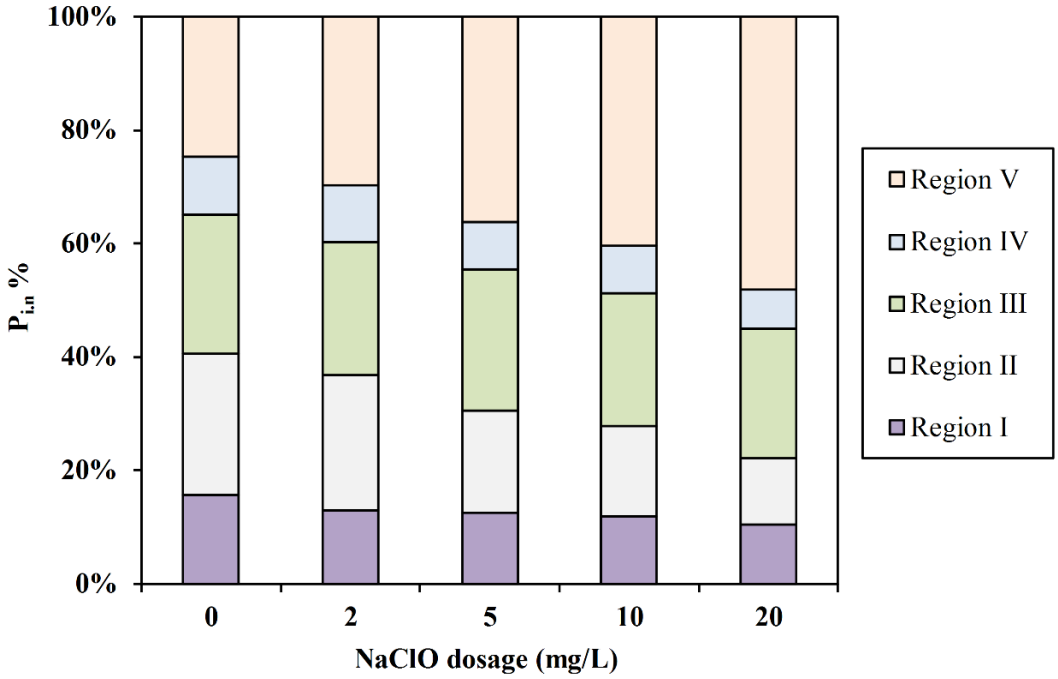

Figure 5.3 FRI distribution of released DOM from activated sludge after 30 min exposure to NaClO.

5.3.3 Formation of byproducts after exposure of activated sludge to NaClO

Byproducts generated from chlorination have been seriously due to their potential toxicity and adverse effects on the water ecosystem and public health. In this study, the formation of disinfection byproducts (DBPs) is expectable since the present organic matter can be easily oxidized by NaClO. Although several components of released DOM have been already identified by the EEM fluorescence analysis, further investigation on the formation of the DBPs and their impacts on receiving water body are still needed. TOCl, TOBr and TOI in the released DOM were determined in this study, while the sum of these three specific organic halides can be considered as TOX reflecting the total halogenated DBPs. **Figure 5.4** showed the TOCl and TOBr concentrations in the DOM produced from activated sludge after exposure to different NaClO doses, while none of the specific TOX can be detected in the control of NaClO treatment. It should also be noted that the concentration of TOI was not detectable, while relatively low levels of TOBr detected in the released DOM likely might originate from bromides in activated sludge. During chlorination, bromide was

oxidized by NaClO to HOBr/OBr^-, which then reacted with organic matter to generate brominated byproducts. It has been demonstrated that brominated byproducts exhibited dozens to hundreds of times higher toxicity than their chlorinated analogues (Liu and Zhang 2014, Pals et al. 2013, Richardson and Ternes 2014, Yang and Zhang 2013). Rapid increases in TOCl and TOBr concentrations were observed when the NaClO dosage was increased from 2 to 20 mg/L. The TOX concentration was in the range of 14.3 mg/L to 68.7 mg/L as Cl. Compared to the NaClO dosage at 2 mg/L, the TOCl concentration increased by 62%, 287% and 377%, and the TOBr level increased by 33%, 158% and 267%, when the NaClO dosage increased to 5, 10 and 20 mg/L, respectively.

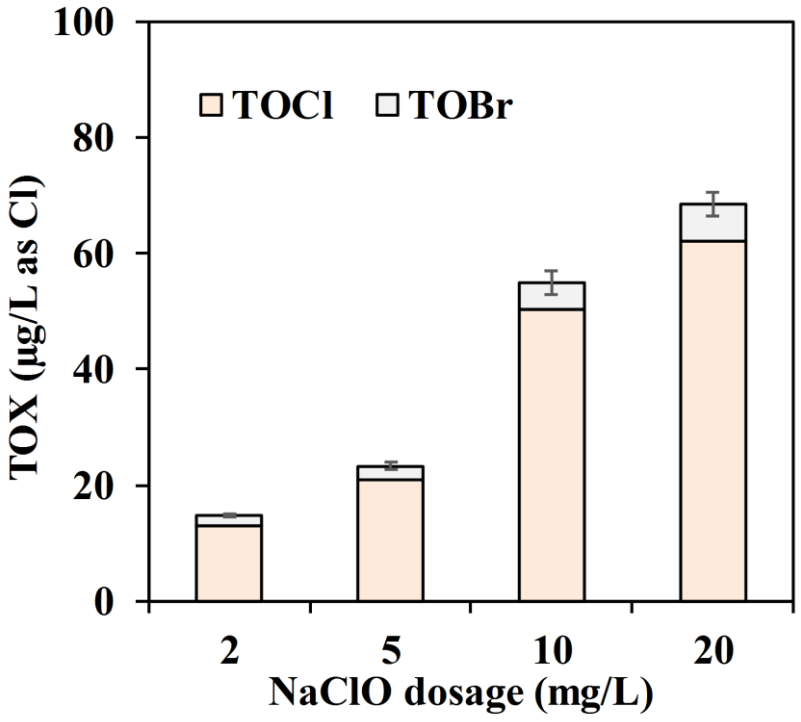

Figure 5.4 TOCl and TOBr concentrations in the released DOM from activated sludge after 30 min exposure to NaClO.

Figure 5.5 shows the ESI-tqMS PIS spectra of m/z 35 of the DOM released after exposure to different doses of NaClO for 30 min. The total ion intensity (TII) (of m/z 70 to 400) in each spectrum is approximately proportional to the quantity of all polar chlorinated byproducts in the released DOM. The TII value followed an

ascending order with increasing the NaClO dosage, i.e., 1.91×10^7 (0 mg/L) < 2.81×10^7 (2 mg/L) < 2.34×10^7 (5 mg/L) < 3.28×10^7 (10 mg/L) < 3.64×10^7 (20 mg/L), indicating that the concentration of overall polar chlorinated byproducts increased with the rising NaClO dosage. The TII trend was consistent with that of TOCl as shown in **Figure 5.4**.

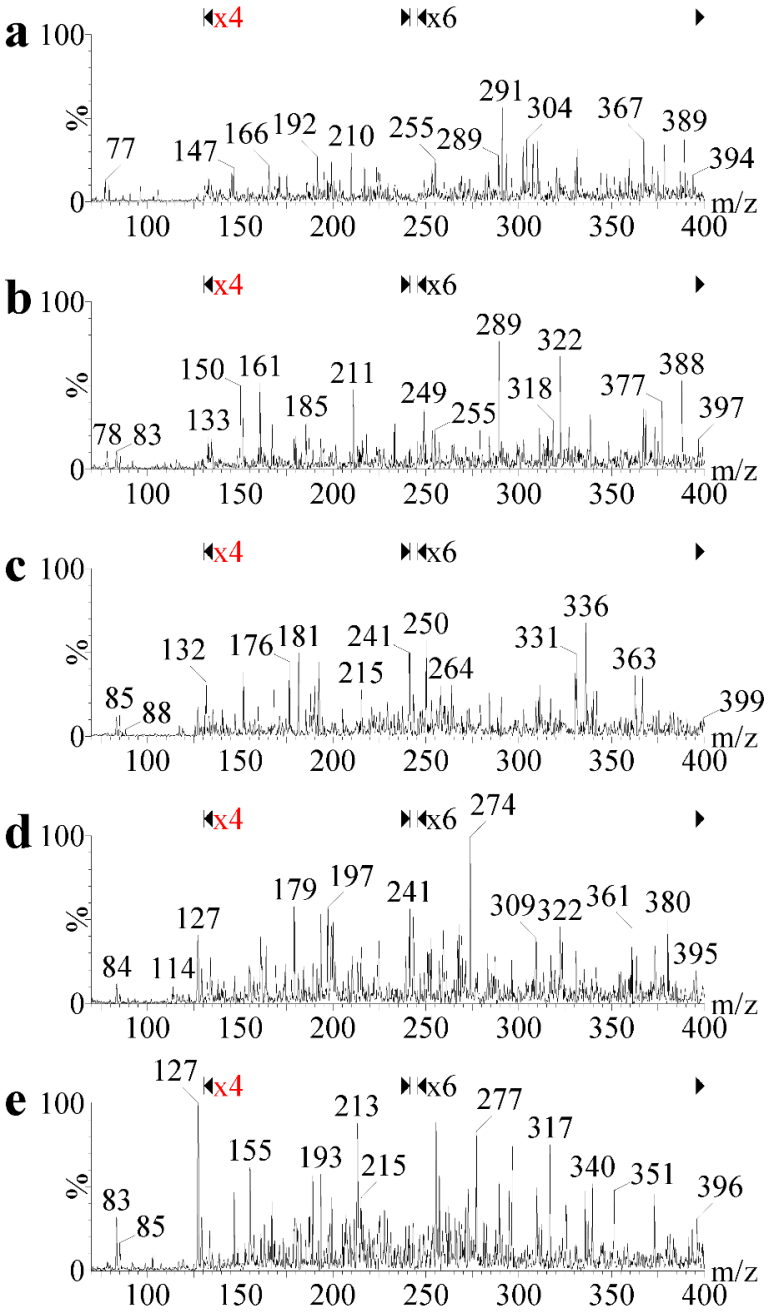

Figure 5.5 ESI-tqMS PIS spectra of m/z 35 of the released DOM from activated sludge after 30 min exposure to (a) 0 mg/L, (b) 2 mg/L, (c) 5 mg/L, (d) 10 mg/L,

and (e) 20 mg/L NaClO. " × 4" and " × 6" in charts indicates that the spectra in the m/z range is magnified by 4 times and 6 times (the y-axes are on the same scale).

Figure 5.6–5.8 showed the chromatograms and spectra of UPLC/ESI-tqMS full scans of m/z 100-210, 200-310 and 300-410, respectively, in the DOM produced from activated sludge dosed with 20 mg/L NaClO. For each ion cluster detected, its structure was proposed based on the retention times and isotopic abundance ratio. A total of 19 chlorinated and brominated byproducts were detected in the sample. Eight of them were confirmed with standard compounds, including dichloroacetic acid (m/z 127/129/131 and m/z 83/85/87), trichloroacetic acid (m/z 161/163/165/167 and m/z 117/119/121/123), bromochloroacetic acid (m/z 171/173/175), 4-chlorophenol (m/z 127/129), 5-chlorosalicylic acid (m/z 171/173), 5-bromosalicylic acid (m/z 215/217), 3,5-dibromo-4-hydroxybenzaldehyde (m/z 277/279/281), and tetrabromopyrrole (m/z 378/380/382/384/386) (**Table 5.3**). The confirmation of 3,5-dibromo-4-hydroxybenzaldehyde and tetrabromopyrrole is exemplified as shown in **Figure 5.9-5.10**, respectively. The retention time, structure and occurrence of some ion clusters are listed in **Table 5.3**. At the NaClO dosage of 2 mg/L, only 5-chloro-6-hydroxyisophthalic acid (m/z 215/217) and 5-bromo-6- hydroxyisophthalic acid (m/z 259/261) were formed. At 5 mg/L NaClO, one more byproduct, 4-chlorophenol (m/z 127/129) was detected. When the NaClO dose was further increased to 10 mg/L, other four byproducts, dichloroacetic acids, trichloroacetic acid, bromochloroacetic acid and 5-bromosalicylic acid were also detected. At the NaClO dose of 20 mg/L, quite a number of halogenated byproducts were found, including all the byproducts detected in the samples with lower NaClO doses. Notably, many of the byproducts detected were aromatic compounds, which have been proven to exhibit significantly higher toxicity than the regulated aliphatic byproducts, i.e., trihalomethanes and haloacetic acids, by World Health Organization and U.S Environmental Protection Agency (Liu and Zhang 2014, Richardson and Ternes 2014, Yang and Zhang 2013). Among the aromatic compounds detected, halo(hydro)benzoquinones are considered as a group of

toxic byproducts which have caused great public concern (Qin et al. 2010, Wang et al. 2014a, Yang and Zhang 2013), and halopyrroles are another group of emerging highly toxic byproducts. Halopyrroles, including tetrabromopyrrole and tribromochloropyrrole (m/z 334/336/338/340/342) were detected when 20 mg/L NaClO was applied. It has been reported that tetrabromopyrrole exhibited 8805 × and 460 × higher developmental toxicity than bromoform and bromoacetic acid, respectively, and approximately 6 × higher developmental toxicity than 2,5-dibromohydroquinone (Yang and Zhang, 2014).

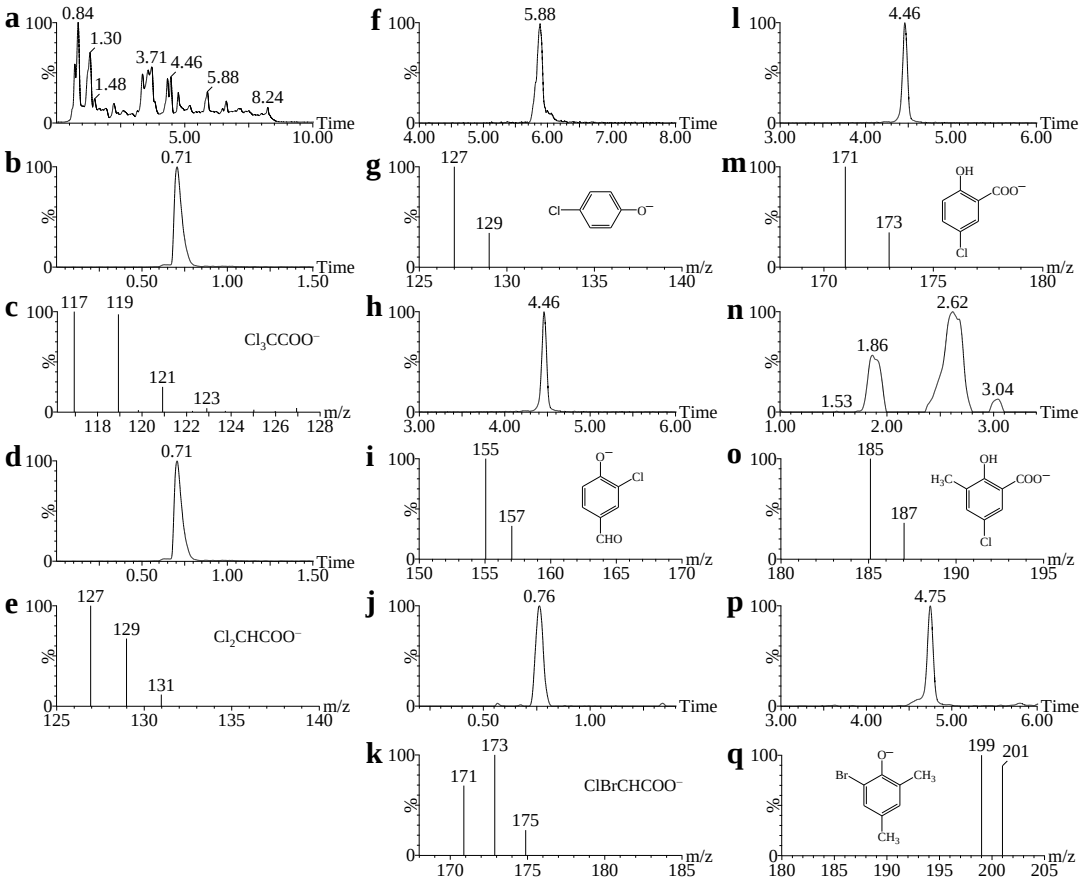

Figure 5.6 (a) UPLC/ESI-tqMS full scan (m/z 100−210) chromatogram of the DOM sample at NaClO dosage of 20 mg/L. Chromatograms and the corresponding spectra of ion clusters (b,c) m/z 117/119/121/123 (27:27:9:1), (d,e) m/z 127/129/131 (9:6:1), (f,g) m/z 127/129 (3:1), (h,i) m/z 155/157 (3:1), (j,k) m/z 171/173/175 (3:4:1), (l,m) m/z 171/173 (3:1), (n,o) m/z 185/187 (3:1), and

(p,q) m/z 199/201 (1:1), respectively. Structure of each ion cluster is inserted in the corresponding spectrum.

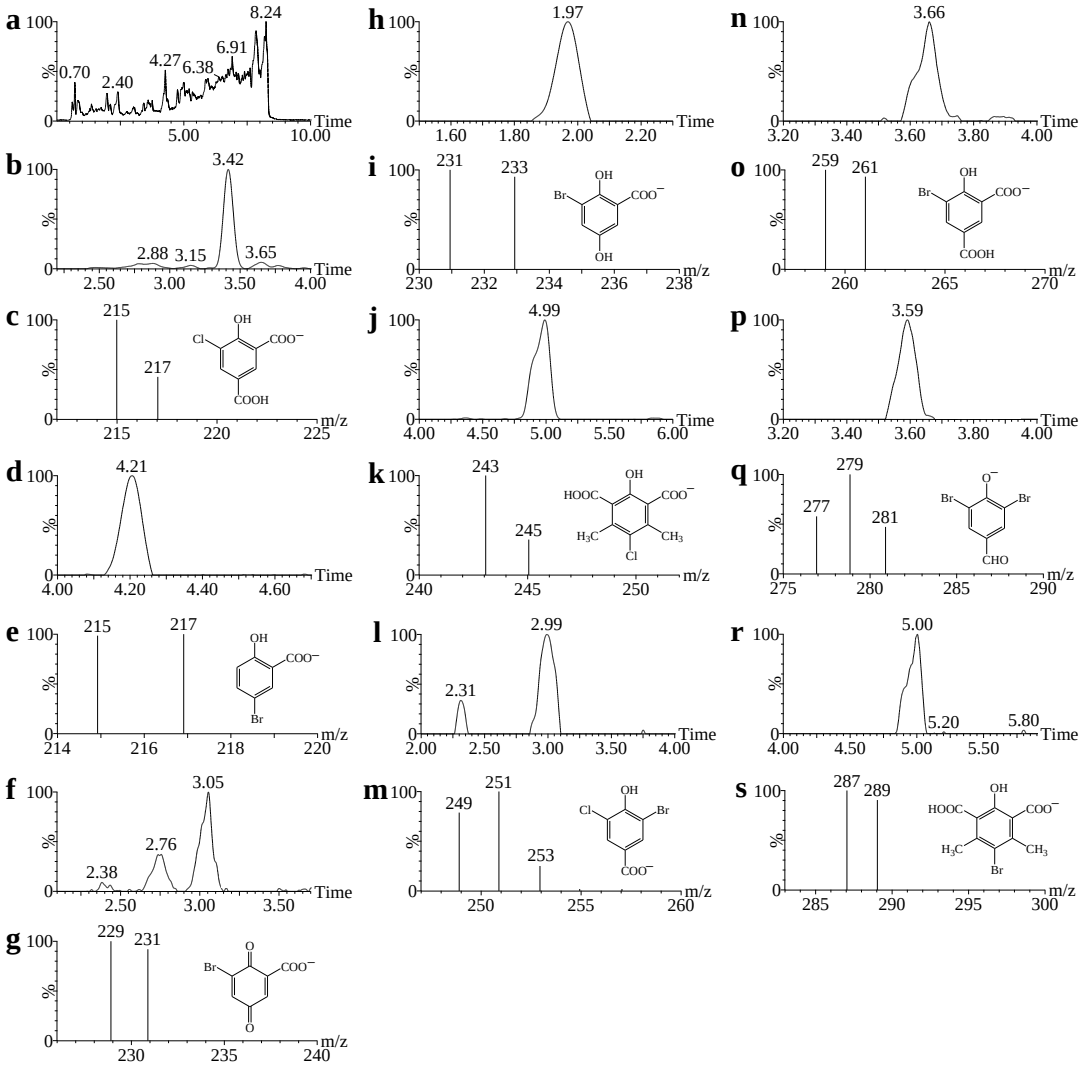

Figure 5.7 (a) UPLC/ESI-tqMS full scan (m/z 200−310) chromatogram of the DOM sample at NaClO dosage of 20 mg/L. Chromatograms and the corresponding spectra of ion clusters (b,c) m/z 215/217 (3:1, retention time 3.42 min), (d,e) m/z 215/217 (1:1, retention time 4.21 min), (f,g) m/z 229/231 (1:1, retention time 3.05 min), (h,i) m/z 231/233 (1:1), (j,k) m/z 243/245 (3:1), (l,m) m/z 249/251/253 (3:4:1, retention time 2.99 min), (n,o) m/z 259/261 (1:1), (p,q) m/z 277/279/281 (1:2:1), and (r,s) m/z 287/289 (1:1), respectively. Structure of each ion cluster is inserted in the corresponding spectrum.

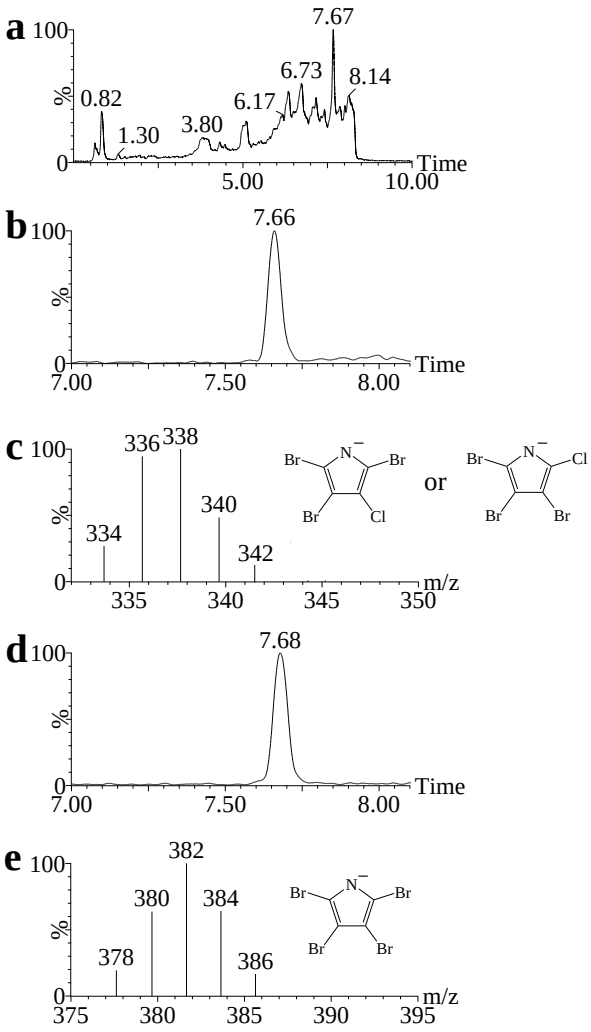

Figure 5.8 (a) UPLC/ESI-tqMS full scan (m/z 300−410) chromatogram of the DOM sample at NaClO dosage of 20 mg/L. Chromatograms and the corresponding spectra of ion clusters (b,c) m/z 334/336/338/340/342 (3:10:12:6:1), and (d,e) m/z 378/380/382/384/386 (1:4:6:4:1), respectively. Structure of each ion cluster is inserted in the corresponding spectrum.

Table 5. 3 Ion clusters of polar halogenated DBPs detected in the released DOM from activated sludge after 30 min exposure to NaClO.

m/z (retention time, min)	Structure	Occurrence (NaClO dose, mg/L)	*m/z* (retention time, min)	Structure	Occurrence (NaClO dose, mg/L)
127/129/131 and 83/83/87[a] (0.71)	$Cl_2CHCOOH$[b]	10, 20	229/231 (3.05)	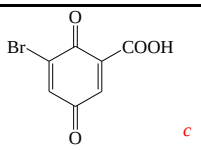 [c]	20
127/129 (5.88)	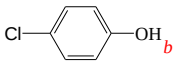 [b]	5, 10, 20	231/233 (1.97)	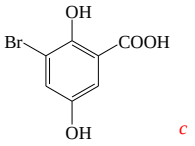 [c]	20
155/157 (4.46)	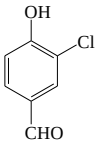 [c]	20	243/245 (4.99)	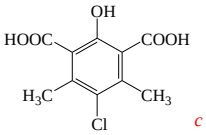 [c]	20
161/163/165/167 and 117/119/121/123[a] (0.71)	Cl_3CCOOH[b]	10, 20	249/251/253 (2.99)	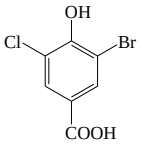 [c]	20
171/173/175 (0.76)	ClBrCHCOOH[b]	10, 20	259/261 (3.66)	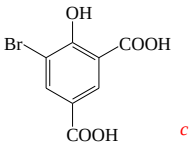 [c]	2, 5, 10, 20
171/173 (4.46)	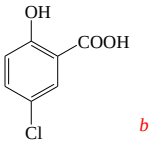 [b]	20	277/279/281 (3.59)	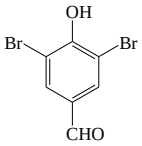 [b]	20
185/187 (2.62)	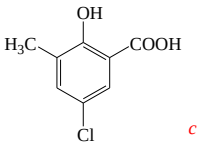 [c]	20	287/289 (5.00)	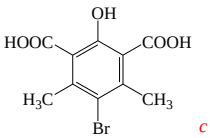 [c]	20
199/201 (4.75)	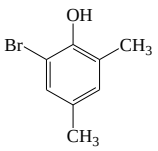 [c]	20	334/336/338/ 340/342 (7.66)	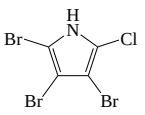 [c]	20
215/217 (3.42)	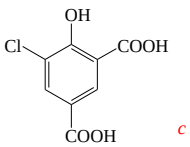 [c]	2, 5, 10, 20		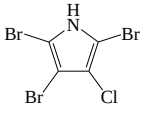 [c]	

215/217 (4.21)	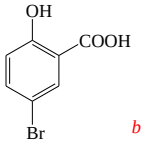 *b*	10, 20	378/380/382/ 384/386 (7.68)	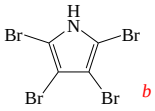 *b*	20

[a] Decarboxylation of these DBPs occurred at the sample cone of ESI-tqMS during analyses;
[b] The sturctures were confirmed with purchased or systhesized standard compounds;
[c] The structures were tentatively proposed, and each structure might have iosomers.

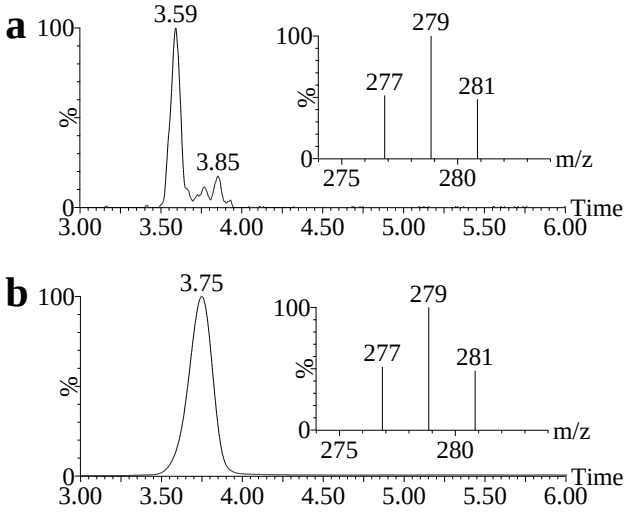

Figure 5.9 (a) UPLC/ESI-tqMS selective ion recording (m/z 277/279/281) chromatograms of the DOM sample at NaClO dosage of 20 mg/L, and (b) 3,5-dibromo-4-hydroxybenzaldehyde standard compound. According to the similar retention times and isotopic ratios obtained in the released DOM sample and standard compound, ion cluster m/z 277/279/281 was confirmed to be 3,5-dibromo-4-hydroxybenzaldehyde.

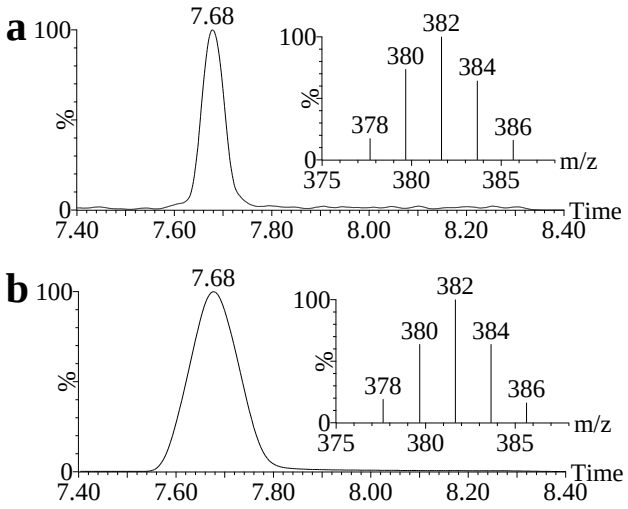

Figure 5.10 (a) UPLC/ESI-tqMS selective ion recording (m/z 378/380/382/384/386) chromatograms of the DOM sample at NaClO dosage of 20 mg/L, and (b) the synthesized tetrabromopyrrole. According to the similar retention times and isotopic ratios obtained in the released DOM sample and synthesized standard compound, ion cluster m/z 378/380/382/384/386 was confirmed to be tetrabromopyrrole.

5.3.4 Engineering implications

On-line chemical cleaning with NaClO is a common method for effective mitigation of membrane fouling in MBR. However, this study clearly showed that NaClO also reacted with suspended biomass, leading to the release of a substantial amount of DOM, most of which was found to be humic-acid like substances and protein-like materials. As discussed above, 24.7 mg/L DOM was produced from bacterial lysis triggered by 20 mg/L NaClO. These released DOM with small molecular sizes may eventually pass through microfiltration membrane and end up in the MBR permeate, worsening the permeate quality (Liang et al. 2007). Besides that, DOM released into the bioreactor may affect the activity of microorganisms in activated sludge. For examples, some presented DOM have been reported to be toxic to microorganisms, inhibit microbial kinetic activity, or adversely affect the settleability of activated sludge (Barker and

Stuckey 1999). Moreover, DOM released may also enhance membrane fouling in MBR. In fact, DOM has been shown to be closely associated with membrane fouling under various operational conditions of MBRs (Bouhabila et al. 2001, Lee et al. 2003, Wisniewski and Grasmick 1998). It is reasonable to consider that DOM produced would adversely impact on the practical operation of MBR.

More importantly, a broad spectrum of halogenated byproducts including haloacetic acids, halophenols, haloquinones and halopyrroles were generated after exposure of activated sludge to NaClO. Given their relatively low molecular weight, these byproducts can easily pass through microfiltration membranes and end up in the permeate of MBR. This may impose potential adverse impacts on ecosystems if the permeate is discharged into receiving water bodies, and human health if such permeate is destined for public water supplies. Toxicological studies have demonstrated that halogenated byproducts might have adverse effects on marine organisms (Liu and Zhang 2014, Yang and Zhang 2013, 2014, 2016). Epidemiological studies also have implied an increased risk of bladder, kidney and colorectum cancers, and an elevated risk of spontaneous abortions and birth defects by consumption of chlorinated drinking water (Cemeli et al. 2006, Villanueva et al. 2004). Therefore, further study may be needed to systematically examine the potential toxicity of the presented byproducts and the fate of these byproducts during practical long-term MBR operation.

5.4 CONCLUSIONS

This study showed the generation of substantial amount of DOM and byproducts after exposure of activated sludge to NaClO during on-line chemical cleaning in MBR. Bacterial lysis and DOM release occurred, and up to 24.7 mg/L as DOC were produced after exposure to NaClO dosage of 0-20 mg/L. The main components of the released DOM were humic acid-like and protein-like substances. As for the byproducts produced during the exposure, 19 polar halogenated byproducts were detected, and eight of them were confirmed. Most of the byproducts were aromatic compounds, especially halopyrroles and

halo(hydro)benzoquinones, which have been shown to be significantly more toxic than the haloaliphatic ones. This study probably for the first time characterized the DOM and byproducts produced during on-line chemical cleaning in MBR, and this may raise serious concerns on the current membrane cleaning strategy by NaClO and more importantly on public health if the permeate of MBR is reused or recycled for various applications.

CHAPTER 6 FATE OF DISSOLVED ORGANIC MATTER AND BYPRODUCTS GENERATED FROM ON-LINE CHEMICAL CLEANING WITH SODIUM HYPOCHLORITE IN MBR

6.1 INTRODUCTION

In chapter 5, it is well established that NaClO, as a strong oxidant, could also trigger serious sludge foaming and dissolved organic matter (DOM) release during on-line chemical cleaning of MBR. These suggest that part of DOM present in MBR may originate from on-line chemical cleaning with NaClO instead of the raw sewage. Therefore, there is an urgent need to systematically examine the fate of the emerging micropollutants generated through chemical cleaning with NaClO in MBR. Meanwhile, in chapter 5, a broad spectrum of halogenated DBPs have been identified in the DOM derived from on-line chemical cleaning with NaClO, most of which were found to be haloaromatic compounds. It has been known that haloaromatic byproducts exhibited substantially more toxicity than haloaliphatic ones (Liu and Zhang 2014). The presence of toxic byproducts in the MBR permeate may compromise water reuse and recycling, and pose serious concern on ecosystem and public health as well. It appears imperative to evaluate the possible fate of these emerging byproducts in MBR, but limited information is available on this aspect thus far.

Therefore, this study aimed to investigate the fates of the DOM and halogenated DBPs produced through on-line chemical cleaning with NaClO in MBR. For this purpose, excitation emission matrix fluorescence with parallel factor analysis

---

The content in this chapter has been published as: Cai, W., Liu, J., Zhu, X., Zhang, X., and Liu, Y. (2017). Fate of dissolved organic matter and byproducts generated from on-line chemical cleaning with sodium hypochlorite in MBR. Chem. Eng. J. 323, 233-242.

(EEM-PARAFAC) was employed to acquire the componential information of the DOM. Total organic halogen (TOX) analysis was conducted to measure the formation of overall halogenated byproducts, and (UPLC)/ESI-tqMS was applied to further identity the byproducts. It is expected that this study can offer deeper insights into the fate of chemical cleaning-associated DOM and DBPs, which should shed light on the current operation of practical MBR and more importantly, on the reuse and recycle of MBR permeate.

6.2 MATERIALS AND METHODS

6.2.1 Chemical reagents

NaClO stock solution of 4%–4.99% was purchased from Sigma-Aldrich and further standardized by N, N-diethyl-p-phenylenediamine (Hach, USA) before usage. 4 bromo-2-chlorophenol (99%), 3,5-dibromo-4-hydroxybenzoic acid (98%), 3,5 dibromo-4-hydroxybenzaldehyde (98%) were ordered from Acros Organics, Indofine, and Alfa Aesar, respectively. Other standard compounds including chlorobromoacetic acid (97%), dichloroacetic acid (>99%), trichloroacetic acid (>99%), dibromoacetic acid (>99%), 5-bromosalicylic acid (90%), 5-chlorosalicylic acid (98%), 2,4,6-trichlorophenol (98%), 2,4,6-tribromophenol (99%), and iodoacetic acid (>99%) were obtained from Sigma-Aldrich. Organic solvents (HPLC grade) including acetonitrile, methyl tert-butyl ether (MtBE), methanol, and all the other chemicals (reagent grade) were also purchased form Sigma-Aldrich.

6.2.2 DOM generation

Activated sludge was collected from a local wastewater treatment plant in Singapore, and acclimatized in a chemostat with a synthetic substrate containing CH_3COONa (690 mg/L), glucose (313 mg/L), NH_4Cl (200 mg/L), K_2HPO_4 (60 mg/L) and other trace minerals for one month. Prior to use, the activated sludge was washed thrice with 10 mM phosphate buffered saline (PBS) solution. The standardized NaClO solution was then dosed to three reactors for having initial

NaClO concentrations of 0, 5 and 20 mg/L, respectively. Such initial NaClO dosages were determined according to the previous studies in chapter 3, 4 and 5, representing control, relatively low and relatively high contents of the reagent. Dissolved oxygen was provided through aeration for a contact duration of 30 min, after which nearly all the chlorine was consumed. After 30-min exposure to 0 to 20 mg/L NaClO, the residual free chlorine was undetectable, and the residual combined chlorine in the range of 0-0.7 mg/L, was further quenched with $Na_2S_2O_3$ according to stoichiometric reaction. Thereafter, a part of the supernatant was collected for DOM analysis.

6.2.3 DOM biodegradation test and further removal in MBR

As illustrated in **Figure 6.1**, after 30-min contact of activated sludge with NaClO, 1.5 L of sludge suspension (i.e. generated DOM and NaClO-treated biomass) was fed into a laboratory-scale aerobic MBR equipped with 75 cm^2 of 0.22 mm PVDF membrane. The permeate flux was controlled at 30 L/m^2h by automatic pump adjustment (Cole Parmer, USA), and 10 mM PBS solution was used as MBR influent. The permeate was collected over one hydraulic retention time (HRT) of 6.7 h. Meanwhile, for evaluating the maximum biodegradability of generated DOM possibly occurred in MBR, another 1.5 L of these sludge suspension was incubated in a reactor for 6.7 h without membrane filtration. Afterwards, the supernatant from the reactor was collected for further analysis. For each DOM, the DOC concentration was measured by organic carbon analyzer (Shimadzu, Japan), representing its total concentration of organic substances.

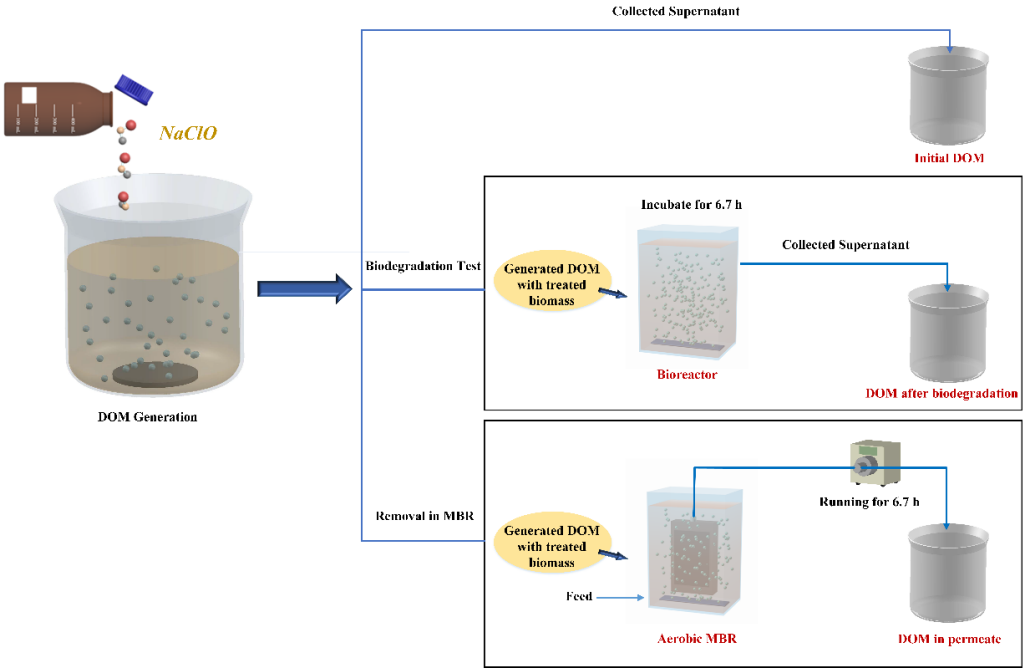

Figure 6.1 Schematic illustration of experimental process.

6.2.4 EEM-PARAFAC analysis

Each DOM sample collected from the experiments was mixed with Milli-Q water according to 1:1 ratio. A fluorescence spectrophotometer (LS55, Perkin Elmer Company, USA) was employed to obtain the spectra of fluorescence EEM. In brief, excitation scanned from 250 to 500 nm at 5 nm intervals, while emission was scanned between 250 and 550 nm with 0.5 nm increment. The fluorescence spectra corresponding to the blank (Milli-Q water) was subtracted from each measured EEMs, and the fluorescence intensities were further normalized by the Raman peak of Milli-Q water at excitation wavelength of 350 nm. Thereby, the unit of EEM intensity present in this study was Raman 350 (R.U.) (Lawaetz and Stedmon 2009). Afterwards, the EEMs of 56 DOM samples obtained from the experiments were subject to PARAFAC modelling by using Matlab R2013a software with DOMFluor toolbox following the protocols described by Stedmon and BrO (2008). For each component, the obtained maximum fluorescence intensity (Fmax) was used to represent its relative concentration.

6.2.5 Determination of TOX and (UPLC)/ ESI-tqMS analysis

TOX is further differentiated into total organic chlorine (TOCl), total organic bromine (TOBr) and total organic iodine (TOI). TOX concentration in each DOM sample was measured according to the method described in chapter 5. Briefly, all chlorinated, brominated and iodinated byproducts were converted to Cl^-, Br^-, and I^-, respectively, and then the Cl^- and Br^- were quantified with an ion chromatograph, and the I^- was quantified with Waters UPLC/ESI-tqMS. The detailed procedure was illustrated in the section of 5.2.4 of chapter 5.

Besides, to detect and identify individual halogenated byproducts, each DOM sample was analysed by (UPLC)/ ESI-tqMS. Prior to analyses, the DOM was pretreated and concentrated with details described in the section of 5.2.5 of chapter 5. By doing so, the byproducts in the DOM (with the volume of 2000 mL) were concentrated in 2 mL of 50% aqueous acetonitrile. The concentrated sample was subjected to ESI-tqMS precursor ion scans of *m/z* 35/37 and *m/z* 79/81, with which all electrospray-ionizable chlorinated and brominated byproducts were selectively detected (Pan and Zhang 2013a, Zhai et al. 2014). The operation parameters of ESI-tqMS were set according to a previous study in chapter 5. Moreover, coupled with UPLC, ESI-tqMS full scans at different *m/z* ranges (i.e., *m/z* 100−160, 150−210, 200−260, 250−310, 300−360, 350−410, 400−460, and 450−510) were conducted. The gradient of water-methanol binary eluent and operational parameters of UPLC/ESI-tqMS were also set based on the method described in chapter 5. For a molecular ion detected and potentially represented a halogenated byproduct, UPLC/ESI-tqMS product ion scans were conducted at the corresponding retention time (RT). Then, the structure of the byproduct was proposed based on the retention time, isotopic ratio, and fragment ions detected in product ion scans.

6.3 RESULTS AND DISCUSSION

6.3.1 Fate of total DOM in MBR

Figure 6.2 showed the concentration profiles of DOM produced after the exposure of activated sludge to NaClO, DOM after biodegradation and DOM in MBR permeate respectively. The initial generation of DOM in the range of 4.9-29.6 mg/L was positively related to the NaClO dosage. After incubation with biomass for 6.7 h, the measured DOM concentrations became lower and only 4.5-14.3 mg/L can be found, suggesting 8.2%-51.7% of generated DOM were biodegraded under the conditions studied. Comparatively, DOM concentrations in MBR permeate ranged from 5.1-18.2 mg/L, resulting in a highest removal of around 39% due to the combined effects of biodegradation and membrane retention in MBR.

At the low NaClO dosage of 5 mg/L, 30.5% of DOM generated can be degraded biologically versus 39.6% ultimately removed by MBR. Since the above DOM biodegradability represented the maximum potential of microbial degradation in MBR, it appeared that membrane or developed fouling layer retained part of DOM. On the other hand, it was observed that the DOM biodegradability (51.7%) significantly exceeded removal rate (38.5%) at NaClO dosage of 20 mg/L. This implied that DOM generated at the higher NaClO dosage of 20 mg/L was more readily biodegradable, and DOM biodegradability was related to the dosage of NaClO applied. It should also be noted that a significant amount of DOM eventually ended up in the permeate, i.e. 9.3 mg/L and 18.2 mg/L at the NaClO dosages of 5 mg/L and 20 mg/L, respectively. In fact, this may raise serious concerns about discharge, reuse and recycle of such MBR permeate.

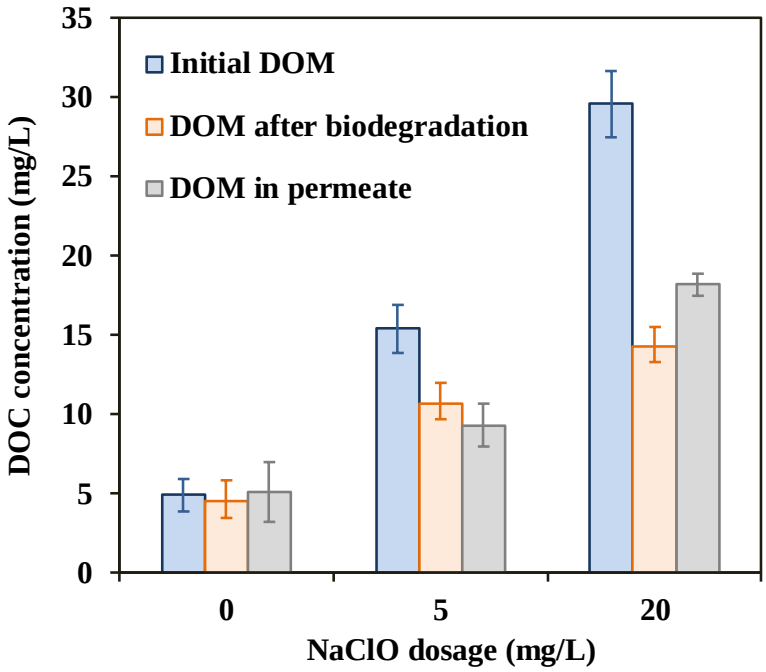

Figure 6.2 DOC concentrations of initial DOM, DOM after biodegradation and DOM in permeate, derived from activated sludge after 30-min exposure to 0 mg/L, 5 mg/L and 20 mg/L NaClO.

6.3.2 Componential analysis of DOM

In the previous study of chapter 5, the composition of generated DOM was analysed by traditional EEM technique of peak selection. However, such analysis might be biased due to the spectral overlaps of different fluorophore groups. Therefore, in this study, a statistical modelling method, namely PARAFAC, was coupled to further decomposed the EEMs into individual components with unique fluorescence features. This allows effectively tracking the fate of independent organic components in water systems. **Figure 6.3** showed that three individual components were successfully identified in DOM, while **Table 6.1** further summarized respective peak locations and possible sources of these components by comparing with those reported in the literature. Component 1 (C1) with the peak at the excitation/emission wavelengths (Ex/Em) of 275/357 nm was assigned to protein-like matter. Component 2 (C2) with primary and secondary maxima at Ex/Em of 265/456 nm and 360/456 nm was a combination of traditional peak A and peak C. By comparing with many other investigations

listed in **Table 6.1**, C2 was identified as terrestrial-like humic substances. In addition, the spectral features of component 3 (C3) at the Ex/Em of 320/390 nm were similar to marine humic materials, which were also considered as DOM altered by microbial reprocessing.

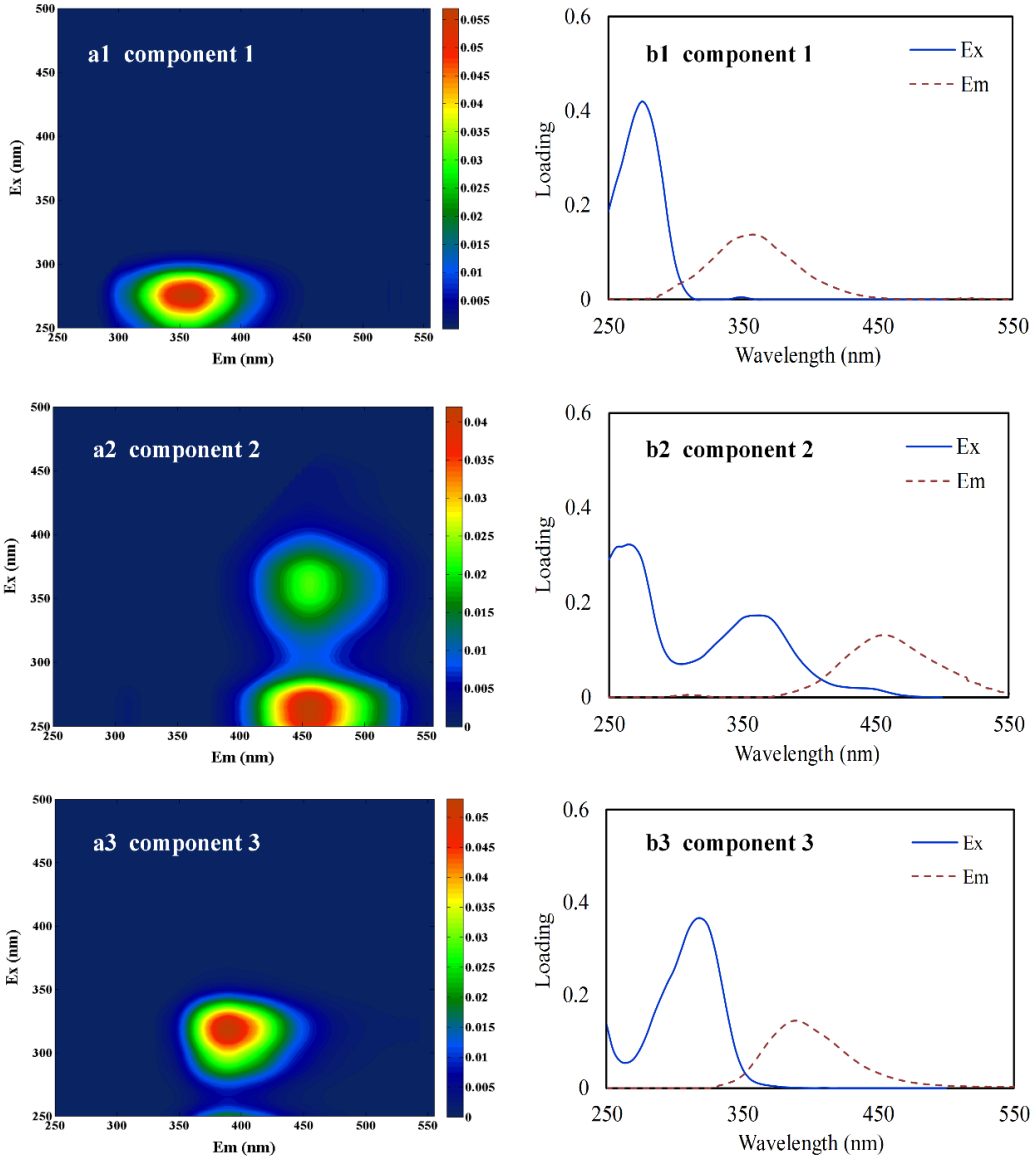

Figure 6.3 (a1-a4) Contour plots of three different fluoresence components identified by PARAFAC modelling and (b1-b4) their corresponding excitation/emission loadings.

Table 6.1 PARAFAC component locations and descriptions**.**

Component	Approximate location	Traditional Peaks [a]	Reported similar PARAFAC components	Descriptions and probable sources
C1	275/357	Peak T 275/340	C1 280/358 (Phong and Hur 2015) C7 280/344 (Stedmon and Markager 2005) C3 280/350 (Hur et al. 2014)	Amino acids, free or bound in proteins
C2	265 (360)/456	Peak A 260/380–460 Peak C 350/420–480	C3 270 (360)/478 (Stedmon et al. 2003) C1 260 (360)/460 (Aryal et al. 2015) C1 250/452 (Kowalczuk et al. 2009)	Terrestrial humic-like substances
C3	320/390	Peak M 312/380-420	C4 325 (250)/416 (Stedmon et al. 2003) C2 315/418 (Murphy et al. 2008) C4 305 (<260)/378 (Yamashita and Jaffé 2008)	Marine humic materials, and microbial derived components

[a] Based on the study by Coble (1996)

Furthermore, **Figure 6.4a–c** showed the respective F_{max} values of three identified components in various DOM. In the fresh DOM produced, the F_{max} values of C1 and C2 were positively related to the NaClO dosage, while the increase in C2 was more significant than that of C1. In fact, such observation was consistent with the previous study in chapter 5. However, after biodegradation of DOM for 6.7 h, the F_{max} value of C1 decreased substantially, suggesting the higher biodegradation of protein-like materials compared with the other two humic-like components. **Figure 6.4d** further showed the differences in F_{max} between the initial DOM and remaining DOM after biodegradation. The significant difference was observed for C1 especially at the high NaClO dosage. However, C2 and C3 appeared hardly biodegradable probably due to the highly recalcitrant nature of humic substances (Tang et al. 2007). These results suggested that protein-like substances (e.g. C1) were more readily biodegradable than those humic-like substances (e.g. C2 and C1). It should also be noted that majority of the detectable components generated by NaClO were eventually ended up in the permeate. For example, about 76.7% of initial C1 and 85.3% of C2 were found in the MBR

permeate at the NaClO dosage of 20 mg/L, suggesting that the protein-like and humic-like substances were, in fact, poorly removed biologically and retained physically by the microfiltration membrane in MBR.

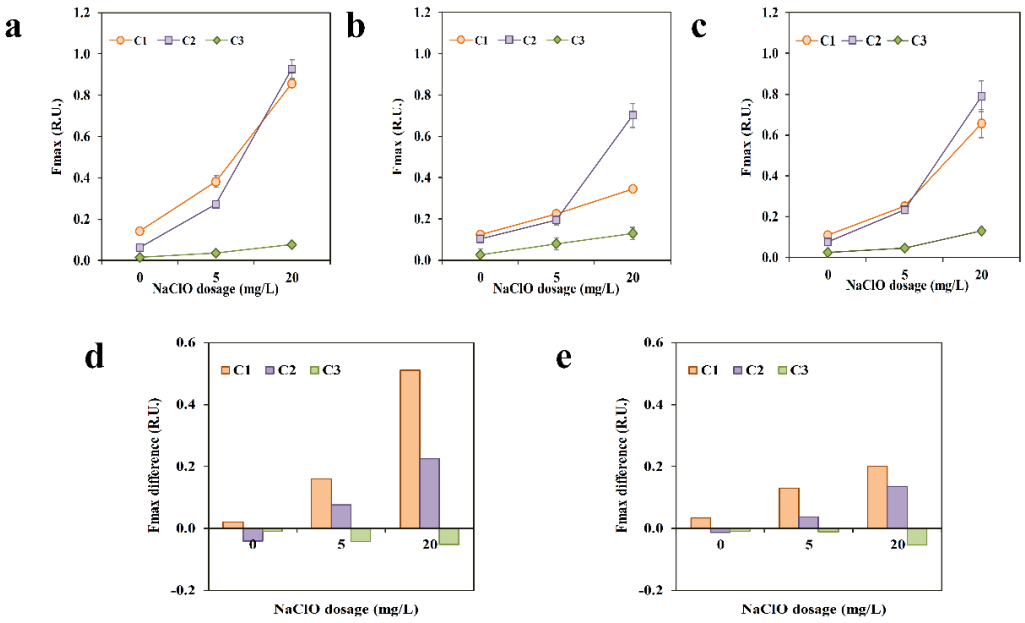

Figure 6.4 F_{max} values of fluorescence components of (a) initial DOM, (b) DOM after biodegradation and (c) DOM in permeate, derived from activated sludge after 30-min exposure to 0 mg/L, 5 mg/L and 20 mg/L NaClO; (d) F_{max} difference between initial DOM and DOM after biodegradation; (e) F_{max} difference between initial and permeate DOM.

In this above study, two types of humic-like substances were identified via EEM-PARAFAC modelling analysis, i.e., the terrestrial humic-like substances (C2) and the marine humic substances (C3). This may reveal the possible structure variation of humic-like materials due to the fact that fluorescent property of a substance is mainly related to its molecular structure. For example, **Figure 6.4d-e** showed that a part of C2 was eliminated by MBR, while C3 could not be removed, reflecting the possible differences in their chemical structures. In addition, it was found that a shift towards the shorter excitation maximum was caused by the changes in absorption spectra, whereas a blue shift in the emission maxima was indicative of structural changes (e.g., fragmentation of large

molecules, decrease of conjugated bonds in a chain structure or aromatic rings, or elimination of amine, hydroxyl and carbonyl groups) (Coble 1996). These in turn suggest that C3 with the shorter emission maxima should consist of smaller or less aromatic molecules as compared to C2, and C2 with larger or more complex structure may be readily biodegraded into simpler compounds or easily retained by membrane, which was also manifested by the relatively higher removal efficiency illustrated in **Figure 6.4d-e**. In addition, it should be noted that F_{max} value of C3 tended to slightly increase accompanied by the microbial degradation of C2, suggesting that C3 might be, to a contain degree, derive from the biodegradation of C2.

6.3.3 Fate of halogenated byproducts in MBR

The presence of halogenated organic compounds in water bodies has attracted increasing concerns in the recent years due to their potential threats to ecosystems and human health. Despite the reported generation of halogenated byproducts during on-line chemical cleaning in chapter 5, little has been known about their subsequent fate in MBR. In this study, TOCl, TOBr and TOI produced upon NaClO exposure were measured respectively, while TOX was calculated as the total concentration of halogenated byproducts.

As TOX in control was not detectable and no specific TOI was identified in the DOM produced in this study, **Figure 6.5a** showed the respective TOCl and TOBr concentrations in the DOM generated at different NaClO dosages of 5-20 mg/L. It can be seen that TOCl accounted for more than 90% of TOX, and remaining 10% of TOBr may be originated from bromide in activated sludge. In general, brominated byproducts are ten to hundred times more toxic than their chlorinated analogs (Ding et al. 2013, Pan and Zhang 2013a). Both TOCl and TOBr concentrations tended to increase rapidly with increasing the NaClO dosage in the range of 5 mg/L to 20 mg/L, while the highest TOX concentration was 73.7 mg/L as Cl. As can be seen in **Figure 6.5b-c**, 22.2% and 9.5% of TOX produced at 5 mg/L and 20 mg/L NaClO were biodegraded, while correspondingly 37.6% and 15.5% of TOX were eventually removed by MBR. Since the biodegradability

represents the maximum level of biodegradation possibly occurred in MBR, these results suggested that microfiltration membrane with fouling layer indeed retained some byproducts in the MBR. Moreover, TOBr seemed more biodegradable and readily eliminated than TOCl, e.g. 39.3% of TOBr was removed in the MBR compared with 14.1% of TOCl removal at the 20 mg/L NaClO. It should be realized that the removability of TOCl and TOBr tended to decrease with increasing the NaClO dosage in the range of 5 to 20 mg/L. This can be attributed to the generation of more recalcitrant byproducts with complex structures (e.g. aromatic compounds) at higher NaClO dosage, as evidenced by the results in **Table 6.2**.

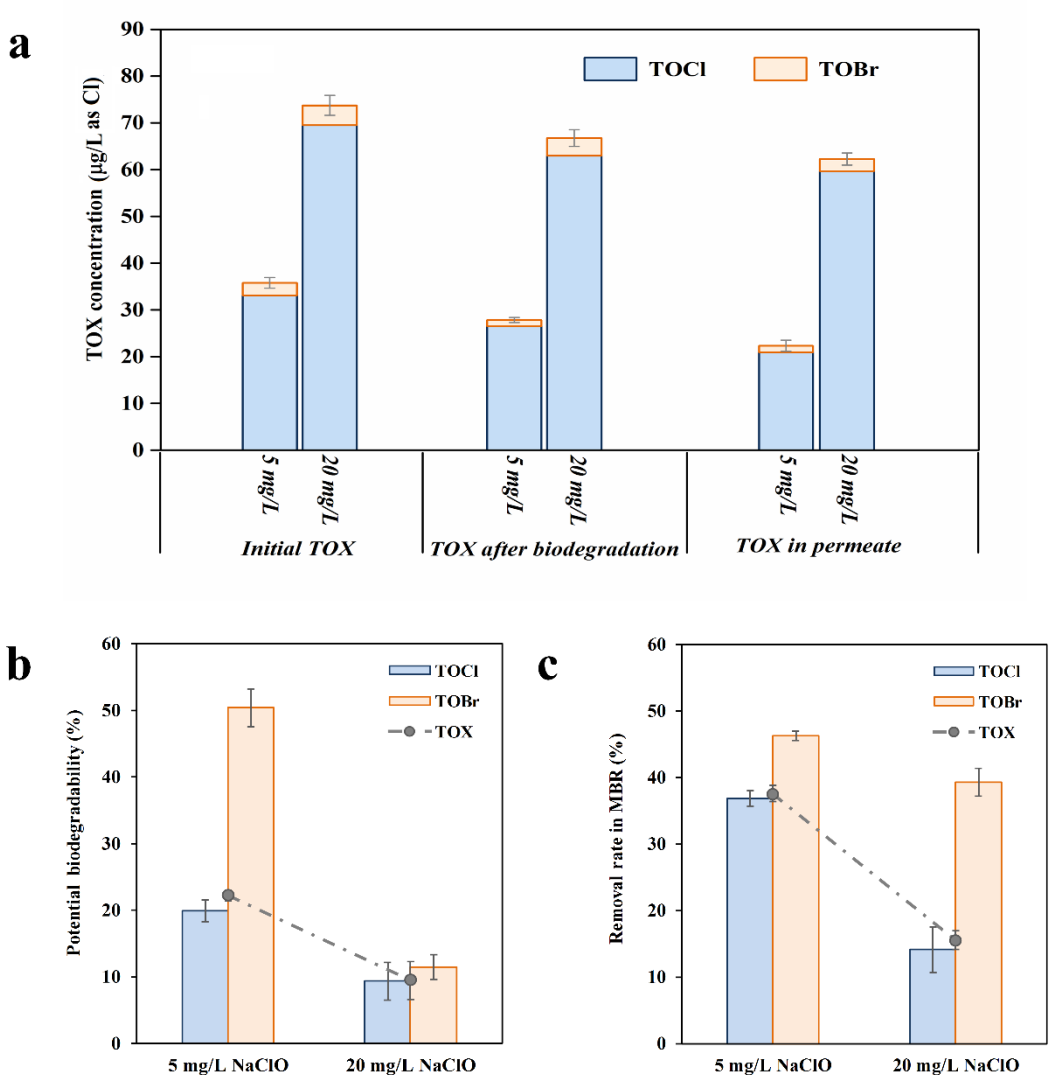

Figure 6.5 (a) TOX concentrations of initial DOM, DOM after biodegradation and DOM in permeate, derived from activated sludge after 30-min exposure to 5 and 20 mg/L NaClO. (b) DBP potential biodegradability (c) DBP removal rate in MBR. (The error bar represents the variation scale of the total DBP concentrations).

Based on the UPLC/ESI-tqMS full scans of the DOM generated at 20 mg/L NaClO, the structures of 25 specific chlorinated and brominated byproducts were identified, nine of which were confirmed with corresponding standard compounds (**Table 6.2**).
In fact, the polar DBP species identified in initially generated DOM were all detected after biodegradation and in MBR permeate, i.e. these 25 halogenated byproducts cannot be completely biodegraded or totally removed in the MBR studied.

According to UPLC/ESI-tqMS full scan chromatographs, the concentration of each detected byproduct was quantified by the peak areas of its ion clusters, and these byproducts exhibited remarkably different biodegradabilities and removabilities (**Figure 6.6**). At the NaClO dosage of 5 mg/L, 8 out of 11 byproducts could be biodegraded with their potential biodegradability of 2.6-56.7%, whereas 9 out of these 11 byproducts were removed in MBR with their removal efficiency ranged from 13.4 to 72.5%. Notably, dibromoacetic acid (m/z 215/217/219) could be eliminated the most easily, indicative of its distinctive features to be readily biodegraded or physically retained by membrane. As for 20 mg/L NaClO, 17 out of 25 detected byproducts produced at 20 mg/L NaClO could be biodegraded to a range of 2.1-41.2%, while 24 of them could be partially removed in MBR with the removal efficiency of 2.0-56.9%, which were lower than those at 5 mg/L NaClO. As discussed above, this observation is probably due to the generation of recalcitrant byproducts at higher NaClO dosage. It should be noted that most of confirmed aromatic byproducts, including 5-chlorosalicylic acid (m/z 171/173), 5-bromosalicylic acid (m/z 215/217), 3,5-dibromo-4-hydroxybenzaldehyde (m/z 277/279/281) and 3,5-dibromo-4-

hydroxybenzoic acid (m/z 293/295/297), could be significantly removed in MBR. However, the concentrations of trichloroacetic acid (m/z 117/119/121/123) and dichloroacetic acid (m/z 127/129/131), on the contrary, marginally increased after microbial degradation especially at the NaClO dosage of 5 mg/L (**Figure 6.6a**). In fact, haloacetic acids (HAAs) have been known as a group of disinfection byproducts which are preferably biodegradable (Bayless and Andrews 2008, Zhang et al. 2009). Therefore, the increase in the concentrations of trichloroacetic acid and dichloroacetic acid observed in this study might be due to microbial decomposition of complex aromatic byproducts. Meanwhile, the removal efficiency of the brominated DBPs was found to be higher than that of the chlorinated DBPs, e.g. 72.5% of dibromoacetic acid and 56.9% of 5-bromosalicylic acid generated were removed in MBR. Despite the considerable removal of detected compounds, it should be highlighted that about 62.4% and 84.5% of total halogenated byproducts produced at 5 mg/L and 20 mg/L NaClO were found in the MBR permeate (**Figure 6.5**), which should be properly addressed if the reuse and recycle of such permeate are considered.

Table 6.2 Ion clusters of polar halogenated byproducts detected in various DOM

m/z (RT, min)	Structure	Occurrence[c] (NaClO dose)	*m/z* (RT, min)	Structure	Occurrence[c] (NaClO dose)
117/119/121/123 (2.13)	Cl_3CCOOH[a] (decarboxylated)	5 mg/L 20 mg/L	127/129/131 (1.10)	$Cl_2CHCOOH$[a]	5 mg/L 20 mg/L
151/153 (0.54)	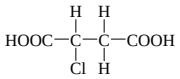 [b]	5 mg/L 20 mg/L	151/153 (1.62)	$BrCH_2CH_2COOH$[b]	20 mg/L
155/157 (4.21)	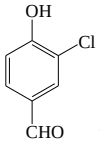 [b]	5 mg/L 20 mg/L	159/161 (2.43)	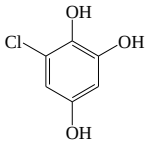 [b]	20 mg/L
171/173/175 (1.48)	$ClBrCHCOOH$[a]	5 mg/L 20 mg/L	171/173 (3.55)	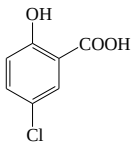 [a]	20 mg/L
185/187 (2.70)	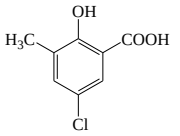 [b]	5 mg/L 20 mg/L	185/187 (5.42)	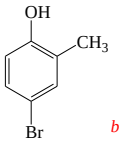 [b]	5 mg/L 20 mg/L

187/189 (2.97)	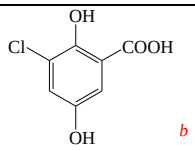 [b]	20 mg/L	189/191/193 (3.55)	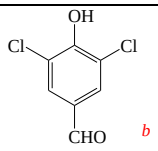 [b]	5 mg/L 20 mg/L
195/197 (0.59)	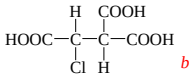 [b]	5 mg/L 20 mg/L	203/205 (2.52)	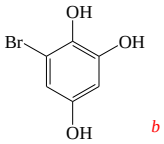 [b]	20 mg/L
205/207/209 (2.74)	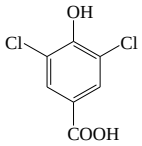 [b]	20 mg/L	205/207/209 (6.47)	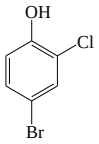 [a]	20 mg/L
215/217/219 (1.56)	$Br_2CHCOOH$ [a]	5 mg/L 20 mg/L	215/217 (3.34)	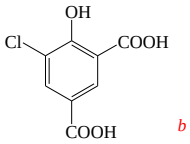 [b]	20 mg/L
215/217 (4.29)	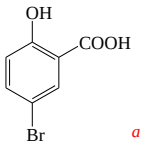 [a]	20 mg/L	229/231 (3.08)	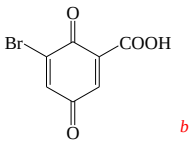 [b]	20 mg/L
233/235/237 (3.64)	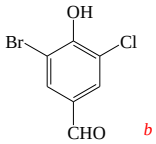 [b]	20 mg/L	243/245 (5.48)	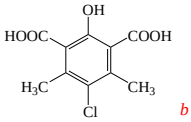 [b]	5 mg/L 20 mg/L
249/251/253 (3.15)	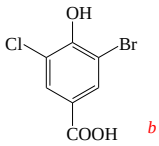 [b]	20 mg/L	277/279/281 (3.68)	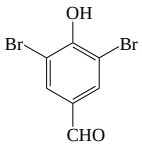 [a]	20 mg/L
293/295/297 (3.40)	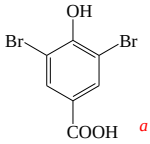 [a]	20 mg/L			

[a]The sturctures were confirmed with purchaesed standard compounds.
[b]The structures were tentatively proposed, and each structure might have iosomers.
[c]All the byproduct species intially formed also existed in MBR permeate.

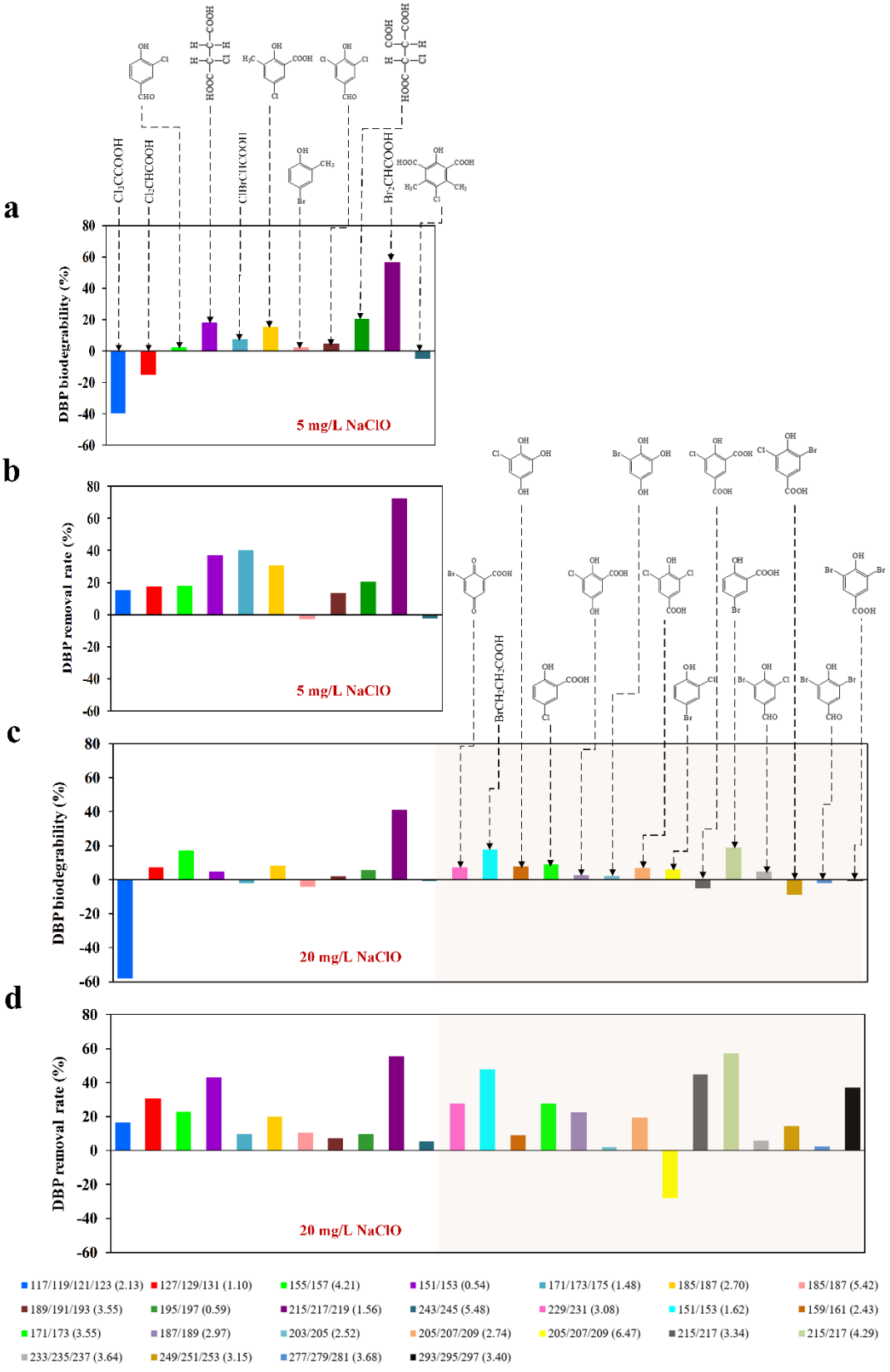
a
b
c
d
DBP biodegrability (%)
DBP removal rate (%)
5 mg/L NaClO
20 mg/L NaClO
Cl3CCOOH
Cl2CHCOOH
ClBrCHCOOH
Br2CHCOOH
BrCH2CH2COOH
117/119/121/123 (2.13)
127/129/131 (1.10)
155/157 (4.21)
151/153 (0.54)
171/173/175 (1.48)
185/187 (2.70)
185/187 (5.42)
189/191/193 (3.55)
195/197 (0.59)
215/217/219 (1.56)
243/245 (5.48)
229/231 (3.08)
151/153 (1.62)
159/161 (2.43)
171/173 (3.55)
187/189 (2.97)
203/205 (2.52)
205/207/209 (2.74)
205/207/209 (6.47)
215/217 (3.34)
215/217 (4.29)
233/235/237 (3.64)
249/251/253 (3.15)
277/279/281 (3.68)
293/295/297 (3.40)

Figure 6.6 Potential biodegradability and removal rate of individual byproducts in MBR, derived from activated sludge after 30-min exposure to 5 mg/L and 20 mg/L NaClO.

This study revealed that a broad spectrum of DOM and byproducts were inevitably generated during on-line chemical cleaning of MBR. Most of them were highly recalcitrant and not readily removable by biodegradation and membrane retention. As a consequence, the safety of such permeate is seriously concerned. To mitigate such an emerging situation, the frequency of on-line chemical cleaning should be minimized by proper engineering design of membrane module, while off-line membrane cleaning should also be considered. In addition, attention has also be given to non-chemical cleaning methods including use of scouring agents (e.g. granular activated carbon), bursting of microbubbles for removing fouling layer and EPS (Aslam et al. 2017, Wang et al. 2016, Lee et al. 2016, Lee et al. 2015).

6.4 CONCLUSIONS

This study probably for the first time explored the fate of the DOM and byproducts generated by on-line chemical cleaning with NaClO in MBR. It was shown that about 39% of the DOM generated could be removed in MBR under the conditions studied. The analysis of PARAFAC revealed that protein-like substances were more readily biodegradable than the humic-like substances. As for emerging DBPs, 25 types of chlorinated and brominated byproducts were detected, and nine of which were further confirmed with standard compounds. It was found that most of DBPs detected belonged to aromatic compounds with higher potential toxicity than aliphatic ones. 62.4% and 84.5% of total halogenated byproducts generated at 5 and 20 mg/L NaClO were ultimately found in the MBR permeate. This study indeed attempted to trigger new thinking on current operational practice of MBR as well as to raise the concern on permeate safety when water reuse and recycle are considered.

CHAPTER 7 CONCLUSIONS AND RECOMMENDATIONS

7.1 CONCLUSIONS

This study investigated the various microbial responses to NaClO and their potential impacts on MBR performance, and the following conclusions can be drawn.

Inevitable contact of activated sludge with NaClO occurred during on-line chemical cleaning with NaClO in MBR. However, NaClO exposure could trigger bacterial lysis and reduce surface hydrophobicity of sludge floc. Meanwhile, the production of EPS and AI-2 was significantly enhanced leading to a faster microbial attachment on membrane surface. More importantly, survived bacteria after exposure to NaClO were more inclined to adhere onto membrane surface than dead bacteria, which can be considered as the defensive response of survived microorganisms to the potential damage exerted by NaClO. As a result, this phenotype may aggravate membrane biofouling formation and reduce membrane performance in MBR.

Upon the exposure to NaClO, significant bacterial death and overproduction of oxidative stress occurred. Compared with respective control at the same viability, the stressed biomass after the exposure to NaClO exhibited a higher tendency to attach on membrane surface. For stressed bacteria, more viable bacteria tended to closely adhere onto membrane surface, especially on the bottom fouling layer while the upper layer predominantly consisted of dead bacteria, eventually leading to the formation of stratification structure of biofilm. Without oxidative stress, on the contrary, dead bacteria preferentially adhered onto membrane surface resulting in a mixed-culture morphology of biofouling layer. This biofilm-forming phenotype revealed that biofilm helped mitigate the potential

damages and confer a survival superiority to bacteria under various unfavourable conditions.

Accompanied by NaClO-triggered bacterial lysis, substantial amount of DOM (up to 24.7 mg/L as DOC) were generated upon exposure to NaClO dosage of 0-20 mg/L. The main components were characterized as humic acid-like and protein-like substances. Moreover, rapid increases in TOCl and TOBr concentrations were observed with the NaClO dosage rising from 2 to 20 mg/L, and the total halogenated concentration was in the range of 14.3 mg/L to 68.7 mg/L as Cl. 19 polar halogenated byproducts were successfully detected, and eight of them were confirmed with corresponding standards. Most of the byproducts were aromatic compounds, especially halopyrroles and halo(hydro)benzoquinones, which have been shown to be significantly more toxic than the haloaliphatic ones. Consequently, these results clearly demonstrated the possible generation of micropollutants through on-line chemical cleaning with NaClO in MBR, which raises concern about MBR performance as well as public health.

Fate of the DOM and byproducts generated from exposure of biomass to NaClO was further examined. It was shown that about 39% of the produced DOM could be removed from MBR at a run of 1 HRT, and protein-like substances were more readily eliminated than two types of humic-like substances. In terms of emerging DBPs, it was found that TOBr were more biodegradable and readily removed in MBR than TOCl. Despite various removal efficiencies of individual byproducts achieved, 62.4% and 84.5% of overall halogenated byproducts generated at 5 and 20 mg/L NaClO were still found in the MBR permeate. As a result, with the potential toxicity, these micropollutants ended up in permeate may bring in significant impacts on ecosystems as well as public health if the permeate of MBR is reused or recycled for various applications.

7.2 RECOMMENDATIONS

Future studies are recommended in the following aspects:

(1) In practical on-line chemical cleaning operation, highly frequent cleaning (approximately 3-120 d) with NaClO are often employed to keep a constant permeate flux. It is expectable that consecutive exposure of biomass to NaClO can bring in more significant impacts on microorganisms and system performance than a single contact. Therefore, a systematical investigation about the microbial responses to long-term consecutive cleaning with NaClO should be conducted. Moreover, the adaptation of microorganisms and their population changes should also be examined over a long-term operation.

(2) Although NaClO is the most commonly employed cleaning agent in MBR, several other reagents, such as NaOH, HCl and citric acid, are also frequently used in cleaning membranes in MBR. Moreover, NaClO is often combined with these reagents for achieving better cleaning performance. Hence, there will be a need to explore the microbial responses to other widely-used detergents, in order to better understanding of the overall impacts of on-line chemical cleaning on MBR operation.

REFERENCES

Abdullah, S.Z. and Berube, P.R. (2013). "Assessing the effects of sodium hypochlorite exposure on the characteristics of PVDF based membranes." Water Research **47**(14): 5392-5399.

Ahmed, Z., Cho, J., Lim, B.R., Song, K.G. and Ahn, K.H. (2007). "Effects of sludge retention time on membrane fouling and microbial community structure in a membrane bioreactor." Journal of Membrane Science **287**(2): 211-218.

Al-Amoudi, A. and Lovitt, R.W. (2007). "Fouling strategies and the cleaning system of NF membranes and factors affecting cleaning efficiency. " Journal of Membrane Science **303**(1): 4-28.

Albasi, C., Bessiere, Y., Desclaux, S. and Remigy, J. (2002). "Filtration of biological sludge by immersed hollow-fiber membranes: influence of initial permeability choice of operating conditions." Desalination **146**(1): 427-431.

Allie, Z., Jacobs, E., Maartens, A. and Swart, P. (2003). "Enzymatic cleaning of ultrafiltration membranes fouled by abattoir effluent." Journal of Membrane Science **218**(1): 107-116.

Alnaizy, R., Abdel-Jabbar, N., Aidan, A. and Abachi, N. (2012). "Modeling and dynamic analysis of a membrane bioreactor with backwash scheduling." Desalination and Water Treatment **41**(1-3): 186-194.

Ang, W.S., Tiraferri, A., Chen, K.L. and Elimelech, M. (2011). "Fouling and cleaning of RO membranes fouled by mixtures of organic foulants simulating wastewater effluent." Journal of Membrane Science **376**(1): 196-206.

APHA, AWWA, WEF, 2012. Standard Methods for the Examination of Water and Wastewater, Washington, DC.

Argüello, M., Alvarez, S., Riera, F. and Alvarez, R. (2003). "Enzymatic cleaning of inorganic ultrafiltration membranes used for whey protein fractionation." Journal of Membrane Science **216**(1): 121-134.

Argüello, M., Alvarez, S., Riera, F. and Alvarez, R. (2005). "Utilization of enzymatic detergents to clean inorganic membranes fouled by whey proteins." Separation and Purification Technology **41**(2): 147-154.

Arkhangelsky, E., Kuzmenko, D., Gitis, N.V., Vinogradov, M., Kuiry, S. and Gitis, V. (2007). "Hypochlorite cleaning causes degradation of polymer membranes." Tribology Letters **28**(2): 109-116.

Arts, I.S., Gennaris, A. and Collet, J.F. (2015). "Reducing systems protecting the bacterial cell envelope from oxidative damage." FEBS Letters **589**(14): 1559-1568.

Aryal, R., Lee, B.K., Beecham, S., Kandasamy, J., Aryal, N. and Parajuli, K. (2015). "Characterisation of road dust organic matter as a function of particle size: a PARAFAC approach." Water, Air, & Soil Pollution **226**(2): 1-10.

Aslam, M., Charfi, A., Lesage, G., Heran, M. and Kim, J. (2017). "Membrane bioreactors for wastewater treatment: a review of mechanical cleaning by scouring agents to control membrane fouling." Chemical Engineering Journal **307**: 897–913.

Azami, H., Sarrafzadeh, M.H. and Mehrnia, M.R. (2011). "Fouling in membrane bioreactors with various concentrations of dead cells." Desalination **278**(1): 373-380.

Baker, A. (2001). "Fluorescence excitation-emission matrix characterization of some sewage-impacted rivers." Environmental Science & Technology **35**(5): 948-953.

Barker, D.J. and Stuckey, D.C. (1999). "A review of soluble microbial products (SMP) in wastewater treatment systems." Water Research **33**(14): 3063-3082.

Bayless, W. and Andrews, R.C. (2008). "Biodegradation of six haloacetic acids in drinking water." Journal of Water and Health **6**(1): 15-22.

Benarde, M.A., Snow, W.B., Olivieri, V.P. and Davidson, B. (1967). "Kinetics and mechanism of bacterial disinfection by chlorine dioxide." Applied microbiology **15**(2): 257-265.

Bouhabila, E.H., Ben Aïm, R. and Buisson, H. (2001). "Fouling characterisation in membrane bioreactors." Separation and Purification Technology **22-23**: 123-132.

Bremere, I., Kennedy, M., Michel, P., van Emmerik, R., Witkamp, G.J. and Schippers, J. (1999). "Controlling scaling in membrane filtration systems using a desupersaturation unit." Desalination **124**(1): 51-62.

Bremere, I., Kennedy, M.D., Johnson, A., van Emmerik, R., Witkamp, G.J. and Schippers, J.C. (1998). "Increasing conversion in membrane filtration systems using a desupersaturation unit to prevent scaling." Desalination **119**(1): 199-204.

Brepols, C., Drensla, K., Janot, A., Trimborn, M. and Engelhardt, N. (2008). "Strategies for chemical cleaning in large scale membrane bioreactors." Water Science & Technology **57**(3): 457-463.

Bridier, A., Briandet, R., Thomas, V. and Dubois-Brissonnet, F. (2011). "Resistance of bacterial biofilms to disinfectants: a review." Biofouling **27**(9): 1017-1032.

Cabiscol, E., Tamarit, J. and Ros, J. (2010). "Oxidative stress in bacteria and protein damage by reactive oxygen species." International Microbiology **3**(1): 3-8.

Cai, W., Liu, J., Zhang, X., Ng, W.J. and Liu, Y. (2016). "Generation of dissolved organic matter and byproducts from activated sludge during contact with sodium hypochlorite and its implications to on-line chemical cleaning in MBR." Water Research **104**: 44-52.

Cai, W. and Liu, Y. (2016). "Enhanced membrane biofouling potential by on-line chemical cleaning in membrane bioreactor." Journal of Membrane Science **511**: 84-91.

Cemeli, E., Wagner, E.D., Anderson, D., Richardson, S.D. and Plewa, M.J. (2006). "Modulation of the cytotoxicity and genotoxicity of the drinking water disinfection byproduct iodoacetic acid by suppressors of oxidative stress." Environmental Science & Technology **40**(6): 1878-1883.

Ceron-Vivas, A., Morgan-Sagastume, J.M. and Noyola, A. (2012). "Intermittent filtration and gas bubbling for fouling reduction in anaerobic membrane bioreactors." Journal of Membrane Science **423**: 136-142.

Chang, I.S. and Kim, S.N. (2005). "Wastewater treatment using membrane filtration-effect of biosolids concentration on cake resistance." Process Biochemistry **40**(3): 1307-1314.

Chang, I.S., Le Clech, P., Jefferson, B. and Judd, S. (2002). "Membrane fouling in membrane bioreactors for wastewater treatment." Journal of Environmental Engineering 128(11): 1018-1029.

Chang, I.S. and Lee, C.H. (1998). "Membrane filtration characteristics in membrane-coupled activated sludge system-the effect of physiological states of activated sludge on membrane fouling." Desalination **120**(3): 221-233.

Chen, D. and Columbia, M. (2011). "Enzymatic control of alginate fouling of dead-end MF and UF ceramic membranes." Journal of Membrane Science **381**(1): 118-125.

Chen, H., Zheng, X., Chen, Y., Li, M., Liu, K. and Li, X. (2014). "Influence of copper nanoparticles on the physical-chemical properties of activated sludge." Plos One **9**(3): e9871.

Chen, W., Westerhoff, P., Leenheer, J.A. and Booksh, K. (2003). "Fluorescence excitation-Emission matrix regional integration to quantify spectra for dissolved organic matter." Environmental Science & Technology **37**(24): 5701-5710.

Cheryan, M. (1998). Ultrafiltration and microfiltration handbook, CRC press.

Cho, B.D. and Fane, A.G. (2002). "Fouling transients in nominally sub-critical flux operation of a membrane bioreactor. " Journal of membrane science **209**(2): 391-403.

Cho, M., Kim, J., Kim, J.Y., Yoon, J. and Kim, J.H. (2010). "Mechanisms of Escherichia coli inactivation by several disinfectants." Water Research **44**(11): 3410-3418.

Choo, K.H. and Lee, C.H. (1996). "Membrane fouling mechanisms in the membrane-coupled anaerobic bioreactor." Water research **30**(8): 1771-1780.

Chu, L. and Li, S. (2006). "Filtration capability and operational characteristics of dynamic membrane bioreactor for municipal wastewater treatment." Separation and Purification Technology **51**(2): 173-179.

Chua, H.C., Arno, T.C. and Howell, J.A. (2002). "Controlling fouling in membrane bioreactors operated with a variable throughput." Desalination **149**(1-3): 225-229.

Çiçek, N., Franco, J.P., Suidan, M.T., Urbain, V. and Manem, J. (1999). "Characterization and comparison of a membrane bioreactor and a conventional activated-sludge system in the treatment of wastewater containing high-molecular-weight compounds." Water Environment Research **71**(1): 64-70.

Coble, P.G. (1996). "Characterization of marine and terrestrial DOM in seawater using excitation emission matrix spectroscopy." Marine Chemistry **51**(4): 325-346.

Cogan, N. and Chellam, S. (2009). "Incorporating pore blocking, cake filtration, and EPS production in a model for constant pressure bacterial fouling during dead-end microfiltration." Journal of Membrane Science **345**(1): 81-89.

Conibear, T.C.R., Collins, S.L. and Webb, J.S. (2009). "Role of Mutation in Pseudomonas aeruginosa Biofilm Development." Plos One **4**(7): e6289.

Cory, R.M. and McKnight, D.M. (2005). "Fluorescence spectroscopy reveals ubiquitous presence of oxidized and reduced quinones in dissolved organic matter." Environmental Science & Technology **39**(21): 8142-8149.

Costa, A.R., de Pinho, M.N. and Elimelech, M. (2006). "Mechanisms of colloidal natural organic matter fouling in ultrafiltration." Journal of Membrane Science **281**(1): 716-725.

Costerton, J.W., Lewandowski, Z., Caldwell, D.E., Korber, D.R. and Lappinscott, H.M. (1995). "Microbial biofilms." Annual Review of Microbiology **49**: 711-745.

Çulfaz, P.Z., Wessling, M. and Lammertink, R.G.H. (2011). "Fouling behavior of microstructured hollow fiber membranes in submerged and aerated filtrations." Water research **45**(4): 1865-1871.

De Araujo, C., Balestrino, D., Roth, L., Charbonnel, N. and Forestier, C. (2010). "Quorum sensing affects biofilm formation through lipopolysaccharide synthesis in Klebsiella pneumoniae." Research in Microbiology **161**(7): 595-603.

Derlon, N., Massé, A., Escudié, R., Bernet, N. and Paul, E. (2008). "Stratification in the cohesion of biofilms grown under various environmental conditions." Water Research **42**(8-9): 2102-2110.

Desai, M., Bühler, T., Weller, P. and Brown, M. (1998). "Increasing resistance of planktonic and biofilm cultures of Burkholderia cepacia to ciprofloxacin and ceftazidime during exponential growth." Journal of Antimicrobial Chemotherapy **42**(2): 153-160.

Ding, G., Zhang, X., Yang, M. and Pan, Y. (2013). "Formation of new brominated disinfection byproducts during chlorination of saline sewage effluents." Water Research **47**(8): 2710-2718.

Do, V.T., Tang, C.Y., Reinhard, M. and Leckie, J.O. (2012a). "Degradation of polyamide nanofiltration and reverse osmosis membranes by hypochlorite." Environmental science & technology **46**(2): 852-859.

Do, V.T., Tang, C.Y., Reinhard, M. and Leckie, J.O. (2012b). "Effects of chlorine exposure conditions on physiochemical properties and performance of a polyamide membrane mechanisms and implications." Environmental Science & Technology **46**(24): 13184-13192.

Doederer, K., Gernjak, W., Weinberg, H.S. and Farré, M.J. (2014). "Factors affecting the formation of disinfection by-products during chlorination and chloramination of secondary effluent for the production of high quality recycled water." Water Research **48**: 218-228.

Doyen, W., Mues, W., Molenberghs, B. and Cobben, B. (2010). "Spacer fabric supported flat-sheet membranes: a new era of flat-sheet membrane technology." Desalination **250**(3): 1078-1082.

Dubois, M., Gilles, K.A., Hamilton, J.K., Rebers, P.A. and Smith, F. (1956). "Colorimetric method for determination of sugars and related substances." Analytical Chemistry **28**(3): 350-356.

Dukan, S., Belkin, S. and Touati, D. (1999). "Reactive oxygen species are partially involved in the bacteriocidal action of hypochlorous acid." Archives of Biochemistry and Biophysics **367**(2): 311-316.

Dukan, S. and Touati, D. (1996). "Hypochlorous acid stress in Escherichia coli: resistance, DNA damage, and comparison with hydrogen peroxide stress." Journal of Bacteriology **178**(21): 6145-6150.

Fan, F. and Zhou, H. (2007). "Interrelated effects of aeration and mixed liquor fractions on membrane fouling for submerged membrane bioreactor processes in wastewater treatment." Environmental Science & Technology **41**(7): 2523-2528.

Flemming, H.C., Schaule, G., Griebe, T., Schmitt, J. and Tamachkiarowa, A. (1997). "Biofouling—the Achilles heel of membrane processes." Desalination **113**(2): 215-225.

Flemming, H.C. and Wingender, J. (2010). "The biofilm matrix." Nature Reviews Microbiology **8**(9): 623-633.

Fukuzaki, S. (2006). "Mechanisms of actions of sodium hypochlorite in cleaning and disinfection processes." Biocontrol Science **11**(4): 147-157.

Fuqua, W.C., Winans, S.C. and Greenberg, E.P. (1994). "Quorum sensing in bacteria: the Luxr-Luxi family of cell density-responsive transcriptional regulators." Journal of Bacteriology **176**(2): 269-275.

Gao, D.W., Zhang, T., Tang, C.Y.Y., Wu, W.M., Wong, C.Y., Lee, Y.H., Yeh, D.H. and Criddle, C.S. (2010) "Membrane fouling in an anaerobic membrane bioreactor: Differences in relative abundance of bacterial species in the membrane foulant layer and in suspension." Journal of Membrane Science **364**(1): 331-338.

Gao, W., Lin, H., Leung, K., Schraft, H. and Liao, B. (2011). "Structure of cake layer in a submerged anaerobic membrane bioreactor." Journal of Membrane Science **374**(1): 110-120.

Giraldo, E. and LeChevallier, M. (2007). "Let them wear cake." Water Environment & Technology **19**(3): 46-51.

Goldman, G., Starosvetsky, J. and Armon, R. (2009). "Inhibition of biofilm formation on UF membrane by use of specific bacteriophages." Journal of Membrane Science **342**(1–2): 145-152.

Gomes de Melo, B.A., Motta, F.L. and Andrade Santana, M.H. (2016). "Humic acids: Structural properties and multiple functionalities for novel technological developments." Materials Science & Engineering: C **62**: 967-974.

Grélot, A., Busnot, A., Grelier, P., Tazi-Pain, A., Heijnen, M. and Grasmick, A. (2009). "A new and appropriate fibre sheet configuration for MBR technologies." Desalination and Water Treatment **6**(1-3): 25-32.

Grelot, A., Machinal, C., Drouet, K., Tazi-Pain, A., Schrotter, J., Grasmick, A. and Grinwis, S. (2008). "In the search of alternative cleaning solutions for MBR plants." Water Science & Technology **58**(10): 2041-2049.

Gui, P., Huang, X., Chen, Y. and Qian, Y. (2003). "Effect of operational parameters on sludge accumulation on membrane surfaces in a submerged membrane bioreactor." Desalination **151**(2): 185-194.

Guo, L., Lu, M., Li, Q., Zhang, J., Zong, Y. and She, Z. (2014). "Three-dimensional fluorescence excitation-emission matrix (EEM) spectroscopy with regional integration analysis for assessing waste sludge hydrolysis treated with multi-enzyme and thermophilic bacteria." Bioresource Technology **171**: 22-28.

Haas, C.N. and Engelbrecht, R.S. (1980). "Physiological alterations of vegetative microorganisms resulting form chlorination." Journal (Water Pollution Control Federation) **52**(7): 1976-1989.

Han, X., Wang, Z., Wang, X., Zheng, X., Ma, J. and Wu, Z. (2016). "Microbial responses to membrane cleaning using sodium hypochlorite in membrane

bioreactors: Cell integrity, key enzymes and intracellular reactive oxygen species." Water Research **88**: 293-300.

Hashino, M., Katagiri, T., Kubota, N., Ohmukai, Y., Maruyama, T. and Matsuyama, H. (2011). "Effect of surface roughness of hollow fiber membranes with gear-shaped structure on membrane fouling by sodium alginate." Journal of Membrane Science **366**(1): 389-397.

Hassett, D.J., Ma, J.F., Elkins, J.G., McDermott, T.R., Ochsner, U.A., West, S.E.H., Huang, C.T., Fredericks, J., Burnett, S., Stewart, P.S., McFeters, G., Passador, L. and Iglewski, B.H. (1999). "Quorum sensing in Pseudomonas aeruginosa controls expression of catalase and superoxide dismutase genes and mediates biofilm susceptibility to hydrogen peroxide." Molecular Microbiology **34**(5): 1082-1093.

Helbling, D.E. and VanBriesen, J.M. (2007). "Free chlorine demand and cell survival of microbial suspensions." Water Research **41**(19): 4424-4434.

Hoffman, L.R., D'Argenio, D.A., MacCoss, M.J., Zhang, Z.Y., Jones, R.A. and Miller, S.I. (2005). "Aminoglycoside antibiotics induce bacterial biofilm formation." Nature **436**(7054): 1171-1175.

Hong, S., Bae, T., Tak, T., Hong, S. and Randall, A. (2002). "Fouling control in activated sludge submerged hollow fiber membrane bioreactors." Desalination **143**(3): 219-228.

Huang, Z., Ong, S.L. and Ng, H.Y. (2008). "Feasibility of submerged anaerobic membrane bioreactor (SAMBR) for treatment of low-strength wastewater." Water Science & Technology **58**(10): 1925-1931.

Hur, J., Lee, B.M. and Shin, K.H. (2014). "Spectroscopic characterization of dissolved organic matter isolates from sediments and the association with phenanthrene binding affinity." Chemosphere **111**: 450-457.

Hwang, B.K., Lee, W.N., Yeon, K.M., Park, P.K., Lee, C.H., Chang, i.S., Drews, A. and Kraume, M. (2008). "Correlating TMP increases with microbial characteristics in the bio-cake on the membrane surface in a membrane bioreactor. " Environmental Science & Technology **42**(11): 3963-3968.

Hwang, K.J., Chan, C.S. and Tung, K.L. (2009). "Effect of backwash on the performance of submerged membrane filtration. " Journal of Membrane Science **330**(1): 349-356.

Itokawa, H., Thiemig, C. and Pinnekamp, J. (2008). "Design and operating experiences of municipal MBRs in Europe." Water Science & Technology **58**(12): 2319-2327.

Ivanovic, I. and Leiknes, T. (2008). "Impact of aeration rates on particle colloidal fraction in the biofilm membrane bioreactor (BF-MBR)." Desalination **231**(1): 182-190.

Jeison, D. and van Lier, J.B. (2007). "Cake formation and consolidation: main factors governing the applicable flux in anaerobic submerged membrane bioreactors (AnSMBR) treating acidified wastewaters." Separation and Purification Technology **56**(1): 71-78.

Jia, X., Zhu, C., Li, M., Xi, B., Wang, L., Yang, X., Xia, X. and Su, J. (2013). "A comparison of treatment techniques to enhance fermentative hydrogen production from piggery anaerobic digested residues." International Journal of Hydrogen Energy **38**(21): 8691-8698.

Jiang, T., Kennedy, M., Guinzbourg, B., Vanrolleghem, P.A. and Schippers, J. (2005). "Optimising the operation of a MBR pilot plant by quantitative analysis of the membrane fouling mechanism." Water Science & Technology **51**(6-7): 19-25.

Jinhua, P., Fukushi, K. and Yamamoto, K. (2006). "Bacterial community structure on membrane surface and characteristics of strains isolated from membrane surface in submerged membrane bioreactor." Separation Science and Technology **41**(7): 1527-1549.

Joelsson, A., Kan, B. and Zhu, J. (2007). "Quorum sensing enhances the stress response in Vibrio cholerae." Applied and Environmental Microbiology **73**(11): 3742-3746.

Joelsson, A., Liu, Z. and Zhu, J. (2006). "Genetic and phenotypic diversity of quorum-sensing systems in clinical and environmental isolates of Vibrio cholerae." Infection and Immunity **74**(2): 1141-1147.

Judd, S. (2010). The MBR book: principles and applications of membrane bioreactors for water and wastewater treatment Butterworth-Heinemann, Oxford.

Kang, I.J., Yoon, S.H. and Lee, C.H. (2002). "Comparison of the filtration characteristics of organic and inorganic membranes in a membrane-coupled anaerobic bioreactor." Water Research **36**(7): 1803-1813.

Khor, S.L., Sun, D.D., Liu, Y. and Leckie, J.O. (2007). "Biofouling development and rejection enhancement in long SRT MF membrane bioreactor." Process Biochemistry **42**(12): 1641-1648.

Kim, A.S., Chen, H. and Yuan, R. (2006). "EPS biofouling in membrane filtration: an analytic modeling study." Journal of Colloid and Interface Science **303**(1): 243-249.

Kimura, K., Ogawa, N. and Watanabe, Y. (2013). "Permeability decline in nanofiltration/reverse osmosis membranes fed with municipal wastewater treated by a membrane bioreactor." Water Science & Technology **67**(9): 1994-1999.

Kimura, K., Yamato, N., Yamamura, H. and Watanabe, Y. (2005). "Membrane fouling in pilot-scale membrane bioreactors (MBRs) treating municipal wastewater." Environmental Science & Technology **39**(16): 6293-6299.

Kowalczuk, P., Durako, M.J., Young, H., Kahn, A.E., Cooper, W.J. and Gonsior, M. (2009). "Characterization of dissolved organic matter fluorescence in the South Atlantic Bight with use of PARAFAC model: Interannual variability." Marine Chemistry **113**(3–4): 182-196.

Krause, S., Zimmermann, B., Meyer-Blumenroth, U., Lamparter, W., Siembida, B. and Cornel, P. (2010). "Enhanced membrane bioreactor process without chemical cleaning." Water Science & Technology **61**(10): 2575-2580.

Kuberkar, V.T. and Davis, R.H. (2000). "Modeling of fouling reduction by secondary membranes." Journal of Membrane Science **168**(1): 243-258.

Kuzmenko, D., Arkhangelsky, E., Belfer, S., Freger, V. and Gitis, V. (2005). "Chemical cleaning of UF membranes fouled by BSA." Desalination **179**(1): 323-333.

Kweon, J.H., Jung, J.H., Lee, S.R., Hui, H.W., Shin, Y. and Choi, Y.H. (2012). "Effects of consecutive chemical cleaning on membrane performance and surface properties of microfiltration." Desalination **286**: 324-331.

LaPaglia, C. and Hartzell, P.L. (1997). "Stress-induced production of biofilm in the hyperthermophile Archaeoglobus fulgidus." Applied and Environmental Microbiology **63**(8): 3158-3163.

Laspidou, C.S. and Rittmann, B.E. (2002). "A unified theory for extracellular polymeric substances, soluble microbial products, and active and inert biomass." Water Research **36**(11): 2711-2720.

Lawaetz, A.J. and Stedmon, C.A. (2009). "Fluorescence intensity calibration using the raman scatter peak of water." Applied Spectroscopy **63**(8): 936-940.

Le-Clech, P., Chen, V. and Fane, T.A.G. (2006). "Fouling in membrane bioreactors used in wastewater treatment." Journal of Membrane Science **284**(1–2): 17-53.

Le-Clech, P., Jefferson, B. and Judd, S. (2003) "Impact of aeration, solids concentration and membrane characteristics on the hydraulic performance of a membrane bioreactor." Journal of Membrane Science **218**(1): 117-129.

Le-Clech, P., Jefferson, B. and Judd, S. (2005). "A comparison of submerged and sidestream tubular membrane bioreactor configurations." Desalination **173**(2): 113-122.

Lechevallier, M.W., Cawthon, C.D. and Lee, R.G. (1988). "Factors promoting survival of bacteria in chlorinated water-supplies." Applied and Environmental Microbiology **54**(3): 649-654.

Lee, E.J., Kim, K.Y., Lee, Y.S., Nam, J.W., Lee, Y.S., Kim, H.S. and Jang, A. (2012). "A study on the high-flux MBR system using PTFE flat sheet membranes with chemical backwashing." Desalination **306**: 35-40.

Lee, E.J., Kim,Y.H., Lee, C.H., Kim, H.S. and Kim, H.S. (2016). "Effect of different physical conditions on fouling control in in-situ chemical cleaning in place (CIP) for flat sheet membranes fouled by secondary effluents." Chemical Engineering Journal **302**: 128-136.

Lee, E.J., Kim, Y.H., Kim, H.S. and Jang, A. (2015). "Influence of microbubble in physical cleaning of MF membrane process for wastewater reuse." Environmental Science and Pollution Research **22**(11): 8451–8459.

Lee, E.J., Kwon, J.S., Park, H.S., Ji, W.H., Kim, H.S. and Jang, A. (2013). "Influence of sodium hypochlorite used for chemical enhanced backwashing on biophysical treatment in MBR." Desalination **316**: 104-109.

Lee, J., Ahn, W.Y. and Lee, C.H. (2001). "Comparison of the filtration characteristics between attached and suspended growth microorganisms in submerged membrane bioreactor." Water Research **35**(10): 2435-2445.

Lee, S. and Elimelech, M. (2006). "Relating organic fouling of reverse osmosis membranes to intermolecular adhesion forces." Environmental Science & Technology **40**(3): 980-987.

Lee, W., Kang, S. and Shin, H. (2003). "Sludge characteristics and their contribution to microfiltration in submerged membrane bioreactors." Journal of Membrane Science **216**(1): 217-227.

Lesjean, B., Rosenberger, S., Laabs, C., Jekel, M., Gnirss, R. and Amy, G. (2005). "Correlation between membrane fouling and soluble/colloidal organic substances in membrane bioreactors for municipal wastewater treatment." Water Science & Technology **51**(6-7): 1-8.

Li, H., Yang, M., Zhang, Y., Liu, X., Gao, M. and Kamagata, Y. (2004). "Comparison of nitrification performance and microbial community between submerged membrane bioreactor and conventional activated sludge system." Water Science & Technology **51**(6-7): 193-200.

Li, Q. and Elimelech, M. (2004). "Organic fouling and chemical cleaning of nanofiltration membranes: measurements and mechanisms." Environmental Science & Technology **38**(17): 4683-4693.

Li, X.Y. and Chu, H.P. (2003) "Membrane bioreactor for the drinking water treatment of polluted surface water supplies." Water Research **37**(19): 4781-4791.

Li, Y., Zhang, X., Shang, C. and Krasner, S.W. (2011). "Evaluation and improvement of total organic bromine analysis with respect to reductive property of activated carbon." Water Research **45**(3): 1229-1237.

Liang, S., Liu, C. and Song, L. (2007). "Soluble microbial products in membrane bioreactor operation: Behaviors, characteristics, and fouling potential." Water Research **41**(1): 95-101.

Liao, B.Q., Kraemer, J.T. and Bagley, D.M. (2006). "Anaerobic membrane bioreactors: applications and research directions." Critical Reviews in Environmental Science and Technology **36**(6): 489-530.

Liao, B.Q., Catalan, L.J.J., Droppo, I.G. and Liss, S.N. (2004). "Impact of chemical oxidation on sludge properties and membrane flux in membrane separation bioreactors." Journal of Chemical Technology and Biotechnology **79**(12): 1342-1348.

Lim, B.R., Ahn, K.H., Song, K.G. and Cho, J.W. (2005). "Microbial community in biofilm on membrane surface of submerged MBR: effect of in-line cleaning chemical agent." Water Science & Technology **51**(6-7): 201-207.

Lin, H., Liao, B.Q., Chen, J., Gao, W., Wang, L., Wang, F. and Lu, X. (2011). "New insights into membrane fouling in a submerged anaerobic membrane bioreactor based on characterization of cake sludge and bulk sludge." Bioresource Technology **102**(3): 2373-2379.

Lin, H., Xie, K., Mahendran, B., Bagley, D., Leung, K., Liss, S. and Liao, B. (2010). "Factors affecting sludge cake formation in a submerged anaerobic membrane bioreactor." Journal of Membrane Science **361**(1): 126-134.

Lisle, J.T., Broadaway, S.C., Prescott, A.M., Pyle, B.H., Fricker, C. and McFeters, G.A. (1998). "Effects of starvation on physiological activity and chlorine disinfection resistance in Escherichia coli O157:H7." Applied and Environmental Microbiology **64**(12): 4658-4662.

Liu, C., Caothien, S., Hayes, J., Caothuy, T., Otoyo, T. and Ogawa, T. (2001). "Membrane chemical cleaning: from art to science." AWWA 2000 Water Quality Technology Conference.

Liu, J. and Zhang, X. (2013). "Effect of quenching time and quenching agent dose on total organic halogen measurement." International Journal of Environmental Analytical Chemistry **93**(11): 1146-1158.

Liu, J. and Zhang, X. (2014). "Comparative toxicity of new halophenolic DBPs in chlorinated saline wastewater effluents against a marine alga: Halophenolic DBPs are generally more toxic than haloaliphatic ones." Water Research **65**: 64-72.

Liu, J., Zhang, X., Li, Y., (2015). "Effect of boiling on halogenated DBPs and their developmental toxicity in real tap water." *Recent Advances in Disinfection By-Products*. American Chemical Society, Washington, DC, 45–60.

Lowry, O.H., Rosebrough, N.J., Farr, A.L. and Randall, R.J. (1951). "Protein measurement with the folin phenol reagent." Journal of Biological Chemistry **193**(1): 265-275.

Lu, T.K. and Collins, J.J. (2007). "Dispersing biofilms with engineered enzymatic bacteriophage." Proceedings of the National Academy of Sciences **104**(27): 11197-11202.

Lumjiaktase, P., Diggle, S.P., Loprasert, S., Tungpradabkul, S., Daykin, M., Camara, M., Williams, P. and Kunakorn, M. (2006). "Quorum sensing regulates dpsA and the oxidative stress response in Burkholderia pseudomallei." Microbiology **152**: 3651-3659.

Lyko, S., Al-Halbouni, D., Wintgens, T., Janot, A., Hollender, J., Dott, W. and Melin, T. (2007). "Polymeric compounds in activated sludge supernatant-characterisation and retention mechanisms at a full-scale municipal membrane bioreactor." Water Research **41**(17): 3894-3902.

Lyko, S., Wintgens, T., Al-Halbouni, D., Baumgarten, S., Tacke, D., Drensla, K., Janot, A., Dott, W., Pinnekamp, J. and Melin, T. (2008). "Long-term monitoring of a full-scale municipal membrane bioreactor—characterisation of foulants and operational performance." Journal of Membrane Science **317**(1): 78-87.

Ma, J., Wang, Z., Yang, Y., Mei, X. and Wu, Z. (2013). "Correlating microbial community structure and composition with aeration intensity in

submerged membrane bioreactors by 454 high-throughput pyrosequencing." Water Research **47**(2): 859-869.

Madaeni, S.S., Fane, A.G. and Wiley, D.E. (1999). "Factors influencing critical flux in membrane filtration of activated sludge." Journal of Chemical Technology and Biotechnology **74**(6): 539-543.

Maeda, S., Ito, M., Ando, T., Ishimoto, Y., Fujisawa, Y., Takahashi, H., Matsuda, A., Sawamura, A. and Kato, S. (2006). "Horizontal transfer of nonconjugative plasmids in a colony biofilm of Escherichia coli." Fems Microbiology Letters **255**(1): 115-120.

Mah, T.F.C. and O'Toole, G.A. (2001). "Mechanisms of biofilm resistance to antimicrobial agents." Trends in Microbiology **9**(1): 34-39.

Martinez-Sosa, D., Helmreich, B., Netter, T., Paris, S., Bischof, F. and Horn, H. (2011). "Pilot-scale anaerobic submerged membrane bioreactor (AnSMBR) treating municipal wastewater: the fouling phenomenon and long-term operation." Water Science & Technology **64**(9): 1804-1811.

McNab, R., Ford, S.K., El-Sabaeny, A., Barbieri, B., Cook, G.S. and Lamont, R.J. (2003). "LuxS-based signaling in Streptococcus gordonii: autoinducer 2 controls carbohydrate metabolism and biofilm formation with Porphyromonas gingivalis." Journal of Bacteriology **185**(1): 274-284.

Meng, F., Chae, S.R., Drews, A., Kraume, M., Shin, H.S. and Yang, F. (2009). "Recent advances in membrane bioreactors (MBRs): membrane fouling and membrane material." Water Research **43**(6): 1489-1512.

Meng, F. and Yang, F. (2007). "Fouling mechanisms of deflocculated sludge, normal sludge, and bulking sludge in membrane bioreactor." Journal of Membrane Science **305**(1): 48-56.

Meng, F., Zhang, H., Yang, F., Zhang, S., Li, Y. and Zhang, X. (2006). "Identification of activated sludge properties affecting membrane fouling in submerged membrane bioreactors." Separation and Purification Technology **51**(1): 95-103.

Metzger, U., Le-Clech, P., Stuetz, R.M., Frimmel, F.H. and Chen, V. (2007). "Characterisation of polymeric fouling in membrane bioreactors and the

effect of different filtration modes." Journal of Membrane Science **301**(1): 180-189.

Miura, Y., Watanabe, Y. and Okabe, S. (2007). "Membrane biofouling in pilot-scale membrane bioreactors (MBRs) treating municipal wastewater: impact of biofilm formation." Environmental Science & Technology **41**(2): 632-638.

Mo, Y., Chen, J., Xue, W. and Huang, X. (2010). "Chemical cleaning of nanofiltration membrane filtrating the effluent from a membrane bioreactor." Separation and Purification Technology **75**(3): 407-414.

Morgan, J.W., Forster, C.F. and Evison, L. (1990). "A comparative-study of the nature of biopolymers extracted from anaerobic and activated sludges." Water Research **24**(6): 743-750.

Murphy, K.R., Stedmon, C.A., Waite, T.D. and Ruiz, G.M. (2008). "Distinguishing between terrestrial and autochthonous organic matter sources in marine environments using fluorescence spectroscopy." Marine Chemistry **108**(1–2): 40-58.

Navarro, R.R., Hori, T., Inaba, T., Matsuo, K., Habe, H. and Ogata, A. (2016). "High-resolution phylogenetic analysis of residual bacterial species of fouled membranes after NaOCl cleaning." Water Research **94**: 166-175.

Ng, C., Sun, D., Zhang, J., Chua, H., Bing, W., Tay, S. and Fane, A. (2005). "Strategies to improve the sustainable operation of membrane bioreactors." Proceedings of the International Desalination Association Conference, Singapore, 37-45.

Nguyen, K.T., Piastro, K., Gray, T.A. and Derbyshire, K.M. (2010). "Mycobacterial biofilms facilitate horizontal DNA transfer between strains of Mycobacterium smegmatis." Journal of Bacteriology **192**(19): 5134-5142.

Ognier, S., Wisniewski, C. and Grasmick, A. (2002). "Characterisation and modelling of fouling in membrane bioreactors." Desalination **146**(1): 141-147.

Oliveira, R., Melo, L., Oliveira, A. and Salgueiro, R. (1994). "Polysaccharide production and biofilm formation by Pseudomonas-fluorescens: effects

of PH and surface material." Colloids and Surfaces B: Biointerfaces **2**(1-3): 41-46.

Pals, J., Attene-Ramos, M.S., Xia, M., Wagner, E.D. and Plewa, M.J. (2013). "Human cell toxicogenomic analysis linking reactive oxygen species to the toxicity of monohaloacetic acid drinking water disinfection byproducts." Environmental Science & Technology **47**(21): 12514-12523.

Pan, Y. and Zhang, X. (2013a). "Four groups of new aromatic halogenated disinfection byproducts: Effect of bromide concentration on their formation and speciation in chlorinated drinking water." Environmental Science & Technology **47**(3): 1265-1273.

Pan, Y. and Zhang, X. (2013b). "Total organic iodine measurement: A new approach with UPLC/ESI-MS for off-line iodide separation/detection." Water Research **47**(1): 163-172.

Pang, C.M., Hong, P., Guo, H. and Liu, W.T. (2005). "Biofilm formation characteristics of bacterial isolates retrieved from a reverse osmosis membrane." Environmental Science & Technology **39**(19): 7541-7550.

Paul, P. and Hartung, C. (2008). "Modelling of biological fouling propensity by inference in a side stream membrane bioreactor." Desalination **224**(1–3): 154-159.

Pereira, C.S., Thompson, J.A. and Xavier, K.B. (2013). "AI-2-mediated signalling in bacteria." Fems Microbiology Reviews **37**(2): 156-181.

Petrus, H., Li, H., Chen, V. and Norazman, N. (2008). "Enzymatic cleaning of ultrafiltration membranes fouled by protein mixture solutions." Journal of Membrane Science **325**(2): 783-792.

Phong, D.D. and Hur, J. (2015). "Insight into photocatalytic degradation of dissolved organic matter in UVA/TiO2 systems revealed by fluorescence EEM-PARAFAC." Water Research **87**: 119-126.

Pollice, A., Brookes, A., Jefferson, B. and Judd, S. (2005). "Sub-critical flux fouling in membrane bioreactors-a review of recent literature." Desalination **174**(3): 221-230.

Porcelli, N. and Judd, S. (2010). "Chemical cleaning of potable water membranes: a review." Separation and Purification Technology **71**(2): 137-143.

Puspitasari, V., Granville, A., Le-Clech, P. and Chen, V. (2010). "Cleaning and ageing effect of sodium hypochlorite on polyvinylidene fluoride (PVDF) membrane." Separation and Purification Technology **72**(3): 301-308.

Qin, F., Zhao, Y.Y., Zhao, Y., Boyd, J.M., Zhou, W. and Li, X.F. (2010). "A toxic disinfection by-product, 2,6-dichloro-1,4-benzoquinone, identified in drinking water." Angewandte Chemie-International Edition **49**(4): 790-792.

Quinones, B., Dulla, G. and Lindow, S.E. (2005). "Quorum sensing regulates exopolysaccharide production, motility, and virulence in Pseudomonas syringae." Molecular Plant-Microbe Interactions **18**(7): 682-693.

Rachid, S., Ohlsen, K., Wallner, U., Hacker, J., Hecker, M. and Ziebuhr, W. (2000a). "Alternative transcription factor ς^B is involved in regulation of biofilm expression in a Staphylococcus aureus mucosal isolate." Journal of Bacteriology **182**(23): 6824-6826.

Rachid, S., Ohlsen, K., Witte, W., Hacker, J. and Ziebuhr, W. (2000b). "Effect of subinhibitory antibiotic concentrations on polysaccharide intercellular adhesin expression in biofilm-forming Staphylococcus epidermidis." Antimicrobial Agents and Chemotherapy **44**(12): 3357-3363.

Ramesh, A., Lee, D. and Lai, J. (2007). "Membrane biofouling by extracellular polymeric substances or soluble microbial products from membrane bioreactor sludge." Applied Microbiology and Biotechnology **74**(3): 699-707.

Regula, C., Carretier, E., Wyart, Y., Sergent, M., Gésan-Guiziou, G., Ferry, D., Vincent, A., Boudot, D. and Moulin, P. (2013). "Ageing of ultrafiltration membranes in contact with sodium hypochlorite and commercial oxidant: Experimental designs as a new ageing protocol." Separation and Purification Technology **103**: 119-138.

Richardson, S.D. and Ternes, T.A. (2014). "Water analysis: Emerging contaminants and current issues." Analytical Chemistry **86**(6): 2813-2848.

Robles, A., Durán, F., Ruano, M., Ribes, J. and Ferrer, J. (2012). "Influence of total solids concentration on membrane permeability in a submerged

hollow-fibre anaerobic membrane bioreactor." Water Science & Technology **66**(2): 377-384.

Robles, A., Ruano, M., Ribes, J. and Ferrer, J. (2013). "Factors that affect the permeability of commercial hollow-fibre membranes in a submerged anaerobic MBR (HF-SAnMBR) system." Water Research **47**(3): 1277-1288.

Rosenberger, S., Evenblij, H., Poele, S.T., Wintgens, T. and Laabs, C. (2005). "The importance of liquid phase analyses to understand fouling in membrane assisted activated sludge processes-six case studies of different European research groups." Journal of Membrane Science **263**(1-2): 113-126.

Rosenberger, S., Laabs, C., Lesjean, B., Gnirss, R., Amy, G., Jekel, M. and Schrotter, J.C. (2006). "Impact of colloidal and soluble organic material on membrane performance in membrane bioreactors for municipal wastewater treatment." Water Research **40**(4): 710-720.

Rouaix, S., Causserand, C. and Aimar, P. (2006). "Experimental study of the effects of hypochlorite on polysulfone membrane properties. Journal of Membrane Science **277**(1): 137-147.

Samrakandi, M.M., Roques, C. and Michel, G. (1997). "Influence of trophic conditions on exopolysaccharide production: bacterial biofilm susceptibility to chlorine and monochloramine." Canadian Journal of Microbiology **43**(8): 751-758.

Santasmasas, C., Rovira, M., Clarens, F. and Valderrama, C. (2013). "Wastewater treatment by MBR pilot plant: flat sheet and hollow fibre case studies." Desalination and Water Treatment **51**(10-12): 2423-2430.

Scott, J., Neilson, D., Liu, W. and Boon, P. (1998). "A dual function membrane bioreactor system for enhanced aerobic remediation of high-strength industrial waste." Water Science & Technology **38**(4), 413-420.

Sedlak, D.L. and von Gunten, U. (2011). "The chlorine dilemma." Science **331**(6013): 42-43.

Senesi, N. (1990). "Molecular and quantitative aspects of the chemistry of fulvic-acid and its interactions with metal-ions and organic-chemicals: Part II.

The fluorescence spectroscopy approach." Analytica Chimica Acta **232**(1): 77-106.

Sheikholeslami, R. (1999). "Composite fouling-inorganic and biological: A review." Environmental Progress **18**(2): 113-122.

Shemesh, M., Kolter, R. and Losick, R. (2010). "The biocide chlorine dioxide stimulates biofilm formation in bacillus subtilis by activation of the histidine kinase kinc." Journal of Bacteriology **192**(24): 6352-6356.

Shorrock, C. and Bird, M. (1998). "Membrane cleaning: chemically enhanced removal of deposits formed during yeast cell harvesting." Food and Bioproducts Processing **76**(1): 30-38.

Sipma, J., Osuna, M.B., Emanuelsson, M.A. and Castro, P.M. (2010). "Biotreatment of industrial wastewaters under transient-state conditions: process stability with fluctuations of organic load, substrates, toxicants, and environmental parameters." Critical Reviews in Environmental Science and Technology **40**(2): 147-197.

Smith, P.J., Vigneswaran, S., Ngo, H.H., Ben-Aim, R. and Nguyen, H. (2005). "Design of a generic control system for optimising back flush durations in a submerged membrane hybrid reactor." Journal of Membrane Science **255**(1): 99-106.

Sofia, A., Ng, W.J. and Ong, S.L. (2004). "Engineering design approaches for minimum fouling in submerged MBR." Desalination **160**(1): 67-74.

Stedmon, C.A. and Bro, R. (2008). "Characterizing dissolved organic matter fluorescence with parallel factor analysis: A tutorial." Limnology and Oceanography-Methods **6**: 572-579.

Stedmon, C.A. and Markager, S. (2005). "Resolving the variability in dissolved organic matter fluorescence in a temperate estuary and its catchment using PARAFAC analysis." Limnology and Oceanography **50**(2): 686-697.

Stedmon, C.A., Markager, S. and Bro, R. (2003). "Tracing dissolved organic matter in aquatic environments using a new approach to fluorescence spectroscopy." Marine Chemistry **82**(3-4): 239-254.

Strugholtz, S., Sundaramoorthy, K., Panglisch, S., Lerch, A., Brügger, A. and Gimbel, R. (2005). "Evaluation of the performance of different chemicals for cleaning capillary membranes." Desalination **179**(1): 191-202.

Sun, Y., Wang, Y. and Huang, X. (2007). "Relationship between sludge settleability and membrane fouling in a membrane bioreactor." Frontiers of Environmental Science & Engineering in China **1**(2): 221-225.

Swietlik, J., Dabrowska, A., Raczyk-Stanislawiak, U. and Nawrocki, J. (2004). "Reactivity of natural organic matter fractions with chlorine dioxide and ozone." Water Research **38**(3): 547-558.

Swietlik, J. and Sikorska, E. (2004). "Application of fluorescence spectroscopy in the studies of natural organic matter fractions reactivity with chlorine dioxide and ozone." Water Research **38**(17): 3791-3799.

Tang, C.Y., Kwon, Y.N. and Leckie, J.O. (2007). "Fouling of reverse osmosis and nanofiltration membranes by humic acid-Effects of solution composition and hydrodynamic conditions. " Journal of Membrane Science **290**(1-2): 86–94.

Te Poele, S. and Van der Graaf, J. (2005). "Enzymatic cleaning in ultrafiltration of wastewater treatment plant effluent." Desalination **179**(1): 73-81.

Teitzel, G.M. and Parsek, M.R. (2003). "Heavy metal resistance of biofilm and planktonic Pseudomonas aeruginosa." Applied and Environmental Microbiology **69**(4): 2313-2320.

Teychene, B., Guigui, C., Cabassud, C. and Amy, G. (2008). "Toward a better identification of foulant species in MBR processes." Desalination **231**(1): 27-34.

Tran, T.M., Ye, Y., Chen, V., Stuetz, R. and Le-Clech, P. (2013). "Assessment of anti-fouling strategies for membrane coupled with upflow anaerobic sludge blanket (MUASB) process." Environmental Technology **34**(4): 521-528.

Trussell, R.S., Merlo, R.P., Hermanowicz, S.W. and Jenkins, D. (2006). "The effect of organic loading on process performance and membrane fouling in a submerged membrane bioreactor treating municipal wastewater." Water research **40**(14): 2675-2683.

Van den Broeck, R., Krzeminski, P., Van Dierdonck, J., Gins, G., Lousada-Ferreira, M., Van Impe, J.F.M., van der Graaf, J.H.J.M., Smets, I.Y. and van Lier, J.B. (2011). "Activated sludge characteristics affecting sludge filterability in municipal and industrial MBRs: Unraveling correlations using multi-component regression analysis." Journal of Membrane Science **378**(1-2): 330-338.

Van Der Gast, C.J., Jefferson, B., Reid, E., Robinson, T., Bailey, M.J., Judd, S.J. and Thompson, I.P. (2006). "Bacterial diversity is determined by volume in membrane bioreactors." Environmental Microbiology **8**(6): 1048-1055.

Vanysacker, L., Bernshtein, R. and Vankelecom, I.F. (2014). "Effect of chemical cleaning and membrane aging on membrane biofouling using model organisms with increasing complexity." Journal of Membrane Science **457**: 19-28.

Vendeville, A., Winzer, K., Heurlier, K., Tang, C.M. and Hardie, K.R. (2005). "Making 'sense' of metabolism: autoinducer-2, LuxS and pathogenic bacteria." Nature Reviews Microbiology **3**(5): 383-396.

Villanueva, C.M., Cantor, K.P., Cordier, S., Jaakkola, J.J.K., King, W.D., Lynch, C.F., Porru, S. and Kogevinas, M. (2004). "Disinfection byproducts and bladder cancer: a pooled analysis." Epidemiology **15**(3): 357-367.

Villarroel, R., Delgado, S., González, E. and Morales, M. (2013). "Physical cleaning initiation controlled by transmembrane pressure set-point in a submerged membrane bioreactor." Separation and Purification Technology **104**: 55-63.

Wang, J., Zamani, F., Cahyadi, A., Toh, J.Y., Yang, S., Wu, B., Liu, Y., Fane, A.G. and Chew J.W. "Correlating the hydrodynamics of fluidized granular activated carbon (GAC) with membrane-fouling mitigation." Journal of Membrane Science **510**:38-49.

Wang, P., Wang, Z., Wu, Z., Zhou, Q. and Yang, D. (2010). "Effect of hypochlorite cleaning on the physiochemical characteristics of polyvinylidene fluoride membranes." Chemical Engineering Journal **162**(3): 1050-1056.

Wang, S., Guillen, G. and Hoek, E.M. (2005). "Direct observation of microbial adhesion to membranes." Environmental Science & Technology **39**(17): 6461-6469.

Wang, W., Qian, Y., Li, J., Moe, B., Huang, R., Zhang, H., Hrudey, S.E. and Li, X.F. (2014a). "Analytical and toxicity characterization of halo-hydroxyl-benzoquinones as stable halobenzoquinone disinfection byproducts in treated water." Analytical Chemistry **86**(10): 4982-4988.

Wang, X.M., Li, X.Y. and Huang, X. (2007). "Membrane fouling in a submerged membrane bioreactor (SMBR): characterisation of the sludge cake and its high filtration resistance." Separation and Purification Technology **52**(3): 439-445.

Wang, Z., Ma, J., Tang, C.Y., Kimura, K., Wang, Q. and Han, X. (2014b). "Membrane cleaning in membrane bioreactors: a review." Journal Of Membrane Science **468**: 276-307.

Wang, Z., Mei, X., Ma, J., Grasmick, A. and Wu, Z. (2013a). "Potential foulants and fouling indicators in MBRs: a critical review." Separation Science and Technology **48**(1): 22-50.

Wang, Z., Meng, F., He, X., Zhou, Z., Huang, L.N. and Liang, S. (2014c). "Optimisation and performance of NaClO-assisted maintenance cleaning for fouling control in membrane bioreactors." Water Research **53**: 1-11.

Wang, Z., Yu, H., Ma, J., Zheng, X. and Wu, Z. (2013b). "Recent advances in membrane bio-technologies for sludge reduction and treatment." Biotechnology Advances **31**(8): 1187-1199.

Wei, C.H., Huang, X., Ben Aim, R., Yamamoto, K. and Amy, G. (2011). "Critical flux and chemical cleaning-in-place during the long-term operation of a pilot-scale submerged membrane bioreactor for municipal wastewater treatment." Water Research **45**(2): 863-871.

Wei, P., Zhang, K., Gao, W., Kong, L. and Field, R. (2013). "CFD modeling of hydrodynamic characteristics of slug bubble flow in a flat sheet membrane bioreactor." Journal of Membrane Science **445**: 15-24.

Wen, C., Huang, X. and Qian, Y. (1999). "Domestic wastewater treatment using an anaerobic bioreactor coupled with membrane filtration." Process Biochemistry **35**(3): 335-340.

Wisniewski, C. and Grasmick, A. (1998). "Floc size distribution in a membrane bioreactor and consequences for membrane fouling." Colloids and Surfaces A: Physicochemical and Engineering Aspects **138**(2–3): 403-411.

Wu, J., Le-Clech, P., Stuetz, R.M., Fane, A.G. and Chen, V. (2008a). "Effects of relaxation and backwashing conditions on fouling in membrane bioreactor." Journal of Membrane Science **324**(1): 26-32.

Wu, J., Le-Clech, P., Stuetz, R.M., Fane, A.G. and Chen, V. (2008b). "Novel filtration mode for fouling limitation in membrane bioreactors." Water Research **42**(14): 3677-3684.

Wu, Z., Wang, Z., Zhou, Z., Yu, G. and Gu, G. (2007). "Sludge rheological and physiological characteristics in a pilot-scale submerged membrane bioreactor." Desalination **212**(1): 152-164.

Xavier, J.B., Picioreanu, C., Rani, S.A., van Loosdrecht, M.C.M. and Stewart, P.S. (2005). "Biofilm-control strategies based on enzymic disruption of the extracellular polymeric substance matrix-a modelling study." Microbiology **151**: 3817-3832.

Xu, H. and Jiang, H. (2013). "UV-induced photochemical heterogeneity of dissolved and attached organic matter associated with cyanobacterial blooms in a eutrophic freshwater lake." Water Research **47**(17): 6506-6515.

Xu, H. and Liu, Y. (2010). "Control and cleaning of membrane biofouling by energy uncoupling and cellular communication." Environmental science & technology 45(2): 595-601.

Xu, H. and Liu, Y. (2011). "D-Amino acid mitigated membrane biofouling and promoted biofilm detachment." Journal of Membrane Science **376**(1–2): 266-274.

Yamanoi, I. and Kageyama, K. (2010). "Evaluation of bubble flow properties between flat sheet membranes in membrane bioreactor." Journal of Membrane Science **360**(1-2): 102-108.

Yamashita, Y. and Jaffé, R. (2008). "Characterizing the interactions between trace metals and dissolved organic matter using excitation−emission matrix and parallel factor analysis." Environmental Science & Technology **42**(19): 7374-7379.

Yamashita, Y. and Tanoue, E. (2003). "Chemical characterization of protein-like fluorophores in DOM in relation to aromatic amino acids." Marine Chemistry **82**(3-4): 255-271.

Yang, M. and Zhang, X. (2013). "Comparative developmental toxicity of new aromatic halogenated DBPs in a chlorinated saline sewage effluent to the marine polychaete platynereis dumerilii." Environmental Science & Technology **47**(19): 10868-10876.

Yang, M. and Zhang, X. (2014). "Halopyrroles: a new group of highly toxic disinfection byproducts formed in chlorinated saline wastewater." Environmental Science & Technology **48**(20): 11846-11852.

Yang, M. and Zhang, X. (2016). "Current trends in the analysis and identification of emerging disinfection byproducts." Trends in Environmental Analytical Chemistry **10**: 24-34.

Yang, Z., Du, M. and Jiang, J. (2016). "Reducing capacities and redox potentials of humic substances extracted from sewage sludge." Chemosphere **144**: 902-908.

Ye, Y., Clech, P.L., Chen, V. and Fane, A. (2005). "Evolution of fouling during crossflow filtration of model EPS solutions." Journal of Membrane Science **264**(1): 190-199.

Yeon, K.M., Cheong, W.S., Oh, H.S., Lee, W.N., Hwang, B.K., Lee, C.H., Beyenal, H. and Lewandowski, Z. (2008). "Quorum sensing: a new biofouling control paradigm in a membrane bioreactor for advanced wastewater treatment." Environmental Science & Technology **43**(2): 380-385.

You, H., Huang, C., Pan, J. and Chang, S. (2006). "Behavior of membrane scaling during crossflow filtration in the anaerobic MBR system." Separation Science and Technology **41**(7): 1265-1278.

Yu, C.H., Fang, L.C., Lateef, S.K., Wu, C.H. and Lin, C.F. (2010). "Enzymatic treatment for controlling irreversible membrane fouling in cross-flow humic acid-fed ultrafiltration." Journal of Hazardous Materials **177**(1): 1153-1158.

Zeman, L.J. and Zydney, A.L. (1996). Microfiltration and Ultrafiltration: Principles and Applications, CRC Press.

Zhai, H. and Zhang, X. (2011). "Formation and decomposition of new and unknown polar brominated disinfection byproducts during chlorination." Environmental Science & Technology **45**(6): 2194-2201.

Zhai, H., Zhang, X., Zhu, X., Liu, J. and Ji, M. (2014). "Formation of brominated disinfection byproducts during chloramination of drinking water: new polar species and overall kinetics." Environmental Science & Technology **48**(5): 2579-2588.

Zhang, H.F., Sun, B.S., Zhao, X.H. and Gao, Z.H. (2008a). "Effect of ferric chloride on fouling in membrane bioreactor." Separation and Purification Technology **63**(2): 341-347.

Zhang, J., Chua, H.C., Zhou, J. and Fane, A.G. (2006). "Factors affecting the membrane performance in submerged membrane bioreactors." Journal of Membrane Science **284**(1-2): 54-66.

Zhang, P., LaPara, T.M., Goslan, E.H., Xie, Y., Parsons, S.A. and Hozalski, R.M. (2009). "Biodegradation of haloacetic acids by bacterial isolates and enrichment cultures from drinking water systems." Environmental Science & Technology **43**(9): 3169-3175.

Zhang, X.S., Garcia-Contreras, R. and Wood, T.K. (2007). YcfR (BhsA) influences Escherichia coli biofilm formation through stress response and surface hydrophobicity." Journal of Bacteriology **189**(8): 3051-3062.

Zhang, X., Talley, J.W., Boggess, B., Ding, G. and Birdsell, D. (2008b). "Fast selective detection of polar brominated disinfection byproducts in

drinking water using precursor ion scans." Environmental Science & Technology **42**(17): 6598-6603.

Zhou, J., Yang, F.L., Meng, F.G., An, P. And Wang, D. (2007). "Comparison of membrane fouling during short-term filtration of aerobic granular sludge and activated sludge." Journal of Environmental Sciences **19**(11): 1281-1286.

Zhou, Z., He, X., Zhou, M. and Meng, F. (2017). "Chemically induced alternations in the characteristics of fouling-causing bio-macromolecules-Implications for the chemical cleaning of fouled membranes." Water Research **108**: 115-123.

Zsirai, T., Buzatu, P., Aerts, P. and Judd, S. (2012). "Efficacy of relaxation, backflushing, chemical cleaning and clogging removal for an immersed hollow fibre membrane bioreactor." Water Research **46**(14): 4499-4507.